EXPERIMENTAL AND THEORETICAL STUDY OF LONGSHORE CURRENTS ON A PLANE BEACH

by

Cyril Jerome Galvin, Jr.
B.S. Saint Louis University
(1957)
S.M. Massachusetts Institute of Technology
(1959)

Submitted in partial fulfillment
of the requirements for the degree of
Doctor of Philosophy

at the

Massachusetts Institute of Technology
June, 1963

Signature of Author _____
Department of Geology and Geophysics
June, 1963

Certified by _____
Thesis Supervisor

Accepted by _____
Chairman, Departmental Committee on Graduate Students

ABSTRACT

EXPERIMENTAL AND THEORETICAL STUDY OF LONGSHORE CURRENTS ON A PLANE BEACH

by

Cyril Jerome Galvin, Jr.

Submitted to the Department of Geology and Geophysics of the Massachusetts Institute of Technology in June, 1963 in partial fulfillment of the requirements for the degree of Doctor of Philosophy.

Measurements were made of the characteristics of breaking waves and the resulting longshore currents for 34 combinations of wave height (up to 0.22 feet), period (0.90 to 1.50 seconds), and breaker angle (up to 32°), along a 20 foot test section of a 30 foot, plane, smooth concrete beach with a 0.104 slope. The velocity of longshore currents generated on a laboratory beach by plunging breakers depends largely on breaker angle (θ_b) and position along the beach. θ_b determines the longshore component of momentum flux in the breaking wave, and this quantity increases in the downstream direction as the breaker is formed from fluid in the surf zone already moving with a longshore velocity. A differential equation for this non-uniform flow of longshore currents agrees qualitatively with the measured variation of velocity with breaker angle and distance. Mean water level also increases, and the breaker position and runup limit move shoreward, in the downstream direction. Energy is dissipated in the surf zone chiefly by the wave breaking and to a lesser extent by the bore in the runup region. The flow of the longshore current dissipates little energy. Longshore current velocity on a laboratory and a natural beach is approximately equal to the product of g, beach slope, wave period, and $\sin 2\theta_b$.

Techniques were developed to measure longshore current velocity and mean water level in the surf zone, and the measurement of breaker point and angle for plunging waves on a laboratory beach was standardized.

Thesis Supervisor: Peter S. Eagleson

Title: Associate Professor of Civil Engineering.

ACKNOWLEDGEMENTS

Peter S. Eagleson, Associate Professor of Civil Engineering, supervised this thesis. R. L. Bernstein and R. M. Males, undergraduate part-time assistants, aided in taking the data and did much of the data reduction. G. A. Tlapa programmed the continuity correlation for the IBM 1620 computer. The experimental work benefited from the suggestions of research assistants at the Hydrodynamics Laboratory, and the experimental equipment reflects the skill of Wallace Fleming, shop foreman. Several mathematical points were discussed with B. E. Fristedt. This research was begun under Contract No. DA-49-055-eng-16 with the Beach Erosion Board (September 1960 to June 1961), and was continued and completed under Contract Nonr-1841(74) with the Office of Naval Research (June 1961 to June 1963).

TABLE OF CONTENTS

TABLE OF CONTENTS (cont'd)

TABLE OF CONTENTS (cont'd)

LIST OF FIGURES

TABLE OF FIGURES (cont'd)

TABLE OF FIGURES (cont'd)

LIST OF TABLES

LIST OF TABLES (cont'd)

LIST OF SYMBOLS

a	Wave amplitude, 1/2 H	ft.
a_t	Vertical distance between mean water level and trough elevation	ft.
A_L	Area of longshore current channel	ft.^{2}
A_w	Cross-sectional area of breaker carried into surf zone	ft.^{2}
A_W	Cross-sectional area of triangular breaker H_b high and $L_b \cos \theta_b$ long	ft.^{2}
b	Breaker distance, horizontal distance between SWLine and breaker position	ft.
C	Wave speed	ft/sec.
d	Water depth, mean water level to beach surface	ft.
d_b	Mean water depth at breaking, defined as mb	ft.
d_d	Mean water depth between toe of beach and plunger	ft.
D_1, D_1', D_2	Constants in revised momentum analysis	
e	Elevation of mean water level above still water level	ft.
E	Energy flux	ft-lbs/sec.
E_f	Rate of energy dissipation by longshore current per foot length of beach	ft-lbs/sec.ft.
E_{ke}	Kinetic energy flux off test beach in longshore current per foot of test beach	ft-lbs/sec.ft.
E_{pe}	Rate of dissipation in maintaining runup volume above still water level per foot of beach	ft-lbs/sec.ft.
E_w	Rate of energy brought to beach per foot of beach length	ft-lbs/sec.ft.
f	Darcy-Weisbach friction factor	
g	Acceleration due to gravity	ft/sec^2
h_f	Head loss due to friction	ft.lbs/lb.
$\bar{h}$	Mean water level at breaking from solitary wave theory	ft.
h	Trough elevation above beach	ft.
H	Wave height, crest elevation minus trough elevation	ft.
k	Friction factor of Putnam et al. absolute roughness	ft.
k_x	Local horizontal distance between top of beach and SWLine	ft.

LIST OF SYMBOLS (cont'd)

K_1	Proportionality constant in continuity correlation	
L	Wave length from small amplitude theory	ft.
m	Beach slope	ft/ft.
MWL	Mean water level, average water surface elevation	ft.
p	Average particle velocity in area A_w divided by C_b	
P	Energy flux from plunger per foot of crest length	ft-lbs/sec.ft.
Q_L	Mass flux in longshore current	ft^3/sec.
Q_R	Q_L/Q_W	
Q_W	Hypothetical mass flux through wave	ft^3/sec.
r	Runup distance, horizontal distance between SWLine and runup limit	ft.
R	Hydraulic radius of longshore current channel = $d_b/2$	ft.
$\mathbb{R}$	Reynolds number of longshore $4VR/\nu$	
S	Surface force in breaking	lbs.
SWL	Still water level. Free surface of fluid at rest	ft.
SWLine	Intersection of SWL with beach, the x-coordinate axis	
t	Time	sec.
T	Wave period	sec.
u	Particle velocity in head of bore	ft/sec.
V	Average longshore current velocity	ft/sec.
V_{bp}	Longshore current velocity indicated by probe at breaker position	ft/sec.
V_b	Longshore component of velocity in return flow out of surf zone	ft/sec.
$V_{f_{10}}, V_{f_{16}}$	Average velocity of floats at x = 10 and 16 ft.	ft/sec.
V'	V_b/V	
x	Horizontal coordinate distance measured positively along beach from upstream training wall	ft.
y	Distance measured positively offshore from SWLine	ft.
y'	Horizontal coordinate, measured from top of beach	ft.
z	Vertical coordinate measured positively up from SWL	ft.

LIST OF SYMBOLS (cont'd)

subscripts

b	Location at breaker	
d	Location between beach toe and wave generator	
f	Refers to float, or friction	
L	Refers to longshore current	
o	Deep water conditions	
r	Refers to runup limit	
W	Wave at breaking in continuity correlation	
w	Wave at breaking in momentum analysis	
β	d_b/H_b	
γ	Weight density of fluid	lbs/ft^3
ρ	Mass density of fluid	slugs/ft^3
σ	Wave shape factor a_t/H_b	
θ	Angle between wave crest and x-coordinate	degrees

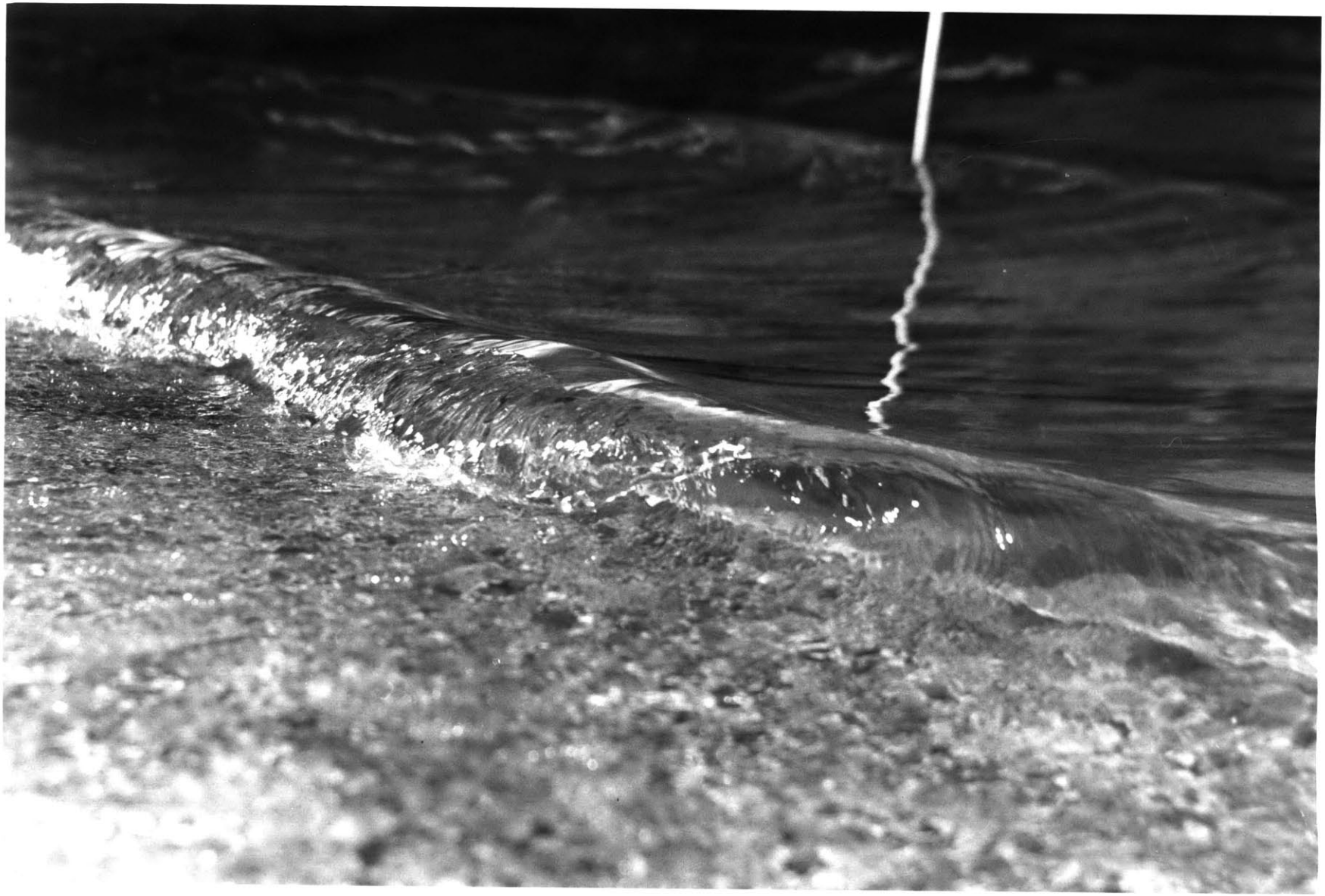

1. INTRODUCTION

1.1 Problem Statement

Longshore currents are currents concentrated between the point of wave breaking and the shoreline and driven parallel to the shoreline, usually by the longshore component of motion in breaking waves.

Longshore currents are of interest to engineers and geologists because they erode, transport, and deposit sediment. Along beaches bordering oceans and large lakes, these currents are capable of transporting hundreds of thousands of cubic yards of sand past a given point during an average year (Johnson, 1956; Brebner and Kennedy, 1959). This is an annual layer one square mile in area and several inches thick.

On natural beaches a quasi-equilibrium often exists between the rate at which sediment is supplied from rivers and cliffs and the rate at which it is transported away by longshore currents, so that net erosion is slight. An example of this equilibrium is the well studied coast of Southern California. Here, all of the beaches studied by Handin (1951, p. 54) with the exception of one 15 mile stretch, "had been in equilibrium during historic time prior to construction of artificial barriors". Sand reaches these beaches "chiefly from streams and to a much lesser extent from erosion of sea cliffs and the sea floor" (Emery, 1960, p. 25). Possibly this is typical of most coasts for it has been estimated that cliffed shorelines of the world erode back at

an average rate of only 1 cm per year and contribute on a worldwide basis about 1/8 km^3 per year to the sea (Kuenen, 1950). Rivers, on the other hand, bring to the sea 5 to 10 km^3 of sediment each year.

Engineering works (breakwaters, groins, dredged channels, and river dams) disturb the equilibrium, accelerating local erosion and deposition along beaches and in harbor entrances. Engineers are therefore interested in the mechanics of longshore currents in order to predict and, if possible, eliminate the unwanted effects of their structures on the environment. Beach Erosion Board Technical Report No. 4 (1961) summarizes and evaluates the literature on the engineering importance of longshore currents.

Coastal processes impart distinctive characteristics to the size distribution of beach sand (Friedman, 1961) as well as to the morphology of the bodies in which this sand occurs. Because the sand in some sandstones has lain, often more than once, on beaches during past geologic time, knowledge of longshore currents is valuable in interpreting the rock record of the past. The land forms produced by longshore currents - spits, hooks, bars, and straight beaches - are sometimes, as fossil forms, important petroleum reservoirs (Bass, 1934).

1.2 Scope of this Investigation

The ultimate aim of studies of longshore currents by engineers or geologists is the quantitative prediction of sediment transport by

longshore currents. Because sediment transport is primarily related to the velocity of the transporting current, it is first necessary to predict this fluid velocity before approaching the more difficult task of predicting sediment transport. The prediction of velocity should be consistent with the basic equations of motion. The correct initial forms of these equations depend critically on the accurate description of the phenomena whose motion these equations are to describe.

Therefore, the logical approach to understanding sediment transport by longshore currents involves first the accurate description of the phenomena generating these currents, then the proper formulation of the equations of motion to predict the velocity of the currents and an experimental verification of this prediction, and finally the investigation of relation between longshore current velocity and sediment transport. Longshore current motion is a compound of flow in open channels and wave motion at and after breaking, and because knowledge of these phenomena is somewhat empirical, it is expected that any formulation of the equations of motion for longshore currents must be liberally alloyed with empiricism.

This investigation deals with the initial steps of experimental description of longshore currents and the analytical prediction of longshore current velocity. Sediment motion is not treated. The experimental phase includes measurements under controlled laboratory conditions of phenomena associated with longshore currents flowing on a particular plane, smooth concrete beach. The analytical phase includes an empirical

relation between longshore current velocity and wave conditions at breaking on laboratory and natural beaches, an order of magnitude analysis of energy dissipation at and after a wave breaks, and a critical analysis of the equations of motion for longshore currents.

2. PREVIOUS INVESTIGATIONS

Literature directly concerned with longshore currents can be divided into three classes: field studies of longshore currents, studies of littoral drift on natural and laboratory beaches, and an analysis (one published paper known to the writer) of the mechanics of longshore currents.

Because longshore currents on natural beaches prompted this study, it is of interest to note what has been learned of them. Early observations, summarized by Johnson (1919), are fragmentary, but the dependence of longshore currents on the breaker angle and wave height was realized by some. The correlation of most longshore currents with breaker angle and wave height was given statistical support by over one thousand qualitative observations along the coast of Southern California (Shepard, 1950). Of particular interest is the repeated observation that longshore currents are unsteady and nonuniform flows on natural beaches (Shepard and Inman, 1950; Putnam, Munk, and Traylor, 1949); the unsteadiness is attributed to the stochastic nature of the incident waves, but the nonuniformity is due to rip currents, for "...most longshore currents can be shown to be related to rips because invariably they can be traced to a locality where the current turns seaward into a rip", (Shepard, 1950). Rip spacing was several hundred to a few thousand feet along most Southern California beaches investigated.

The variability in velocity was such that the standard deviation of longshore current velocity measuredat 15 stations roughly 300 feet apart usually equaled or exceeded the mean of the 15 measurements (Inman and Quinn, 1951). In other words, it is not uncommon on some relatively plane natural beaches (Torrey Pines and Pacific Beach, California) for longshore current velocity to oppose the longshore component of motion in the breaking waves. Inman and Quinn, and Putnam, et al. give measurements of breaker angle, wave height and period, beach slope, and longshore current velocity for some California beaches. Their methods of obtaining these data will be discussed in Section 9.

The material moved by longshore currents is called littoral drift. Savage (1962) summarizes present field and laboratory knowledge of the littoral drift transport rate and discusses techniques useful in laboratory studies of longshore currents. Probably the first physical approach to any aspect of the longshore current problem was an attempt to relate drift transport rate to the longshore component of power supplied by waves. The idea was initially put forward by Munch-Peterson (in 1914 according to Svendson, 1950), was later modified at the Los Angeles district of the Corps of Engineers (Eaton, 1951), and presently exists as Caldwell's (1956) formula based on measurements made on two natural beaches. Data for drift transport rates at Santa Barbara (Johnson, 1952) include all but the angles needed by this formula, but even assuming the most favorable value for the missing angles, the data will not come within an order of magnitude of satisfying the empirical relation.

The momentum analysis of Putnam, et al. (1949) gives a relation between the longshore current velocity, and the independent variables wave height, period, breaker angle, beach slope, and friction parameter. Putting velocities and wave characteristics measured on field and laboratory beaches into this relation, mean values of the friction parameter were obtained and these values of the friction parameter were then used to predict the velocities from which they were derived. This analysis will be discussed in detail later in this paper.

In a review of theories of longshore current motion, Per Bruun (1963) concludes that this momentum solution is the best available for plane beaches, and suggests that for beaches bordered by bias, a continuity relation between the fluid brought in by the breaking waves and that carried out by rips might be useful.

3. EXPERIMENTAL PROGRAM

In some relatively well set problems of fluid mechanics, such as those involving solutions of Laplace's equation, experiments have the role of checking what experience has shown to be an adequate representation of a well described class of phenomena. In other, essentially nonlinear, problems of fluid mechanics, and longshore currents is one of them, experiments have the role of determining what exactly are the physically important features of the phenomenon under investigation. In the latter case, theory should wait on experiment and observation, or risk describing a phenomenon which does not exist.

Experiments designed to describe quantitatively longshore currents on a laboratory beach were performed at the MIT Hydrodynamics Laboratory. In an extensive preliminary investigation, methods were developed to measure four types of data, classified for convenience as types A, B, C, and D (see Table 1). Energy dissipation in the breaking wave, perhaps the most important dependent variable in this study, could not be directly measured, for appropriate instruments do not exist.

One or more of the four types of data are included in 44 runs, identified for convenience by a unique combination of three independent variables: θ_d, H_d, and T. Four values of θ_d, the angle between wave generator and shoreline, divide the runs into Series I(0^o), II(10^o), III(27^o), and IV(51^o). Each series, except I, includes about a dozen tests identified by a unique combination of wave period (T) and wave

height in front of generator (H_d).

TABLE 1 TYPES OF EXPERIMENTAL DATA

Type	Principal measuring device	Quantity measured	Symbol
A	parallel wire resistance gage	wave height	H
		wave speed	C
		wave form	σ
B	breaker locator tape	breaker position	b
		breaker angle	θ_b
		runup limit	r
C	damped piezometers	change in MWL due to waves	e
D	miniature current meter, floats	longshore current velocity	V

Tables A1 and A2 of the Appendix summarize the data available from these experiments according to data type, series, and test number. Series I ($\theta_d = 0^o$) was done only to check a few cases when no longshore currents would be expected.

4. EXPERIMENTAL EQUIPMENT AND PROCEDURE

4.1 Run Conditions

The experiments were conducted in a model basin 45 ft. by 22 ft. by 1.4 ft. containing a movable, plunger-type wave generator 20 ft. long and a smooth concrete beach 30 ft. long and 13 ft. wide with a 1 on 10 slope (see Figures 1, 2, and 3). Offshore water depth was kept at 1.15 ft. Waves, generated at known angles to the beach, advanced onto the beach between training walls. The waves breaking at an angle to the shoreline set up a longshore current which flowed along the test section of the beach and out through an opening between the downstream training wall and the shore. The flow eventually returned to the beach by passing under the plunger.

Table 2 lists the range of the independent variables in these experiments. The values were largely determined by available space and equipment.

4.2 Parallel Wire Resistance Gage (Type A Equipment)

Wave height, speed, and form were obtained using a platinum wire resistance wave gage and Sanborn recording oscillograph, Model 150. The wave gages (see Figure 3) differ from previous models (Dean, 1959; Wiegel, 1956) principally in the addition of connectors between the sensing wires and cable leading to the recorder. For use in and near the surf zone, this connection is made by soldering the 0.036 inch diameter platinum wire

Figure 1. Wave Basin

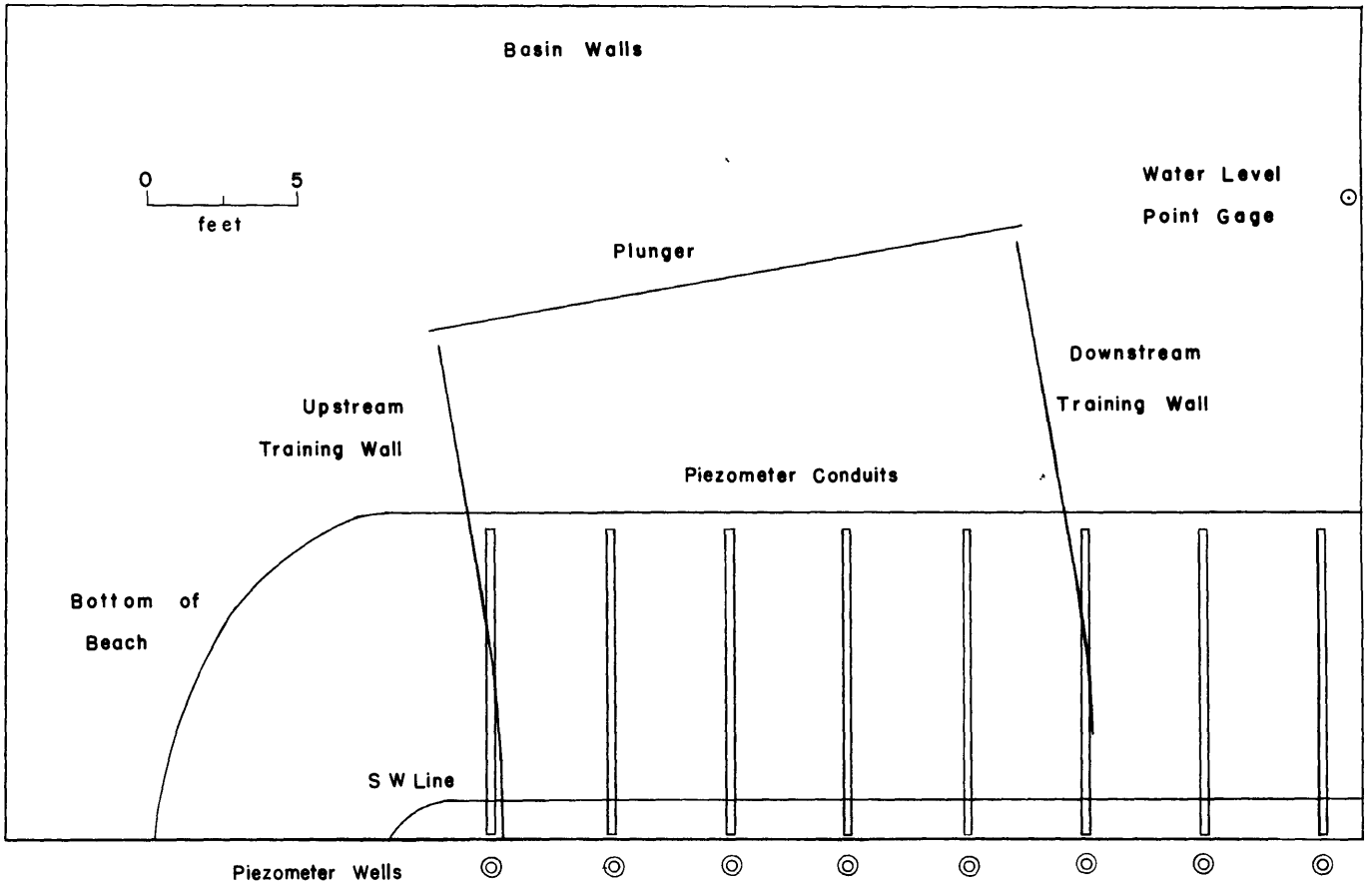

PLAN VIEW OF BASIN

Figure 2. Plan View of Basin

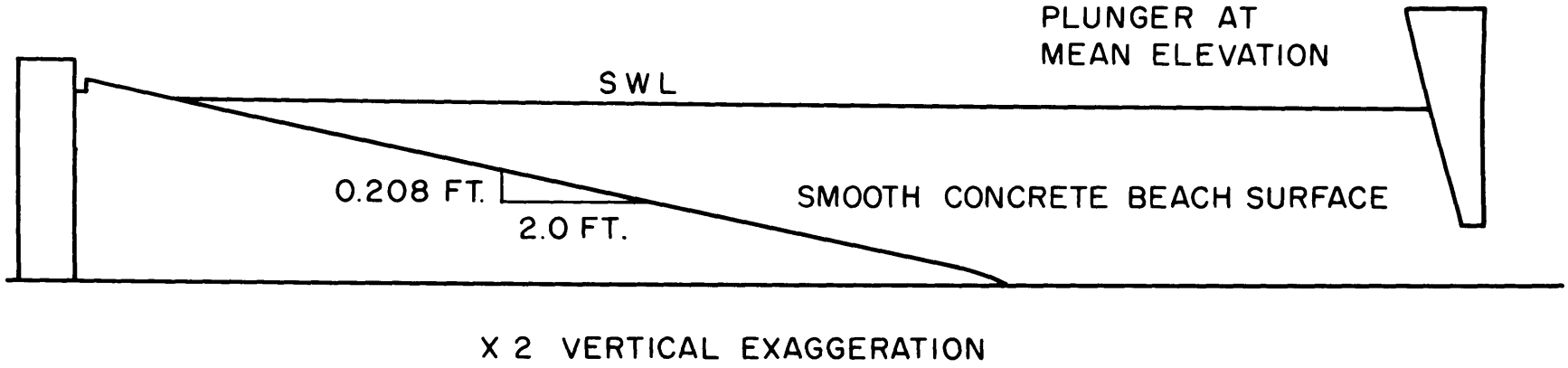

Figure 3. Cross-Section of Beach and Basin

TABLE 2 RUN CONDITIONS

Wave generator angle	(θ_d)	0°, 10°, 27°, 51°
Wave period	(T)	0.90 to 1.50 sec.
Wave height at generator	(H_d)	0.05 to 0.21 ft.
Beach slope	(m)	0.104 ft./ft. overall average 0.109 ft./ft. nearshore average
Beach surface		smooth concrete
Water depth at generator	(d_d)	1.15 ft.
Water temperature		14° to 23°
Length of test beach (between training walls)		$\sim$ 22 ft.
Opening between downstream training wall and SW Line		2.2 ft.
Mean elevation of plunger base above floor		0.40 ft.

Training wall curvature	Series	Curvature
	I	not needed
	II	for refraction of 1.25 sec. wave
	III	none
	IV	for refraction of 1.50 sec. wave.

in an Amphinol female jack (80 M C 2 F) which fits a male plug (80 M C 2M) on the cable. The base of the female jack was covered with a smooth convex coat of beeswax. These modifications prevent the calibration from drifting due to the collection of spray from breaking waves at the connection, and they also make the wires easily detachable from the long lengths of cable. The parallel, 0.036 inch diameter wires of these gages cantilever 5-1/2 inches beyond the connector and are held parallel and 3/16 inch apart by two lucite spacers (see Figure 4).

Calibration. Gages were calibrated by lowering them into still water in one centimeter increments over a range of 6 or 7 cm., and recording on Sanborn paper the change in resistance between the wires. A plot of gage elevation (in cm. above an arbitrary datum) against recorder deflection (in mm.) is reasonably linear and constant for time intervals on the order of 10 hours (see Figure 5). The slope of this curve, in feet of water per mm. of Sanborn paper, is the calibration constant used to obtain wave height.

This static calibration was checked by hermonically oscillating the gage a known vertical distance in still water, following the procedure of Dean (1959). In six tests, differences between static and dynamic calibrations were 2 per cent or less, which approaches the order to which the amplitude of the vertical oscillation can be read.

Gage performance. Because the gages were used in shallow water on a concrete beach containing aluminum channels in the beach surface,

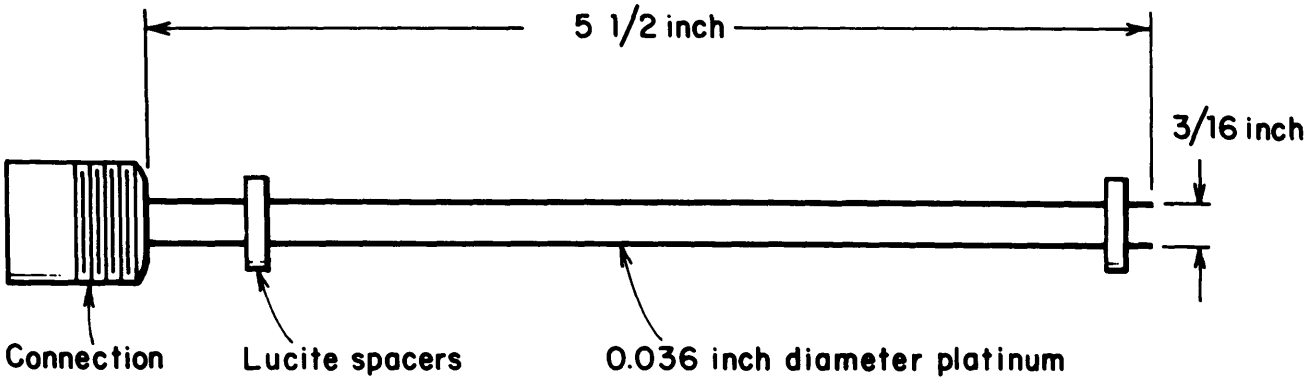

Figure 4. Platinum Wire Resistance Wave Gage

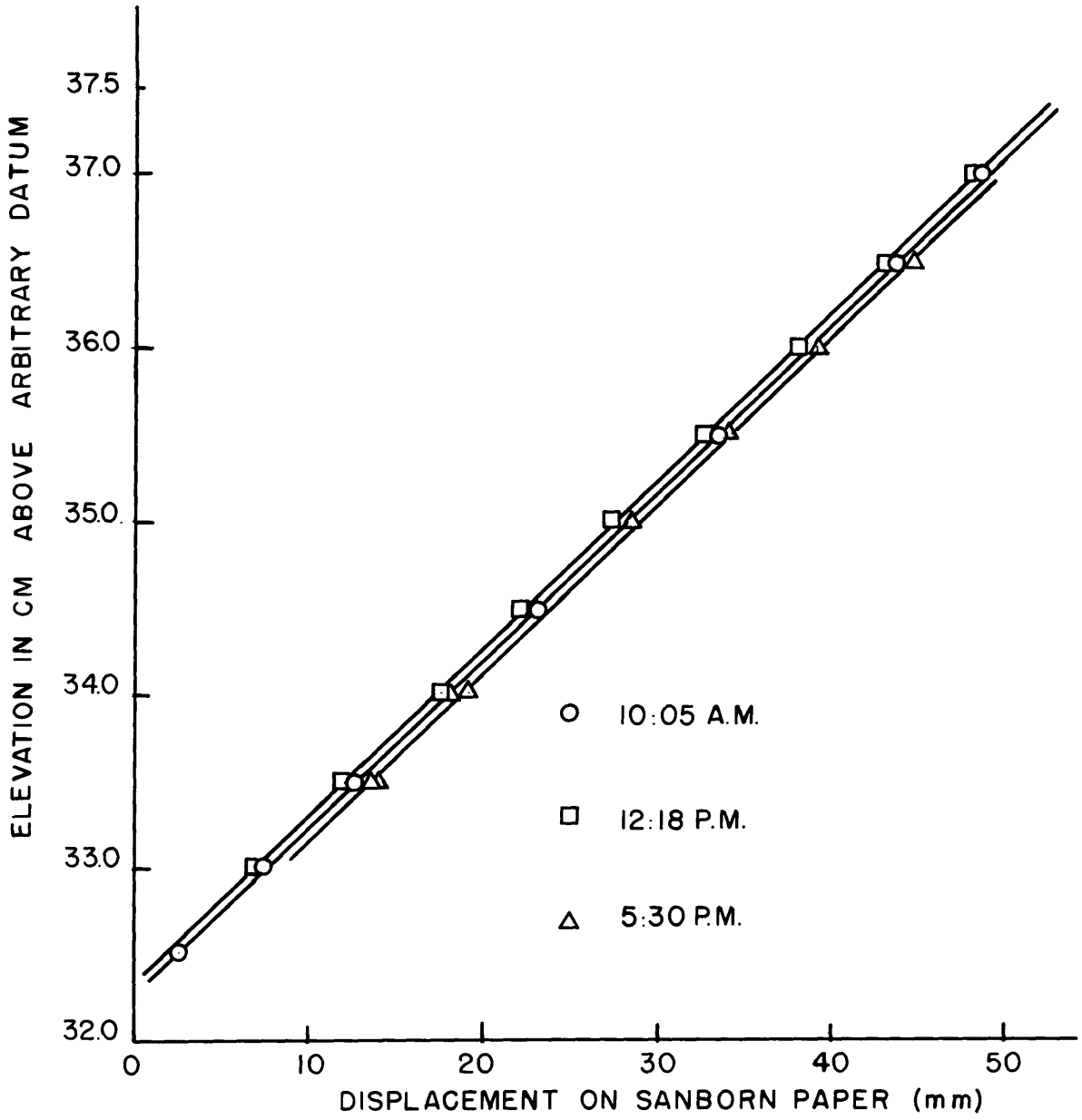

Figure 5. A Calibration Curve for Platinum Wire Resistance Wave Gage

the effects of these surfaces on the calibration were determined. Linearity of calibration was not affected by the free surface in shallow water as long as the probe was 3 mm. below the free surface. The calibration curve obtained with the ends of the two wires in contact with the same concrete surface was indistinguishable from a normal calibration curve. Calibration made in shallow water was affected by the aluminum channels at distances of less than 2 inches, and therefore, gages were not used over the channels. The lucite spacers, as long as they were entirely below or above the free surface, did not affect the slope of the calibration curve, but position of this curve was translated slightly if spray wet the upper spacer.

During a few runs, the platinum wires were accidently bent, but after straightening, a recalibration showed no more than normal variation from the original calibration. J. A. Hoopes (personal communication, 1963) found little variation in sensitivity for large changes in wire spacing. A 100 per cent increase in spacing (from 1/4 to 1/2 inch) decreased the sensitivity only 15 per cent. In normal use, spacing does not change. The wires of the gages are relatively short and stiff; no vibration or severe bending under the action of the waves occurs.

Gages were never wiped while in use. Calibrations before and after a test wiping were indistinguishable, one from the other. Water surface during these runs was clean, and the gages were in water only while in use.

In general, these tests of the performance of parallel wire resistance gages repeat and extend tests reported by Wiegel and Dean, and substantiate Dean's conclusion that actual wave height will not differ by more than 3 to 5 per cent from measured wave height.

Oscillograph. During the tests of the wave gage, an important possible source of experimental error was noted. The stylus of the recorder is held by a spring against the recording paper, and if the spring tension is too high, friction between stylus and paper can cause large errors, particularly when low paper speeds and small deflections of the stylus permit sticking to occur. For this reason, most wave gage data were taken at highest paper speed (100 mm./sec.) and about two thirds of full scale deflection, under which conditions the rapid relative motion between stylus and paper minimizes the friction effect. Whenever recordings were made at low speeds, tension on the stylus was checked. Recording data near the edges of the Sanborn paper was avoided when possible because the response of the stylus in this region is slightly nonlinear.

4.3 Measurement of Wave Height, Speed and Shape (Type A Procedure)

In use, wave gages were suspended from a point gage mounted on a rolling cross bar which traveled on an aluminum frame extending over a 6 ft. by 20 ft. area of the test beach (see Figure 6). Wave height was obtained by averaging the recorded wave height of twenty successive waves passing one calibrated wave gage. Wave shape (temporal variation of water surface elevation at the gage position) could be obtained from these same

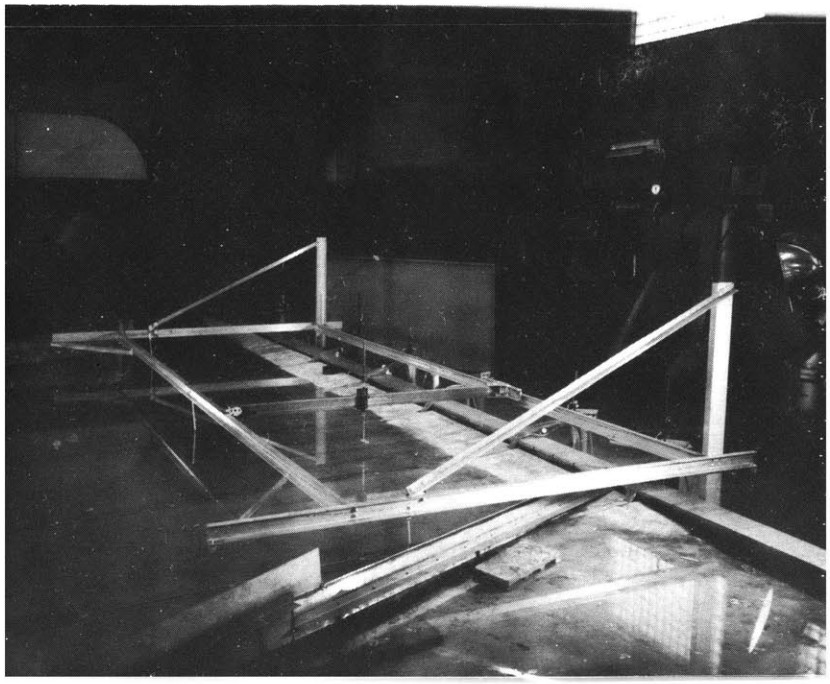

Figure 6. Frame with Rolling Cross-Bar over Test Section of Beach.

recordings. Envelopes of wave height were obtained by moving the calibrated gage slowly from offshore, through the breaker zone, and into the runup region. Wave speed was obtained by averaging the recorded phase lag (Δs in Figure 7) of 20 waves passing two gages fixed 0.25 ft. apart on a line parallel to the direction of wave travel.

These data were always taken at a station in the middle of the test beach and usually also at the upstream and downstream ends of the beach (see Appendix, Table A4). At these stations, wave speed and height were measured at between six and ten locations along a line extending from the top of the runup region to offshore of the breaker.

4.4 Measurement of Breaker Point, Breaker Angle and Runup Limit (Type B Equipment and Procedure)

Definitions. As the breaker begins to plunge, the crest overreaches the concave front of the wave. When viewed from above, this concavity forms a grayish, translucent band along the wave front and is separated from the clear water to the back of the wave by a dark line marking the vertical segment of the wave face (see Figure 8). The position where this dark line first appears in the shoreward moving wave is defined as the breaker point (y_b'). The breaker angle (θ_b) is defined as the angle between the wave crest at the breaker point and the mean shore line. The average maximum position attained by the bore which forms after the wave breaks is defined as the runup limit (y_r').

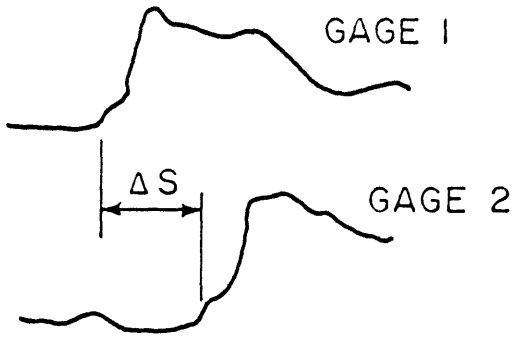

Figure 7. Phase Lag Measured by 2 Wave Gages. Gages Spaced 0.25 feet Apart in Plane Normal to Direction of Wave Propagation. Shape Shown is that of a Bore Forming from the Broken Wave.

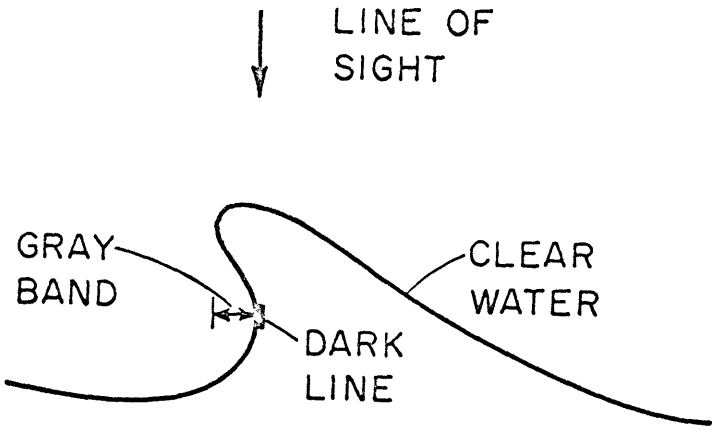

Figure 8. Breaker Point Definition. Position of the First Appearance of Dark Line in the Shoaling Wave is Defined as the Breaker Position.

Breaker locator. Breaker point and breaker angle were measured visually with a breaker locator consisting of two horizontal plates whose front edges had been fixed in the same vertical plane. The lower of those two plates is opaque lucite and pivots from a protractor which can move along the traveling cross bar (see Figure 9). A second lucite plate is fixed on dowels 0.25 feet above the first.

With the plates parallel to the shore line ($\theta = 0$), breaker point was measured by sliding the breaker locator offshore until the dark line defining the breaker point just disappeared beneath the opaque plate. The position of the breaker was then read from a tape on the cross bar. The measurement was repeated by sliding the locator in from offshore and noting the first appearance of the dark line. The average of these two readings was recorded as the breaker position (y_b').

With the breaker locator at the breaker point, breaker angle (θ_b) was measured by pivoting the plates until their front edges fell in the same vertical plane as the wave crest at breaking. The angle was then read directly from the protractor on the breaker locator.

In measurements of both y_b' and θ_b, the observer's line of sight was kept vertical by looking down past the locator in such a way that the front edges of the two plates coincided. θ_b and y_b' were measured by two observers at each of 5 stations along the test section of the beach.

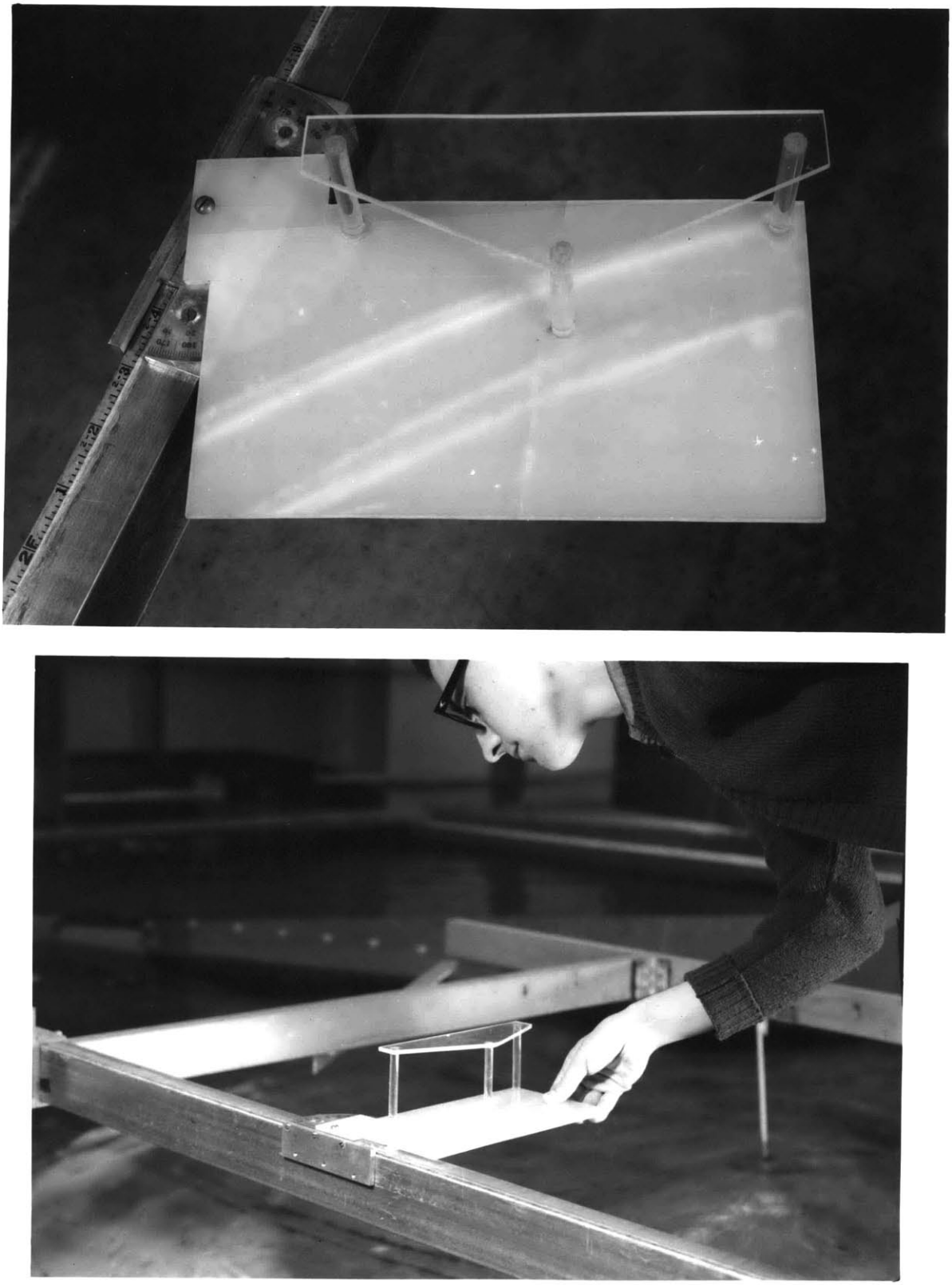

Figure 9. Breaker Locator

Runup limit. The distance between the beach top and runup limit (y_r') was measured with a tape by two observers at the 5 stations where y_b' and θ_b were measured. The conversion of y_r' and y_b', distances measured from the beach top, to r and b, distances measured from still water level, is outlined in Section 5.1.

Repeatability and operator variation. The position of the breaker point and runup limit and the magnitude of the breaker angle are visible over only a small fraction of the wave cycle, and the quantities themselves fluctuate from wave to wave. The average position of these quantities was measured visually in a standard manner by two observers, but in spite of the standardization, the observations are still somewhat subjective.

In evaluating these measurements it is necessary to know what is the agreement among repeated measurements of the same quantity by one observer (repeatability) and what is the difference between measurements of the same quantity by different observers (operator variation). If it can be assumed that the average values of the quantities can be measured in the interval of observation (about 1 minute), then the repeatability and operator variation give measures of the accuracy of the method.

Over a six week interval, y_b', y_r', and θ_b were measured 3 times by one observer for the conditions of test IV 2. In Table B, the repeatability of y_b' and y_r' seems about the same, and the maximum range in any of the 9 sets of repeated y_b' and y_r' readings is 0.16 feet. The important

quantity here is $y_b' - y_r'$, the distance between breaker point and runup limit which is on the order of 2 feet in these tests. If it is assumed that any measurement is within 0.08 feet of the mean, then the 'most probable' error in $y_b' - y_r'$ (Topping, 1955) is $(0.08^2 + 0.08^2)^{1/2}$ or 0.11 feet or about 5 per cent of $y_b' - y_r'$.

In all but 4 of the 38 tests involving type B data the measurements were repeated by a second observer. The operator variation, indicated by Table 3, has maximum ranges of 0.23 feet for measurements of y_b' and 0.09 feet for y_r'. In tests II 2, III 2, IV 2, the absolute value of operator variation averages 0.12 feet for y_b' and 0.03 feet for y_r', but the differences between the average y_b' and y_r' of each observer in these 3 tests is only 0.04 feet and 0.02 feet. This indicates that y_b' is subject to greater uncertainty than y_r', but that systematic differences between observers are small. The experimental data presented in this report (see Appendix) is based on the average y_b' and y_r' of the two observers.

In Table 3, the repeatability of measurements of θ_b is within 8.5 degrees, or 3.5 degrees if one measurement is eliminated, for 5 sets of 3 readings. For the same data, the operator variation ranges up to 6 degrees. Unlike measurements of y_b' and y_r', there is a systematic difference between the measurements of the two observers (see Table 4), but similar to the treatment of y_b' and y_r' data, the values of the angle presented in this report are the average θ_b of the two observers. This choice of θ_b, a critical variable in this study, is explained in Section 5.3.

TABLE 3

REPEATABILITY AND OPERATOR VARIATION FOR Θ_b MEASUREMENT (TEST IV 2)

Measurement	y_b', in ft.		y_r', in ft.		Θ_b, in degrees	
Observer	CJG*	RLB**	CJG	RLB	CJG	RLB
Distance along beach, in feet						
4	2.82		0.54		23.5	
	2.76	3.04,2.79	0.52	0.50	32	26
	2.91		0.46		28.5	
7	2.73		0.46		27	
	2.86	2.73	0.42	0.39	30	30.5
	2.86		0.37		29	
11	2.68				26	
	2.74	2.70			28	31
	2.66				26	
15	2.42		0.32		26.5	
	2.49	2.71,2.62	0.31	0.29	29	33.5
	2.49		0.17		28	
18	2.31		0.35		29	
	2.32	2.29	0.34,0.19	0.25,0.21	30.5	32.5
	2.33		0.31		29	

*Measurements taken on 8/31/63, 9/6/62, 10/11/62

**Measurements taken on 9/6/62

Average difference $y_b' - y_r' \sim 2.25$ ft.

TABLE 4

OPERATOR VARIATION IN AVERAGE BREAKER ANGLE

Series	Date	$\Delta\theta_b^*$ in degrees	$\theta_{b\ AVE}$ in degrees
II	Dec. 1962	2.64	3.5
III	March 1963	2.39	8
IV	Sept. 1962	3.87	17

*$\Delta\theta_b = \theta_{b\ AV\ (RLB)} - \theta_{b\ AV\ (CJG)}$

4.5 Change in Mean Water Level (Type C Equipment and Procedure)

Definitions. The elevation of the surface of a motionless body of water is defined as the still water level (SWL). The intersection of the still water level with a plane beach is called the still water line (SWLine), a term approximately equivalent to shoreline. The time average elevation of a moving water surface is defined as the mean water level (MWL). The elevation of the mean water level measured positively upward from the still water level is defined as the setup elevation, e, (see Figure 10).

$$e = MWL - SWL \qquad (1)$$

Little is known of e, except that it depends on wave energy brought to the beach and is distinguished from wind or tidal setup. Variation in the energy supplied by waves to natural beaches causes the

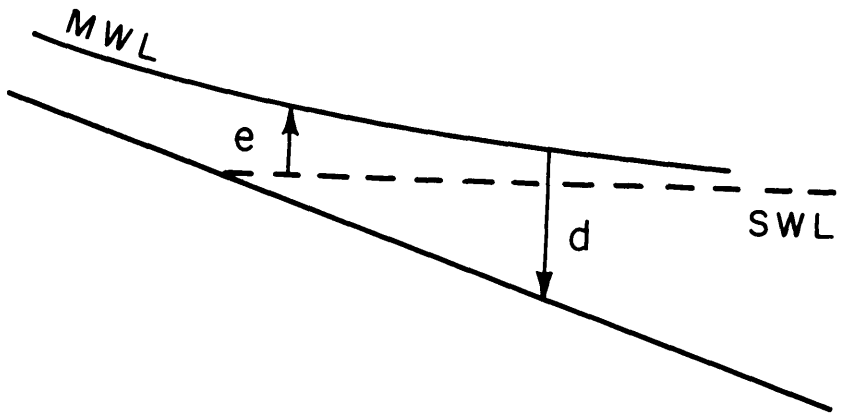

Figure 10. Definition of Change in Mean Water Level (e) and Depth (d)

fluctuating MWL known as surf beat (Munk, 1949), but on natural beaches it is difficult to measure SWL. Because wave setup is a measure of one mechanism of energy dissipation in the surf zone, measurements were made to evaluate its importance.

Piezometer conduits and wells. Eight 10 feet long piezometer conduits were imbedded flush with the surface of the smooth concrete beach, and extend in a direction perpendicular to the shoreline at 4 foot intervals along the beach (see Figure 2). The conduits, consisting of nested aluminum channels, contain 6 smoothly polished 1/16-inch piezometer taps located so that 4 of these taps lie in or near the surf zone (see Figure 11). Three eighth inch ID Tygon tubing leads from each pressure tap through the piezometer conduit and a manifold to a piezometer well,

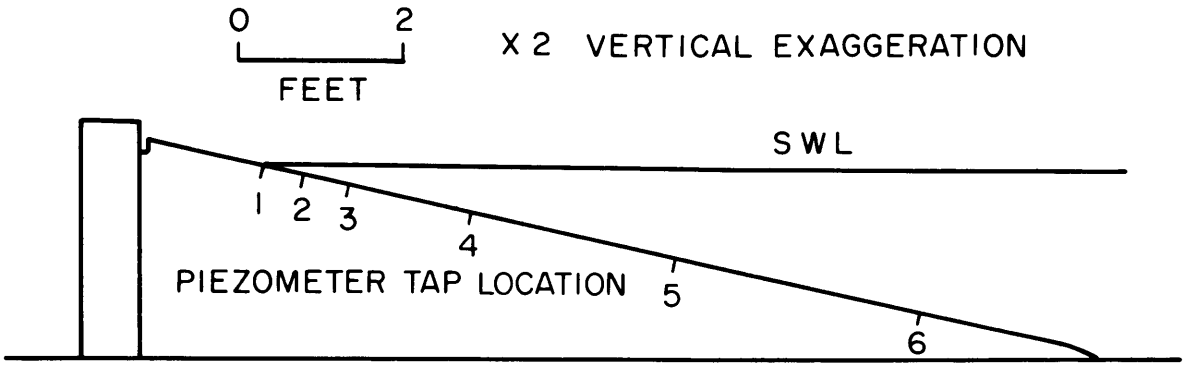

Figure 11. Location of Taps for Damped Piezometer

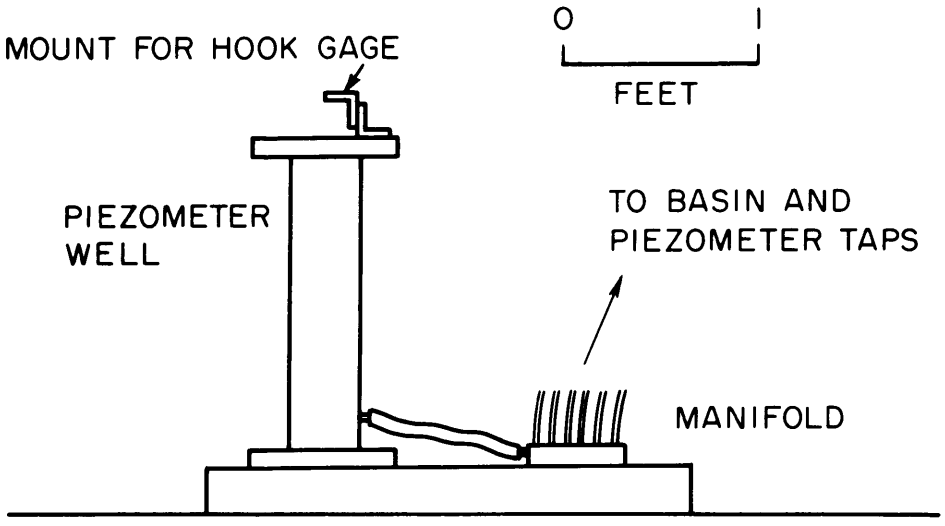

Figure 12. Piezometer Well

which is a 4-inch ID tube with a hook gage to measure water level (see Figure 12).

The large ratio of well-to-tubing diameter and the highly viscous flow in the tubing ($\mathbb{R} \sim 10$) so damps the fluctuation of the water level in the piezometer well that careful observation with a hook gage and flashlight is required to see any periodic response to wave motion in the basin. The viscous damping and diameter ratio are such that the 5 minutes are required for the water level in the tube to adjust to a change of one mm. in the SWL of the basin.

Measurement of e. From the definition of equation 1, it is necessary to measure MWL and SWL to obtain e. SWL was measured in the piezometer well by raising the hook gage to the reflection of a flashlight shining on the water surface. The wave generator was then started and allowed to run for 25 minutes. Then the local mean pressure at the taps was obtained by connecting the different taps, one at a time, to the well through the manifold, and measuring the steady state level in the well with hook gage and flashlight. Steady state level was attained in the well when successive readings of the water surface, ten minutes apart, had a variation of no more than 0.1 mm.

After some practice, readings could be made by different observers with an operator variation of no more than 0.2 mm. Precision was 0.1 mm. The time of each measurement was always recorded.

The final SWL measured at the end of the test was almost always lower than the initial SWL. This drop in SWL was recorded through the test at a damped piezometer well in a quiet section of the basin (water level point gage of Figure 2). From the record of this point gage, the 'evaporation correction', as much as 1.0 mm. in a day's run could be computed for the different times of pressure tap measurements. Indications from theory and experiment are given in Section 5.4 that the piezometer tap beneath the waves measures the mean hydrostatic head, and thus indicates MWL.

4.6 Velocity Measurement (Type D Equipment and Procedure)

Velocity in the longshore current was measured by joint use of floats and a velocity probe (propellor-type miniature current meter). The floats were rectangular solids of softwood 5/8-inch by 5/8-inch by 5/16-inch which floated about 1/4 above water when wet. The velocity probe was an Armstrong Miniflowmeter AWE 183/1 ISSUE A which counts electronically the revolutions of a jewel-mounted propellor in a 5/8-inch diameter housing (see Figure 13). When actuated by uniform flow in the direction of the propellor axis, these counts are convertable to velocity using the manufacturers calibration curve. This curve was repeatedly checked in a towing tank and found to be accurate to within 2 per cent (E.A. Prych, personal communication, 1963).

However, the response of the probe depends upon its orientation with respect to the velocity vector of the fluid, and since fluid

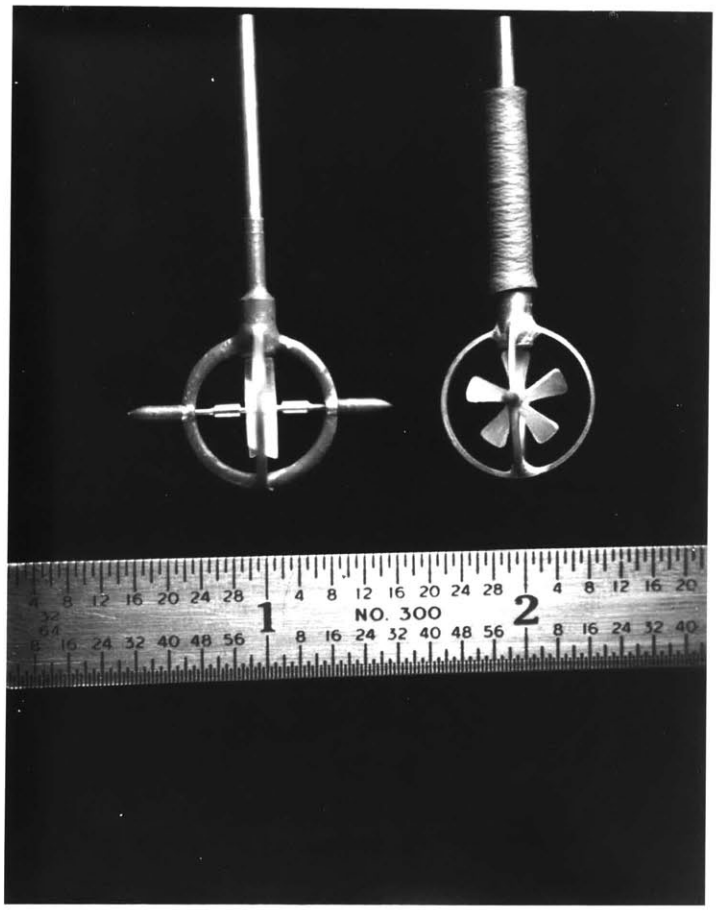

Figure 13. Velocity Probes

velocities in the surf zone vary in an unknown manner, both in magnitude and direction, this instrument cannot be used directly to measure longshore current velocity. Linear relations were found to exist between the apparent velocity given by the probe when aligned with the longshore current and the mean surface velocity obtained by timing the travel of the floats. Calibrations were developed for Series II, III, and IV by comparing the maximum indicated velocity at a station with local float velocity (see Figure 14).

The calibrations are satisfactory, but probably they could be improved by introducing the breaking angle (θ_b) into the curves. Also, since the probe counts the rotation of the propellor regardless of the direction or origin of the current which induces it, the indicated velocity offshore of the breaker and in slow longshore currents may be too high. The calibration curve for Series IV and the few measurements of series I indicate this. Inshore of the SWLine the probe is often exposed during part of the wave cycle.

In 31 tests which included this type of data, velocity was measured with the probe at at least 5, and usually 7, stations along the beach and at each station 3, 4, or 5 measurements were made on a line perpendicular to the shoreline in the surf zone (see Appendix, Table A 7). Each indicated probe velocity is the average of 50 seconds of counting. Whenever possible, probe elevation was at the estimated mean depth.

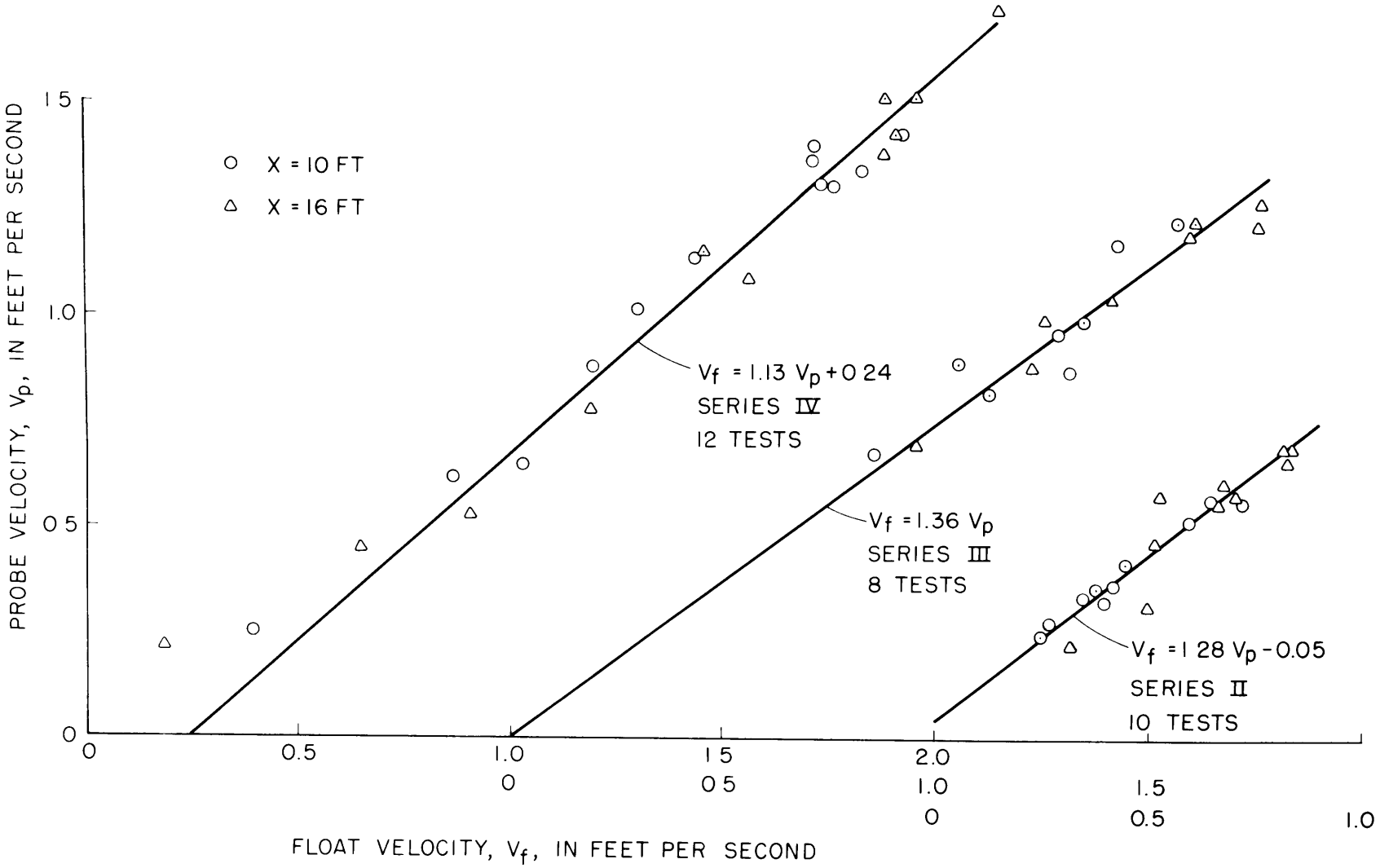

Figure 14. Calibration of Velocity Probes with Surface Floats

The distance traveled by the floats in an integral number of wave periods (4 or 5) was measured with a tape for two sections of the beach in each of the 31 tests. By assuming the velocity varied linearly between these two sections, the mean float velocities were adjusted in all the tests to common positions 10 feet and 16 feet from the upstream training wall. The necessary adjustment was made as small as possible by the initial choice of the section over which to measure the float travel. Each float velocity is the average of 10 measurements during which measurements the floats did not ground on the beach.

TABLE 5

DYE AND FLOAT VELOCITY IN LONGSHORE CURRENTS

Test	Dye Velocity* ft/sec.	Float Velocity* ft/sec.
III 2	1.31	1.33
	1.33	1.32
III 4	1.13	1.24
	1.15	1.23
III 6	0.97	1.00

*each number is the average of 5 measurements over the downstream section of beach. Mid-point of dye patch was timed.

It has been noted (N.H. Brooks, 1963, personal communication; Shepard, 1950) that floats used in the surf are subject to surfboarding effects which make them travel faster than the water particle velocity. To test this effect, races were held between a small quantity of malachite

green-dyed water and the floats. The course was a six foot stretch over the downstream end of the beach, and the wave conditions were those of test III 4 and III 6. The front edge of the dye won 6, lost 2, and tied 2 for test III 4, and won 7, lost 2, and tied 1 for test III 6. It appears from these results that the effects of diffusion on dye balances the effect of higher surface velocity and surfboarding on the floats in these tests. Measured dye and float velocities show occasional differences (Table 5).

4.7 General Basin Conditions

Care was taken to perform the different series and types of experiments under as nearly identical conditions as possible (see Table 2). The plunger to the wave generator was leveled after each change in wave generator position and the mean elevation of the plunger maintained within 0.01 feet. The angle between plunger and shoreline (θ_d) was measured with tape and transit. Training walls were curved for refraction at the 10° and 52° position but not for the 27° position. For all experiments the upstream training walls extended to the top of the beach and the exit width for the longshore currents between the downstream training wall and the shore was maintained to within a few tenths of a foot. SWL was kept to within 0.003 feet of a constant value, a variation which is an order of magnitude less than the variation in basin floor elevation. Water temperature in these experiments ranged from 14° to 23°C.

No attempt was made to study the effect of changing the basin geometry. Wave height just offshore of the breaker showed in some cases a pronounced secular increase in the first few minutes after turning on the wave generator and a gradual approach to steady conditions lasting 20 minutes or so. The data presented in this report were obtained at least 25 minutes after the start of the wave generator.

Wave height, H_d, was measured in front of the plunger to define the wave heights associated with each of the tests, and the results are listed in Table A 1. H_d is the average height of the third through tenth waves to pass the wave gage located in front of the plunger after the start of the plunger. The first couple of waves were smaller due mainly to random starting position of the plunger and the difference between group and phase velocities. Accurate measurements of plunger frequency showed that even at the first complete revolution, after starting, the wave generator had attained its steady state frequency. Reflections from the beach and training walls became measurable after about 10 or 12 waves. These H_d measurements varied about 7 per cent for different positions relative to the plunger, and varied less than 2 per cent for repetitions of the measurement at the same position.

5. EXPERIMENTAL RESULTS

5.1 Coordinate Systems and Definition

The principal coordinate system is a right-handed, rectangular x-y-z system (see Figure 15) in which x follows the still water line (SWLine), y is perpendicular to x and lies in the plane of the still water level (SWL), and z is normal to the x y plane. The origin of this system is the intersection of the SWLine with the first piezometer conduit on the beach (approximately equivalent to the upstream training wall). x is measured positively in the direction of longshore current flow (the downstream direction), y is measured positively toward the wave generator (the offshore direction) and z is measured positively upwards.

As defined in section 4.5, SWL is the elevation of the water surface in the basin when the fluid is not in motion, and SWLine is the intersection of the SWL with the beach.

A second coordinate parallel to the y axis but originating at the top of the beach is defined as the y' coordinate. The difference between y and y' is defined as k_x (see Figure 16). The value of k_x was calibrated against SWL as measured by the water level point gage, and as a function of x. In this way measurements of the various types of data could be referred to a local and temporal value of SWLine, since this quantity fluctuates slightly during a run due to decrease in SWL

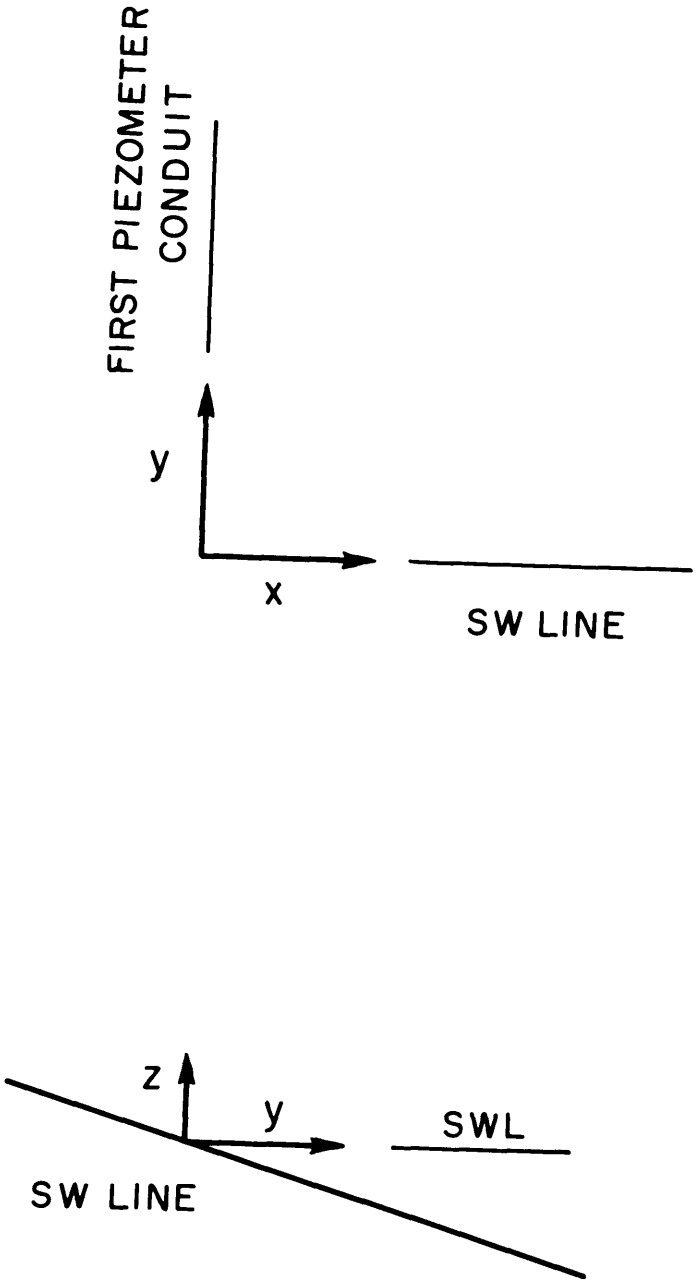

Figure 15. Definition of x-y-z Coordinate System.
Above, Horizontal Plane,
Below, Vertical Plane.

(see Section 4.5) and also varies along the beach due to slight unevenness of the beach surface.

The runup limit y_r' was defined in section 4.4 as the average distance from the top of the beach to the uppermost position of the runup. The runup distance r is defined here as the horizontal distance between SWLine and y_r' (see Figure 16)

$$r = k_x - y_r' \tag{2}$$

The breaker position y_b' was defined in section 4.4 as the distance between the top of the beach and the breaker position. The breaker distance b is defined here as the distance between the breaker position and the SWLine (see Figure 16)

$$b = y_b' - k_x \tag{3}$$

There are three quantities measured in the z coordinate: d, the vertical distance between MWL and the beach surface (see Figure 10), e, the local vertical distance between SWL and MWL, and H, the vertical distance between wave crest and trough. e is measured positively up from SWL, and d is measured positively down from MWL.

Several parts of the beach are frequently referred to (see Figure 17). The shoaling zone lies between the position at which the wave ceases to be a deepwater wave and the breaker point. The surf zone lies between the

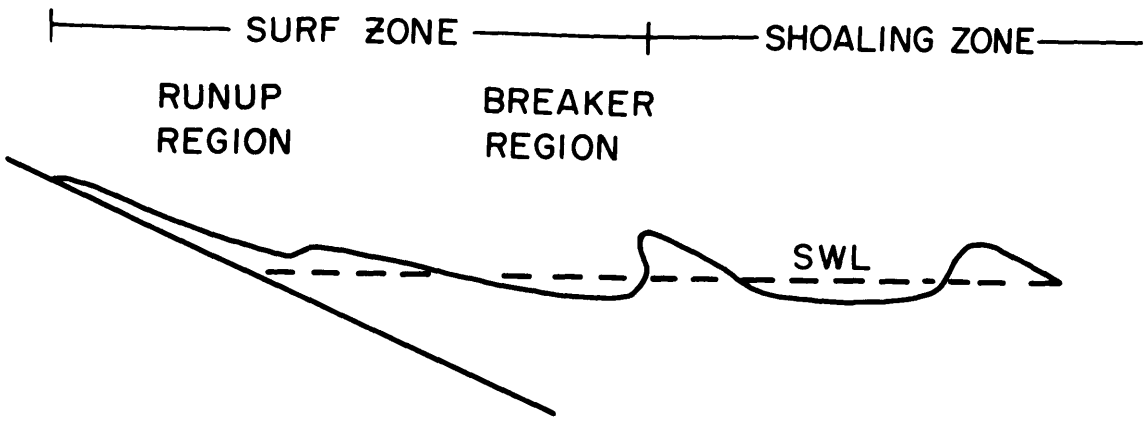

Figure 17. Definitions of Surf Zone, Shoaling Zone, Breaker Region, and Runup Region.

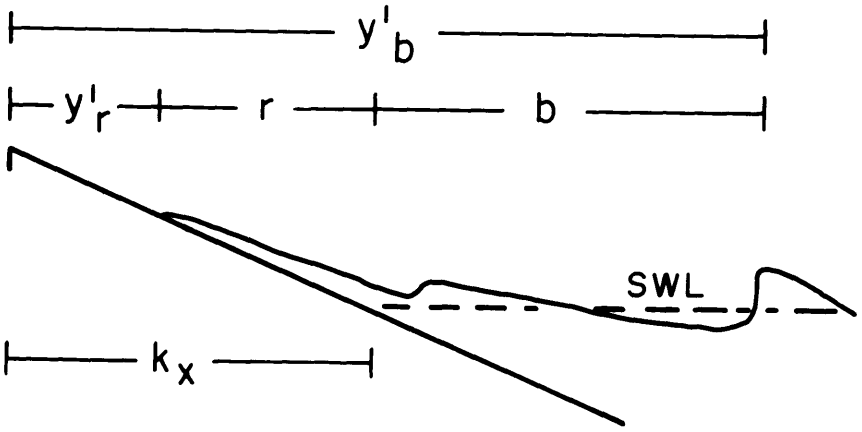

Figure 16. Definitions of Runup Limit (y'_r), Runup Distance, r, Breaker Position (y'_b), Breaker Distance (b), and Position of Still Water Line (k_x).

breaker point and the runup limit. The breaker region is in the offshore segment of the surf zone between the breaker point and the point where the breaking wave re-forms as the runup bore. The runup region is the inshore segment of the surf zone between the point at which the runup bore forms and the runup limit.

The subscript $_b$ refers to quantities measured at the breaker position, the subscript $_d$ refers to quantities measured on the flat, off-beach portion of the basin, and the subscript $_o$ refers to hypothetical deep water quantities obtained from small amplitude theory.

5.2 Wave Height, Shape, and Speed (Type A Data)

Wave height. The resistance wave gage was used to measure wave height at breaking (H_b) and envelopes of wave height through the surf zone; to test the uniformity of wave height conditions over the basin; to measure reflection from the beach; and to establish the wave heights which define the test numbers of the experiments.

The increase in wave height on the beach from the offshore value can be computed from small amplitude theory using Tables of Functions for Gravity Waves (Wiegel, 1954). Measured wave heights offshore and at breaking are listed in Table 6 for Series II data. This table points up the differences in wave height along the beach at the breaker point, and shows that small amplitude theory gives the correct order of magnitude of H_b. Part of the scatter may be due to the fact that the wave height

TABLE 6

COMPARISON OF WAVE HEIGHTS AT BREAKING WITH PREDICTED HEIGHTS FROM SMALL AMPLITUDE THEORY

H_b (ft)	measured	theory	measured	theory	measured	theory	H_d (ft)
x (ft)	3		10		17		
	0.121	0.199	0.192	0.187	0.141	0.206	0.143
	0.134	0.173	0.204	0.169	0.083	0.183	0.121
	0.075	0.153	0.157	0.144	0.102	0.147	0.098
	0.154	0.183	0.198	0.172	0.171	0.183	0.130
	0.171	0.214	0.212	0.165	0.171	0.185	0.156

envelope begins to change rapidly near the breaker point, but most of the variation appears due to intrinsic properties of the wave basin. The theory predicts higher waves at either end of the beach and lower waves in the middle of the beach. The differences among H_b measurements are usually greater than the difference between measurement and theory. The larger wave heights at x = 10 are typical of most of the tests.

A contour map of the wave heights in the basin similar to that presented by Savage (1962, Figure 12) showed that for steady state conditions of test III 2, wave height on the flat portion of the basin varied with location about 10 or 15 per cent from a mean value, and that in the shoaling zone near breaking, variation similar to that in Table 6 is present.

Wave height envelopes were made by traversing from offshore of the breaker position to the runup limit. Typical profiles (see Figure 18) reveal a slight increase in wave height through the shoaling zone to a maximum height just before the breaker point, a decrease in height as the breaker plunges, an increase due to the splash-up, and then a steady decrease as the wave moves toward the runup limit. The location of the breaker position just inshore of the maximum height attained on the envelope is to be expected from the way breaker point is defined in this investigation (see Section 4.4).

Heights of successive waves at the breaker position fluctuated randomly about a mean and these fluctuations may be due to random motion of the breaker position. Because the wave gage is stationary, random changes in the breaker position may shift the position of the gage relative to the envelope (see Figure 18) and this motion effects crest elevation most. Such variation may also be explained by reflected waves which, when they are superimposed on the peaked crests, may cause an increase or decrease in crest height, but when superimposed on the long flat troughs, can only change the trough elevation when the phase is such that the reflected wave subtracts from the trough elevation.

Attempts to correlate the height of a wave at breaking with the height of the runup bore formed from this wave after breaking led to the conclusion that no easily demonstrated correlation exists.

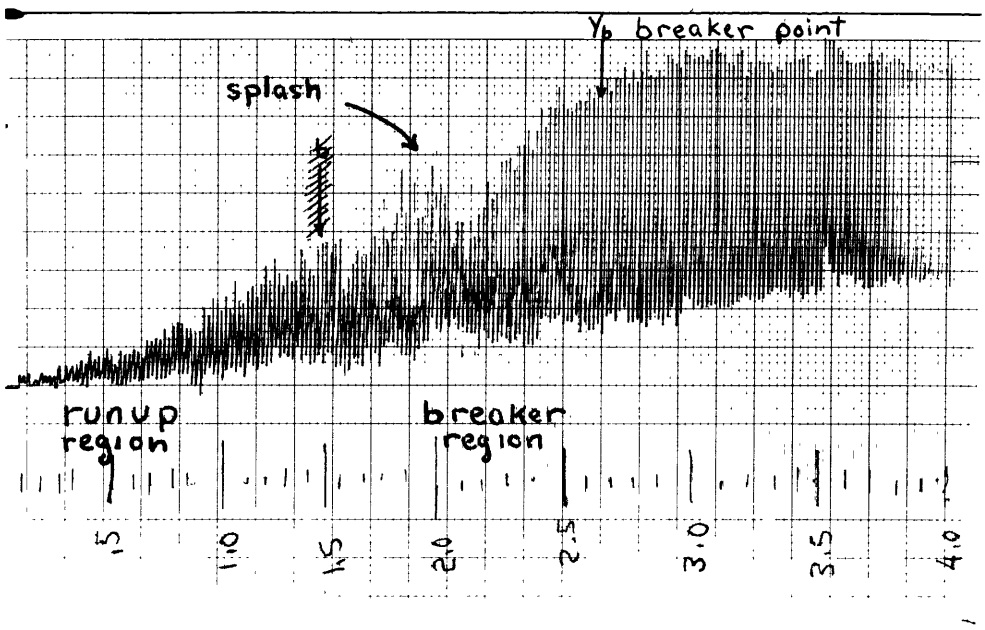

Figure 18. Wave Height Envelope through Surf Zone

In test III 2, reflection coefficient for the beach (defined as the amplitude of the reflected wave divided by the amplitude of the incident wave) was found to be 0.05. The breaker height to depth ratio is discussed in Section 5.6, and the measurement of H_d was discussed in Section 4.7.

Wave shape. Mean water level at a point is the time averaged water surface elevation at that point and wave height H is the difference between the maximum and minimum elevation of that water surface. The shape of the wave, as used here, is the temporal variation of the water surface at a point.

For waves with sinusoidal shape, the mean water level occurs at an elevation above the wave trough of $a_t = 1/2\ H$, but for finite amplitude waves, $a_t < 1/2\ H$ due to the flat troughs. A shape factor, σ, is defined as the ratio a_t/H (see Figure 19) having a maximum value of 0.5.

$$\sigma = \frac{a_t}{H} \tag{4}$$

This ratio is important in computing the total depth from wave crest to beach surface, and also as an indication of the shape of the wave. By graphically averaging the wave shape recorded with wave gage and oscillograph, shape factors were obtained for different positions on the beach (see Table 7). In their field measurements Inman and Quinn, (1951, p. 26) assume, in effect, that $\sigma = 0.25$.

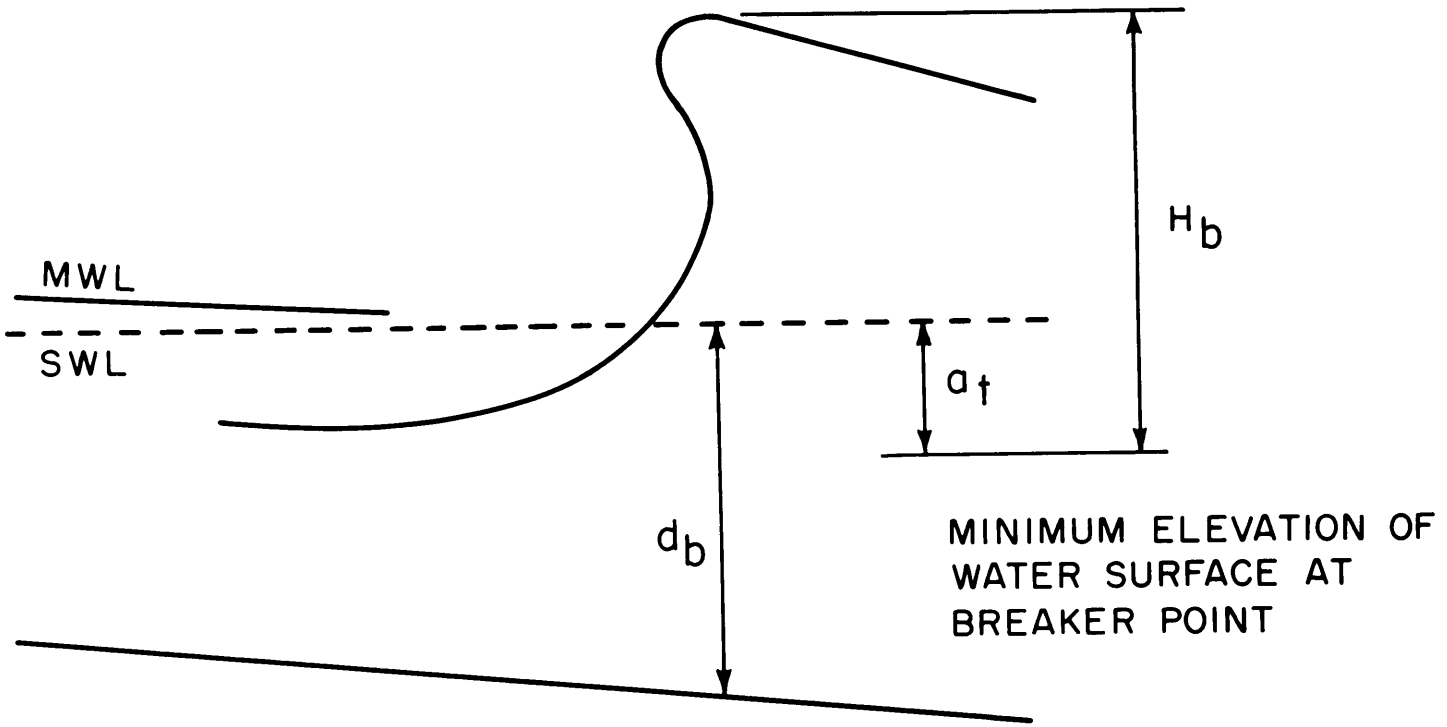

$$\beta \equiv \frac{d_b}{H_b} \qquad \sigma \equiv \frac{a_t}{H_b}$$

Figure 19. Definition of β, Breaker Depth-Breaker Height Ratio, and σ, Wave Shape Factor.

TABLE 7

SHAPE FACTOR VS. POSITION ON BEACH

Test	Position	σ
III 2	several feet offshore of breaker point	0.37 to 0.45
III 2	near the breaker point	0.34, 0.23
II 3	near the breaker point	0.32
III 2	in runup region	0.35 to 0.45

There is some evidence that σ, like H, varies erratically with position on the beach, and even with time, but the data indicate that before approaching the breaker point, shape factor is high, at the breaker point it reaches a minimum, and in the runup region the shape factor is again high. However, the two locations of high σ correspond to different wave shapes. The offshore wave shape is roughly sinusoidal while that in the runup region, as well as the breaker region, is approximately triangular. Wave shape of a wave near breaking did not resemble that of a solitary wave in these experiments, possibly because of the small distance between toe of the beach and the breaker position.

Wave speed. The speed of the wave at breaking, as measured with the pair of wave gages and the oscillograph, changes relatively little as the wave approaches the breaker point. It then decreases to a lower value in the runup region and continues to decrease to the runup limit,

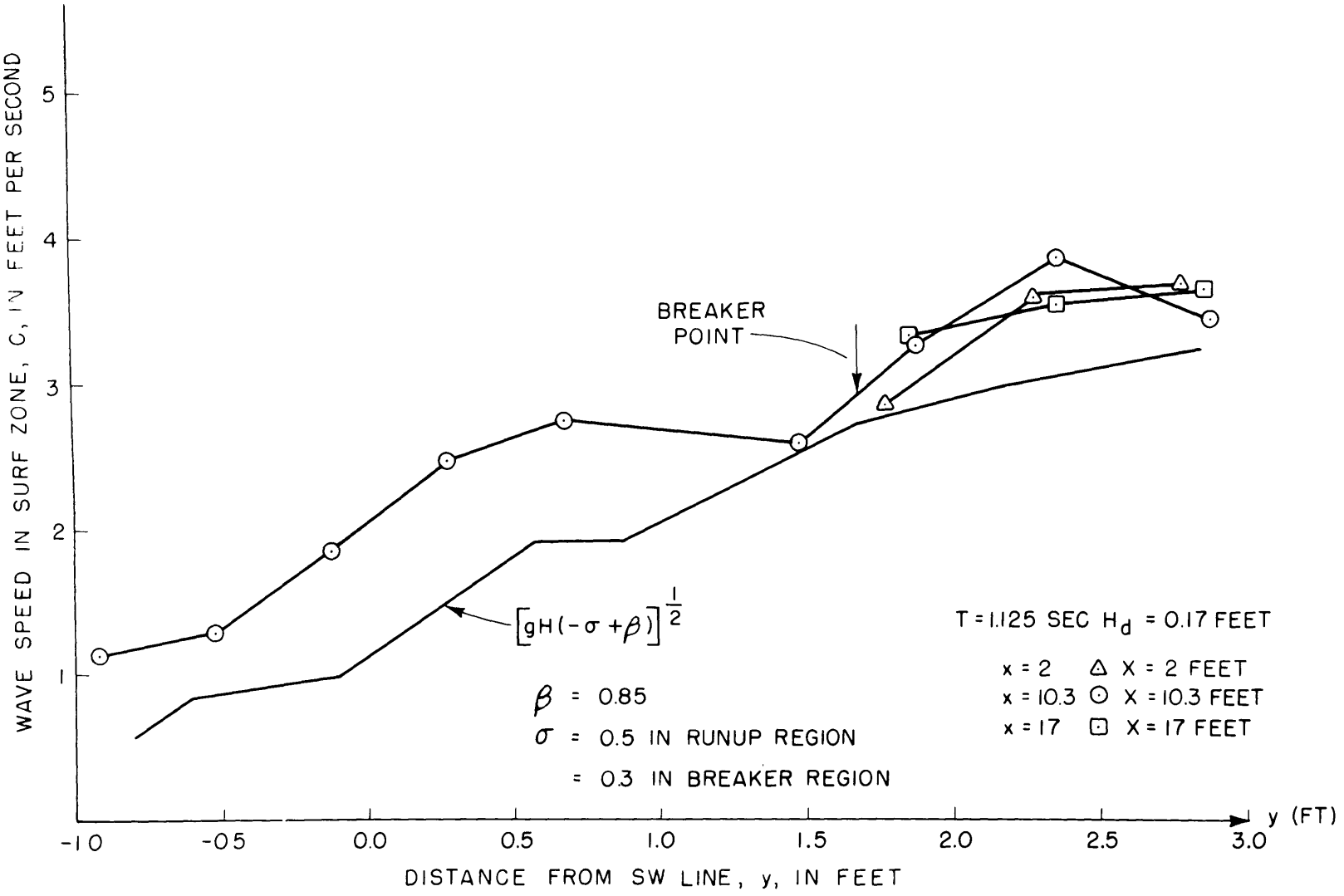

Figure 20. Wave Speed near Breaking and in Runup Region. H measured from Wave Height Envelope.

(see Figure 20). In all cases where profiles of the wave speeds were made through the surf zone, only slight extrapolation of the curve of C versus y is necessary to reach the runup limit, and always the wave speed indicated there by this extrapolation is well above zero (about 1 foot per second or 1/2 to 1/4 of the breaker speed). Because measurements are made nearly to the runup limit, this indicates that the distance over which the runup bore decelerates to zero at the runup limit, is on the order of the gage spacing (0.25 feet) on the laboratory beach.

A wave as such is difficult to define at, and just after, the point at which the plunging crest strikes the water and a wave speed there has little meaning due to the rapid changes in shape with y, although one may be measured from the recordings. When in simultaneous use, the apir of wave gages usually interfered electronically with each other, especially at greater depths of submergence, causing small high frequency oscillations to be superimposed on the recorded wave trace. This effect was almost unnoticeable for the shallow bores in the runup, but was significant when measuring breaker speed. However, most of the uncertainty in wave speed at the breaker point is caused by peculiarities introduced when one of the gages was located too near the point where the plunging crest strikes the water, or by the superposition of small reflected waves. Since each measurement of local wave speed is the average of 20 individual measurements, the effect of shifting breaker position is lessened.

The wave speed at breaking is an important quantity in the analysis of longshore currents, and it is useful to be able to predict it. Figure 21 compares the measured C_b with the wave speed predicted by solitary wave theory and shows that solitary wave theory gives the order of magnitude correctly, but scatters widely for some readings. Several of the divergent readings were remeasured with no significant change in C_b, but it can be noticed that slight irregularities on the recorded wave trace can introduce large errors.

Munk (1949) observes large scatter in the comparison of solitary wave theory with waves on natural beaches, and these data show that this is true of more controlled laboratory conditions as well. As has been observed, it is interesting that solitary wave theory agrees as well as it does with data for asymmetrical breaking waves which travel into water moving with a significant offshore velocity.

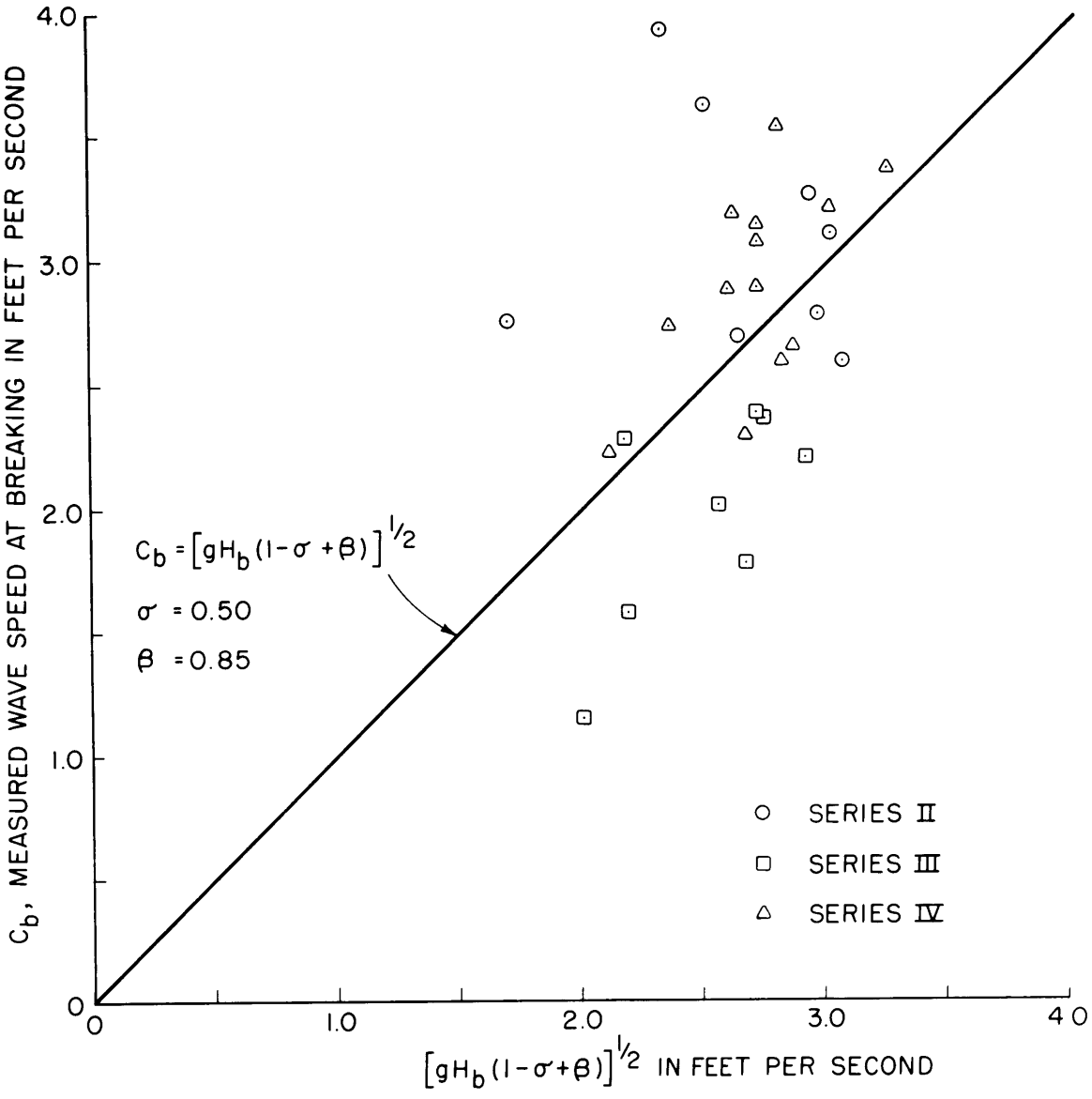

Figure 21. Measured Wave Speed at Breaking Compared with Solitary Wave Theory.

5.3 Breaker and Runup Results (Type B data)

Breaker distance and runup distance are geometrical factors describing the width of the surf zone through which the longshore current flows. In addition, the runup elevation, mr, is a measure of the potential energy stored temporarily in the runup region (see Section 7.2), and the breaker depth d_b = mb is an important variable describing breaker position (see Section 5.4).

The breaker angle Θ_b is among the most important of the variables in this investigation, and probably the most difficult to measure. According to small amplitude theory, the amount that a wave refracts in traveling between two points on a beach is a function of the wave crest angle at the first point, the wave period, and beach slope. In practice, the magnitude of Θ_b depends also on where the breaker point is defined, how plane the beach is, and the observer.

As described in section 4.4, there were consistent differences (on the order of 3 degrees) between the measurements of two observers. By comparing the measured angle of the two observers, separately and as averages, with the theoretical value predicted by small amplitude theory, it was found that the average of the two observed values agreed best with the theory, particularly in series II where the mean angle is small and error is most significant.

Table 8 compares the average observation with the theoretical value. The theoretical value was obtained from Figure 4 of Johnson,

O'Brien, and Isaacs (1948) by entering the graph on the abscissa with d_d/L_o, rising to intersect Θ_d, moving horizontally to d_b/L_o, and reading the angle (Θ_b) there.

TABLE 8

BREAKER ANGLE FROM SMALL AMPLITUDE THEORY AND FROM OBSERVATION

Test No.	Series Θ_b * in degrees	II theory	II observation	III theory	III observation	IV theory	IV observation
2				12.5	14.5	23	29
3		5	5.5			18	15
4		4	4.5	11.5	11	17	19
5		4	5.5	10.5	11.5		
6				10	9		
7				8	6		
8		4	3.5	9	7	15.5	13
9		4.5	4.5	11	8	17	18.5
10		4.5	4.5	11.5	10.5	17.5	21
11		5	5.5	12.5	13.5	17	23
12				8	3.5		
13		4.5	4	11	10.5		

*all measurements at x = 10 feet, and the average of two observers to the nearest half degree.

The observations, which are the averages of 2 readings of each of the two observers, agree well with theory. The agreement is possibly better than should be expected, for finite amplitude effects probably ought

to decrease refraction, thus resulting in observed values of θ_b higher than computed. However, of the 26 observations in Table 8, 12 are greater and 12 are less than the theoretical values.

5.4 Mean Water Level (Type C data)

On a beach bordering a basin of still water, the SWLine marks the upper equilibrium surface of the water mass. On a laboratory beach on which waves are breaking, it is observed that the SWLine is permanently under water and the position of water-beach interface oscillates between the runup limit and a lower elevation which is above the SWLine. The distance over which the interface oscillates is on the order of 1/4 r for the shortest period waves of this study (T = 1.0 seconds) and perhaps r for the longest period waves (T = 1.5 seconds). The water from the bore leaves the runup region by a smooth draining, so that there is no distinctwater-beach interface in the withdrawing part of the cycle.

The mass of water in the runup region has a permanent elevation above the SWL and this elevation represents a conversion of some of the kinetic energy of the breaking wave into potential energy (see Section 7.2).

Piezometer taps located offshore of the SWLine measured the mean elevation of the water above the tap. In the surf zone it is at first surprising that these damped piezometers measure the MWL and not the MWL minus some acceleration head induced by the sudden periodic passage of

the bore. However, there is empirical and theoretical evidence that they do measure only MWL.

Calibrated wave gages were placed in the surf zone before the wave generator was started and the SWL recorded. Then, after running the wave generator for 25 minutes, the bore passing the gage was recorded. By graphical integration of these records and subtracting the recorded SWL, a local value of e was obtained and compared with the average value of e for that y position on the beach. Figure 22 shows the results.

It appears that the piezometer data show a smooth rise in MWL towards the shore, that the MWL at 3 points in the runup region obtained from graphical integration of the oscillograph trace agrees with this piezometer data, and that the wave height envelope is at an elevation indicating a σ between 1/3 and 1/2.

The width of the surf zone in these tests was on the order of 2 or 2.5 feet, the mean depth averaged less than 0.1 feet, and at any one time usually only 1.5 waves occupied this zone. This implies that L/d is about 15, and thus, that conditions approached those of shallow water waves. A measure of the vertical acceleration induced by the passage of a bore is the second time derivative of the water surface elevation at a given position, d^2z/dt^2. Since the damped piezometer measures only the mean effect of the pressure above it (see Section 4.5),

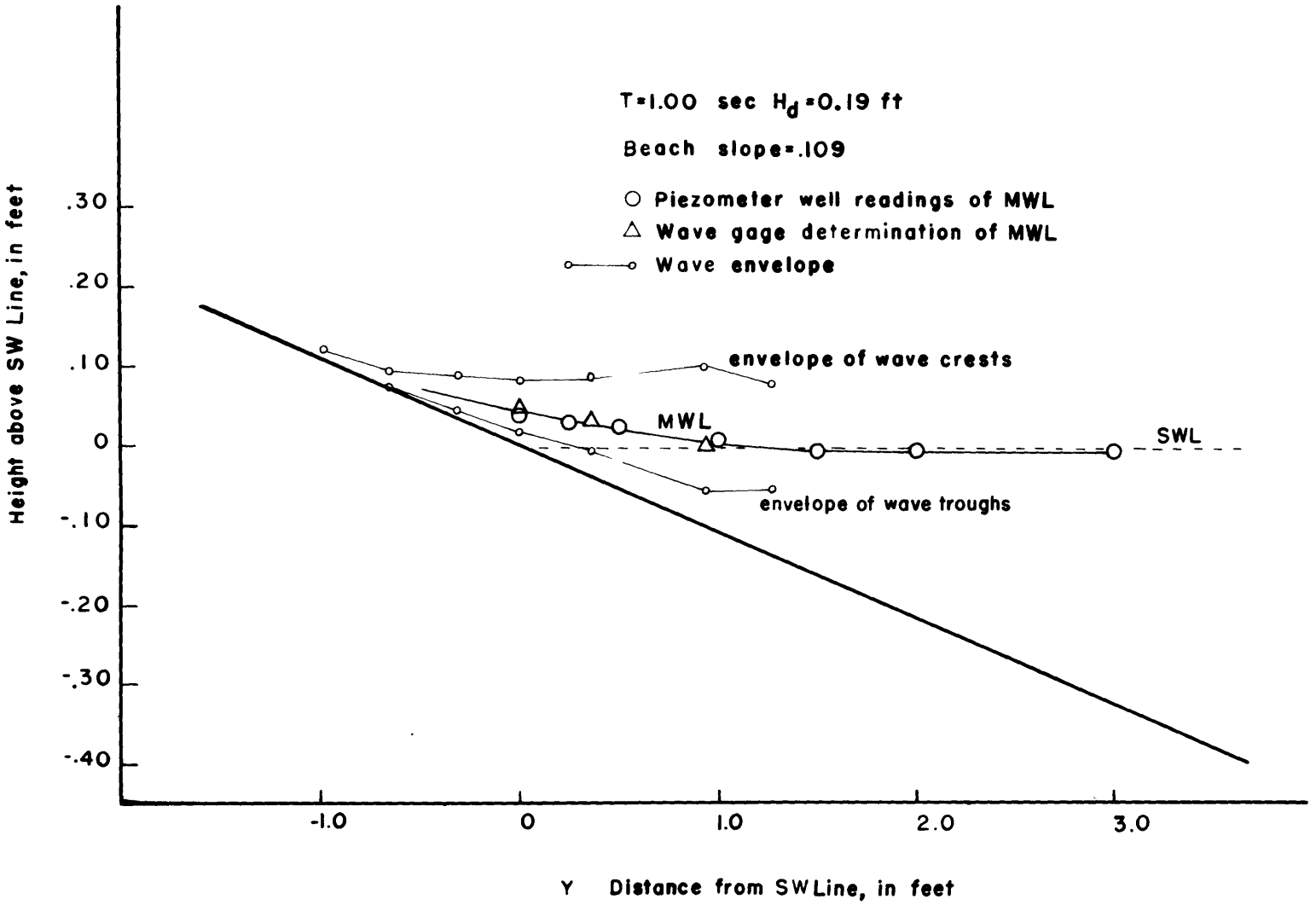

Figure 22. Mean Water Level in Surf Zone from Damped Piezometers and from Graphical Integration of Wave Gage Trace.

a measure of the mean effect of the vertical acceleration felt by the piezometer is

$$\frac{1}{T} \int_0^T \frac{d^2z}{dt^2} \, dt \qquad (5)$$

which, since the bore is periodic, is zero.

A useful rule for computing depth of breaking on this laboratory beach was obtained from analysis of the curves of e versus y. Such curves typically show that e decreases in the offshore direction, becoming zero before the breaker position and very slightly negative at the breaker position. Figure 23 is a histogram of the frequency of e_b magnitudes, where e_b is the difference between MWL and SWL at the breaker point. A mean e_b is about -1mm (0.003 feet) and an average breaking depth is about 0.12 feet; therefore to a good approximation, the breaker depth d_b is the still water depth at the breaker point. For this reason, breaker depth is defined in this report as

$$d_b = mb . \qquad (6)$$

5.5 Longshore Current Velocity (Type D data)

Longshore current velocity is the principal variable of interest in these experiments. The principal empirical conclusions from velocity measurements along the 20 foot test section of the laboratory beach are these:

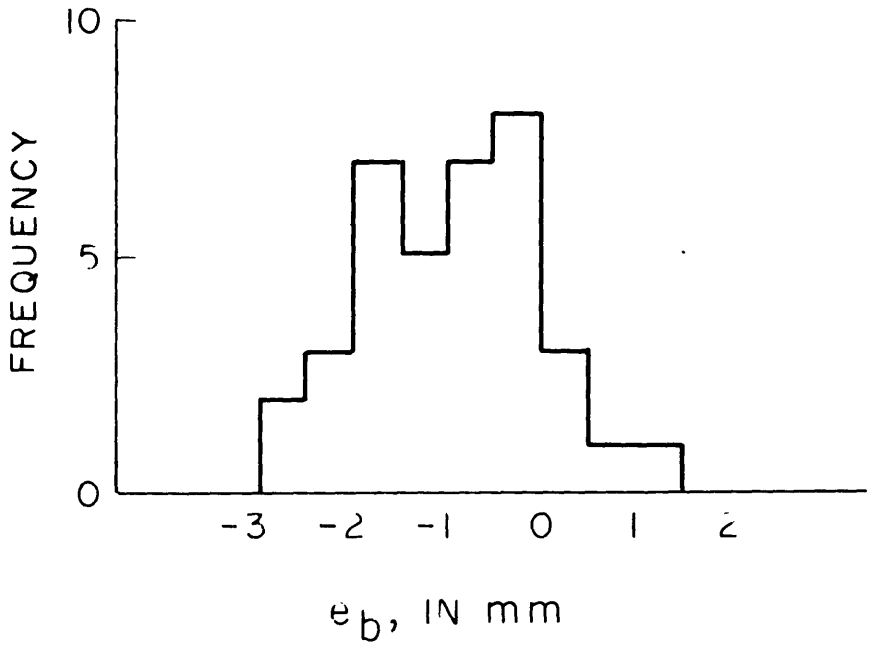

Figure 23. Distribution of Elevation of Mean Water Level at Breaker Position Relative to Still Water Level. Based on Smooth Curves of e versus y, and Measured Breaker Position.

1. Velocity depends on Θ_b, H_b, T, and x.
2. V increases with x (see Figures 26 and 31).
3. At a given x, V increases with Θ_b (see change in velocity for the three calibrations in Figure 14, and the velocity and breaker angle curves of Figure 31).

In the y direction, the maximum measured velocity at a given x occurred most often a few tenths of a foot offshore of the SWLine, and usually drops to a lower value at the breaker point (see Figure 24). Because the velocity probes become exposed over part of the cycle in the runup region, velocity may be higher than indicated there, and since there is much orbital motion in the region offshore of the breaker, velocity is probably less than indicated there. Velocity probe measurements are calibrated against the mean velocity of surface floats approximately in the middle of the surf zone, yet comparison of float and dye velocity indicate that the surface velocities cannot be too far from the mean velocities (see Section 4.6).

Observations of the net particle paths in the shoaling zone were made using dye and paper floats. The observed pattern of the currents is complex and changes with the test conditions. Results of a typical series of observations for bottom, mid-depth, and surface about 1.5 feet offshore of the breaker point are given in Table 9. For test IV 6 there was a noticeable upstream drift at x = 15 and 17 at the same distance offshore.

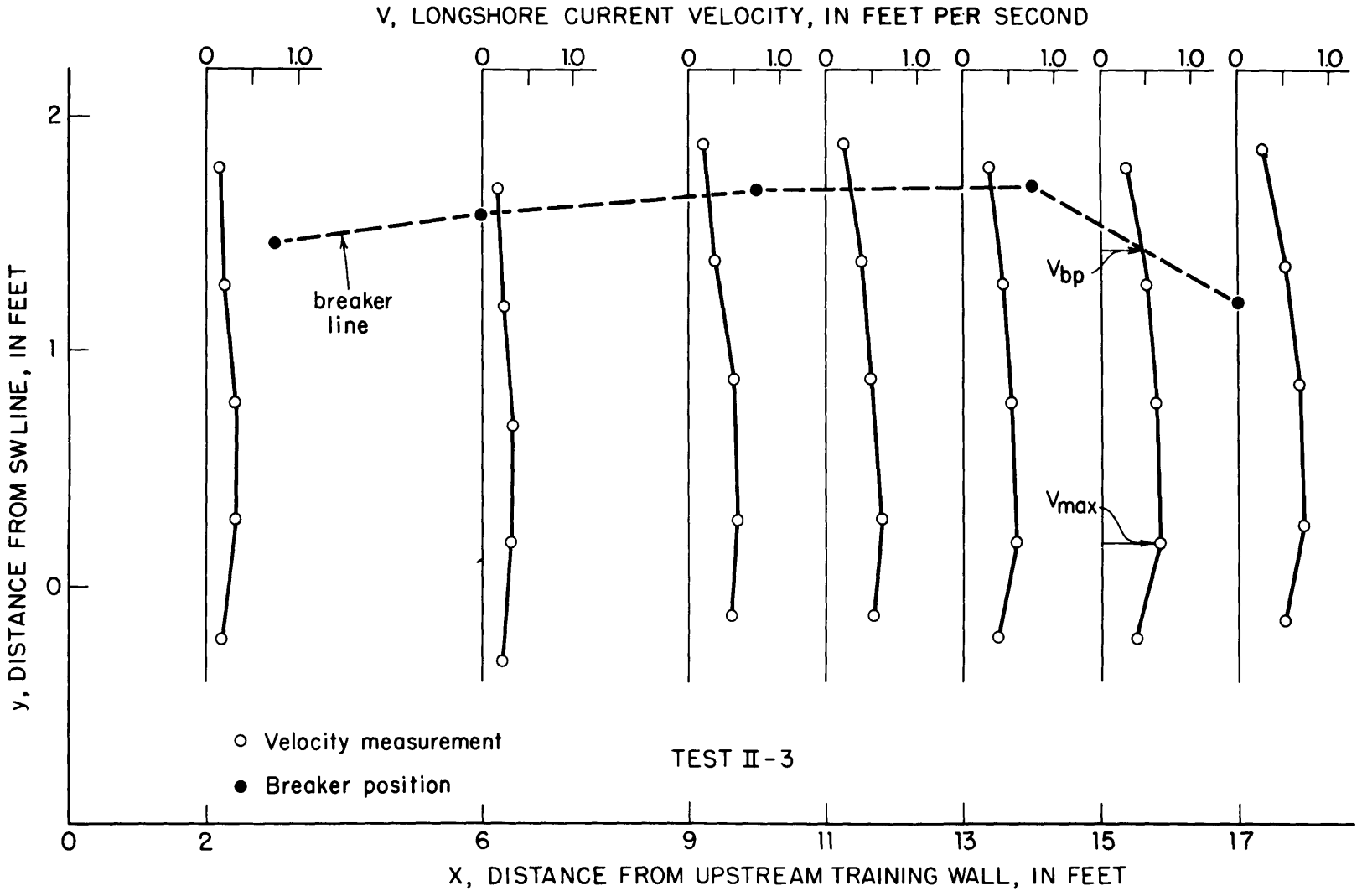

Figure 24. Velocity Distribution in Longshore Current

TABLE 9

NET PARTICLE MOTION IN SHOALING ZONE * (TEST IV 4)

x (ft)	bottom	mid-depth	surface
1	onshore (fast)	onshore (fast)	onshore (fast)
3.5		onshore (very slow)	
5	downstream (slow)		onshore (fast)
8	downstream and offshore (slow)		onshore and downstream (fast)
11	onshore	offshore and downstream	downstream and onshore
15	downstream (no onshore)	slightly offshore	
18	downstream only	downstream only	downstream and slightly onshore

*1.5 ft. offshore of breaker.

Measurements of longshore current velocities (see Figure 31 for examples) always show relatively high initial values, and the qualitative observations of Table 9 support these measurements by showing that, at the upstream end of the beach, fluid is drawn rapidly into the longshore current. After the first initial increase, longshore current velocity grows less rapidly, and the longshore current is supplied mainly from upstream and net transfer across the breaker is reduced. The fluid in the surf zone appears to remain there. There is a notable absence in these observations of strong offshore motion, suggesting that there is no large return flow from the surf zone. The surface velocity in the shoaling zone

shows the most consistent shoreward trend, an observation which supports the idea that fluid which does enter the longshore current is brought there by the breaking wave.

At the downstream end of the beach, some of the fluid, instead of flowing off the test beach in the longshore current, flows offshore along the downstream training wall. This is part of a general counter-clockwise pattern in the test area bounded by the training walls, the plunger and the beach.

5.6 Breaker Height and Depth

Waves break in a depth roughly equal to wave height, and there exist several theoretical criteria demonstrating why this should be so (Miche, 1944; McCowan, 1894). The ratio of the two quantities (mean water depth at the breaker point divided by the wave height at the breaker point, see Figure 19) is defined as β.

$$\beta = \frac{d_b}{H_b} \tag{7}$$

The exact value of β has been the subject of several theoretical, experimental, and field studies, and are summarized here (from Ippen and Kulin, 1955). It is obvious from published results that there is little agreement among the data. It is interesting that the oscillatory waves in field and laboratory are closer to the theory for solitary waves than the solitary waves in the laboratory.

TABLE 10

ESTIMATES OF BREAKER DEPTH - BREAKER HEIGHT RATIOS

Reference	Wave type	Slope	β	$1/\beta$
Iverson (lab)	oscillatory	1:50	1.22	0.82
		1:20	1.19	0.84
		1:10	0.97	1.04
Larras (lab)	oscillatory	1:100	1.46	0.68
		1:50	1.34	0.75
		1:11	1.16	0.86
Series II,III, IV, (lab)	oscillatory	1:10	0.85	1.18
Munk field	oscillatory	?	1.33	0.75
Ippen and Kulin (lab)	solitary	1:44	0.83	1.20
McCowan (theory)	solitary	-	1.28	0.78

The data of this investigation are plotted on Figure 25 along with those of Putnam et al. (1949) and Miche's theory. H_b and d_b are normalized by deepwater wave length L_o ($= 5.12\ T^2$). These data can be approximated by a straight line through the origin with a slope indicating $\beta \sim 0.85$. Unlike these experimental results, the data of Putnam et al. (1949) agree well with the theory, indicating that different criteria were used to determine breaker position or breaker depth.

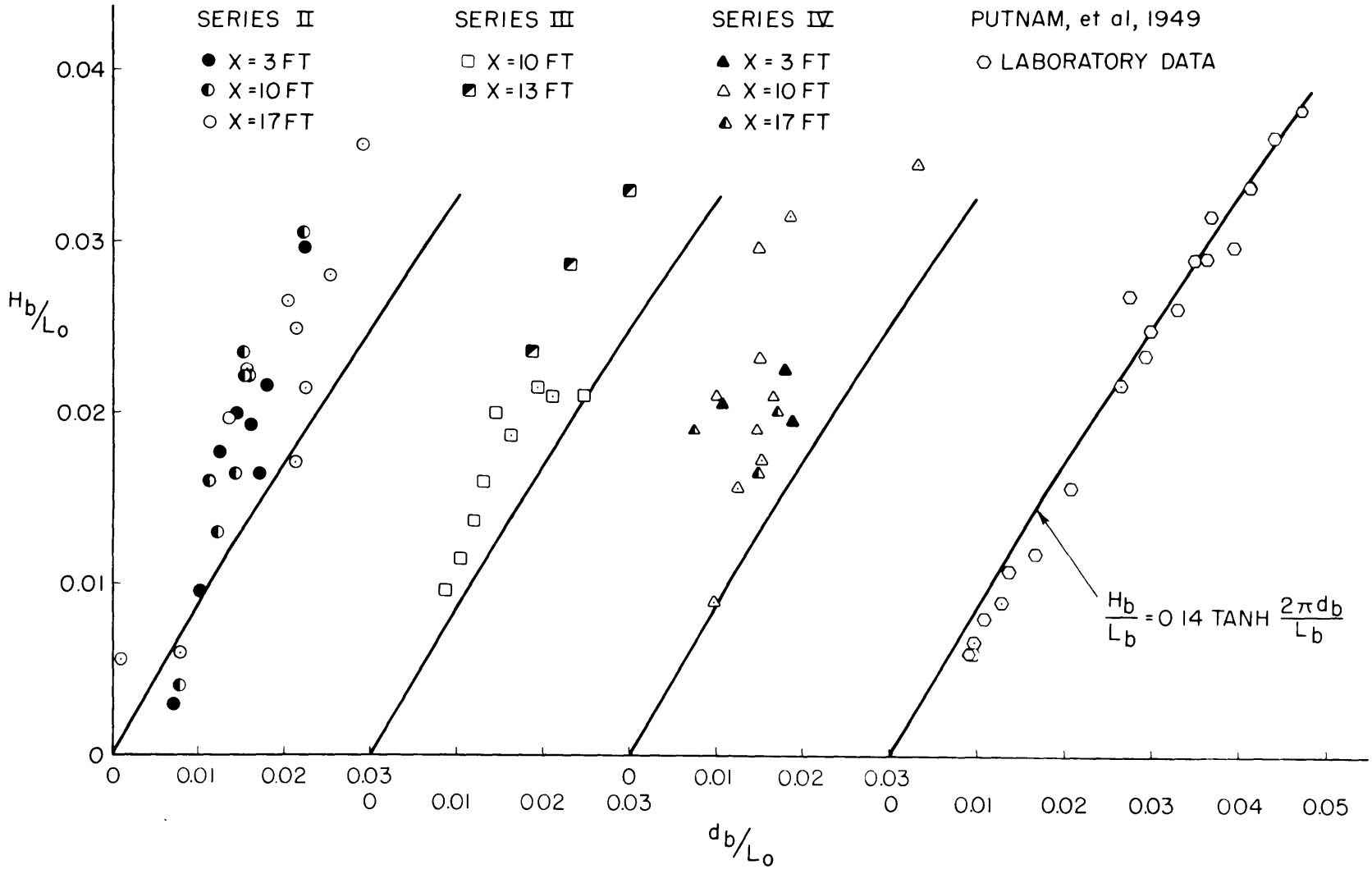

Figure 25. Breaker Height and Breaker Depth. Curve is Miche's Theory.

Part of the problem is the uncertainty in defining mean depth and locating the breaker position, (see Section 4.4). Part of the problem may also lie in the short length of the beach which may not be long enough to permit transformation of the initially sinusoidal wave shape into the solitary wave shape noted in natural conditions by Munk (1949). There appears to be a noticeable variation of β with slope in Table 10, and the observations which come closest to those of this study are those with the most similar slope.

5.7 Non-Uniformity in x

One important result of the laboratory study is the observation that surf conditions are non-uniform in the x direction. The different types of data, considered as a whole, reinforce this interpretation.

Histograms were constructed for each of 5 classes of data showing where the maximum and minimum values of the given variable occurred on the test section of the beach. Figures 26, 27, 28, 29, and 30 each show 6 histograms: the maximum and minimum position of the given variable for all tests in each of the 3 series. In cases where the maximum or minimum occurred at two locations, both were plotted.

Figure 26 shows that velocity maxima occur predominately downstream and the minima upstream for all series. Figure 27 shows that e increases (MWL rises) in the downstream direction also. Series III which does not demonstrate this is based on 3 runs only, and they all for the same test (III 2).

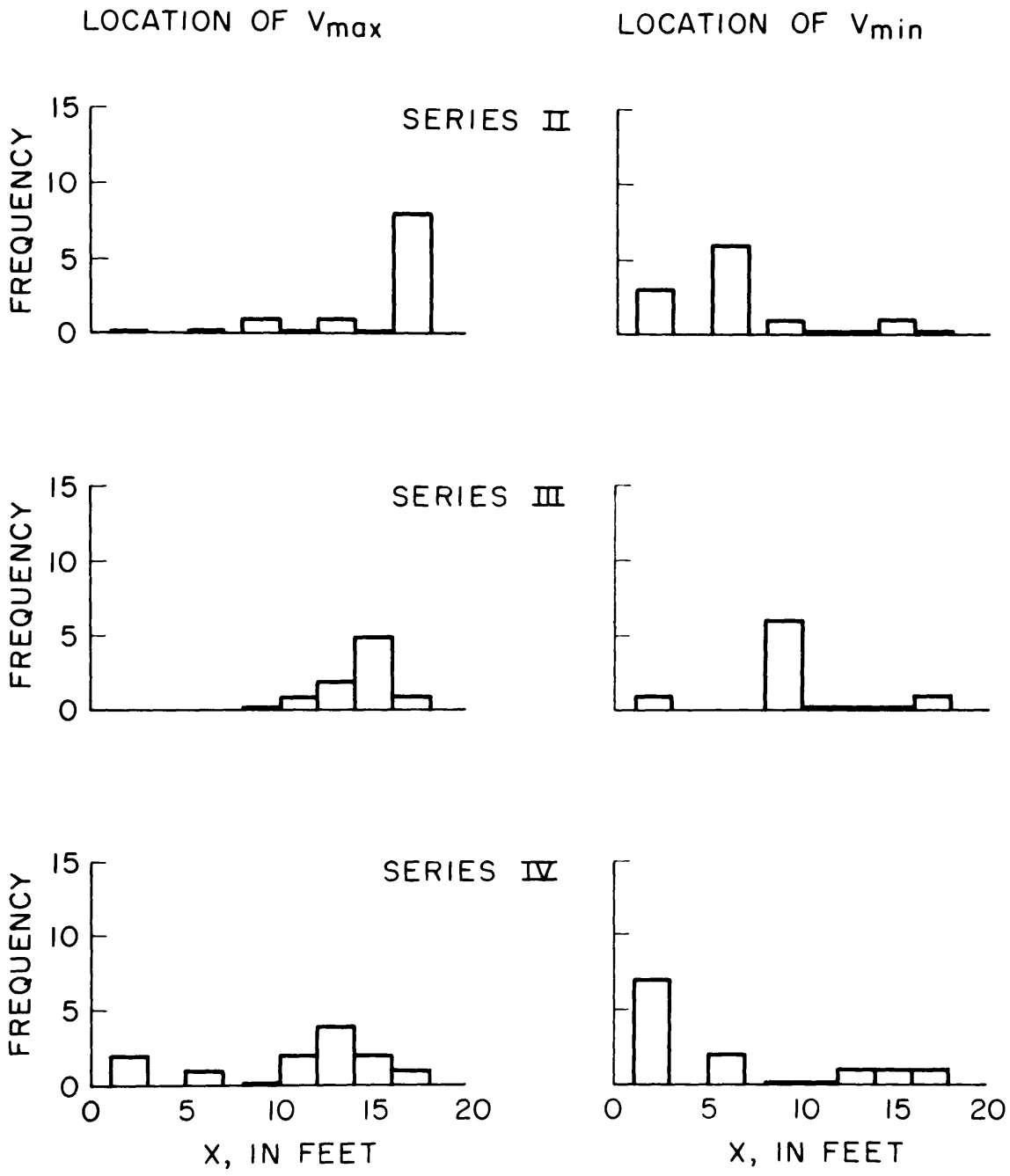

Figure 26. Location of Maximum and Minimum Longshore Current Velocity along Test Beach

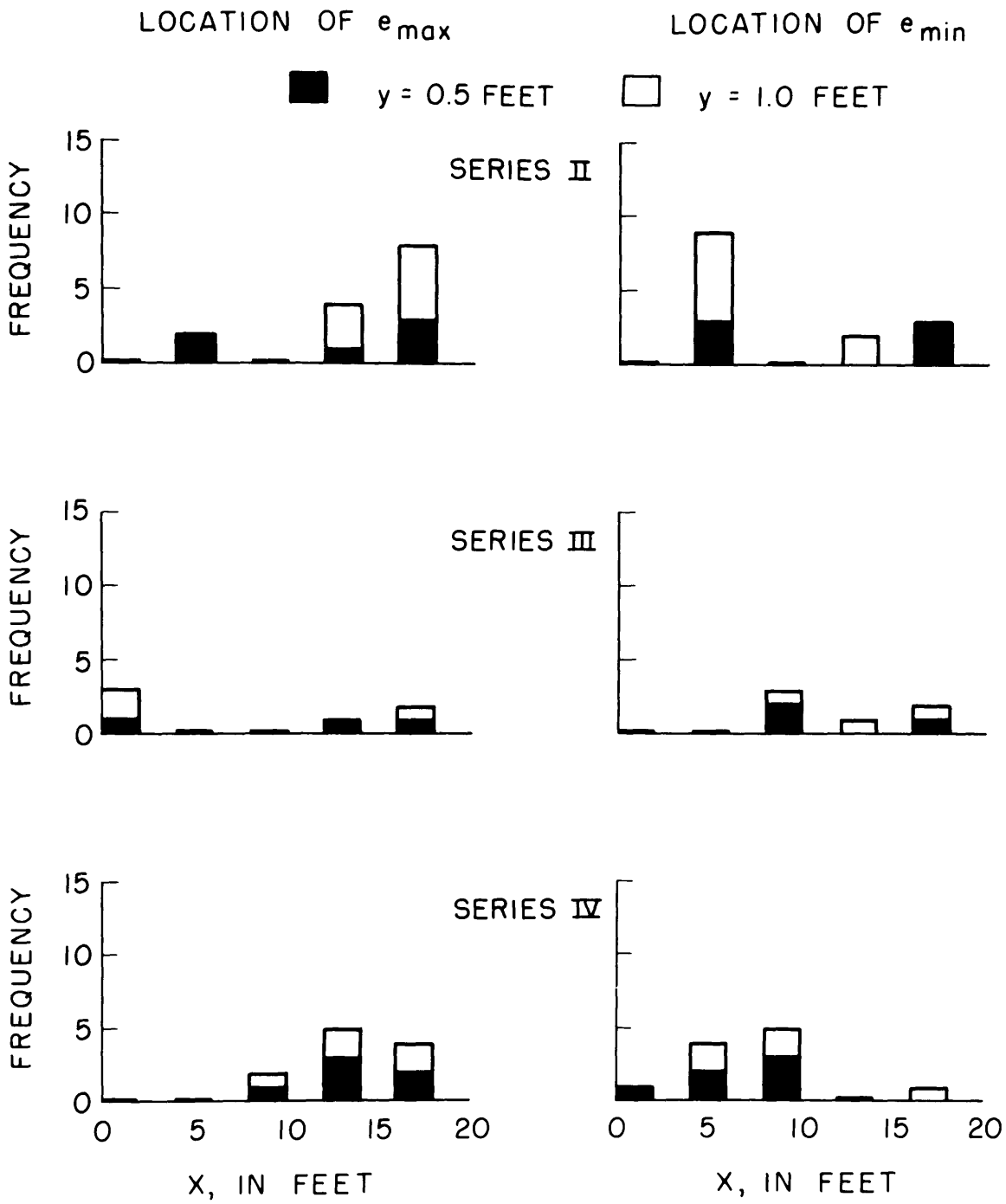

Figure 27. Location of Maximum and Minimum Mean Water Level along Test Beach for Sections 0.5 feet and 1.0 feet Offshore of Still Water Line.

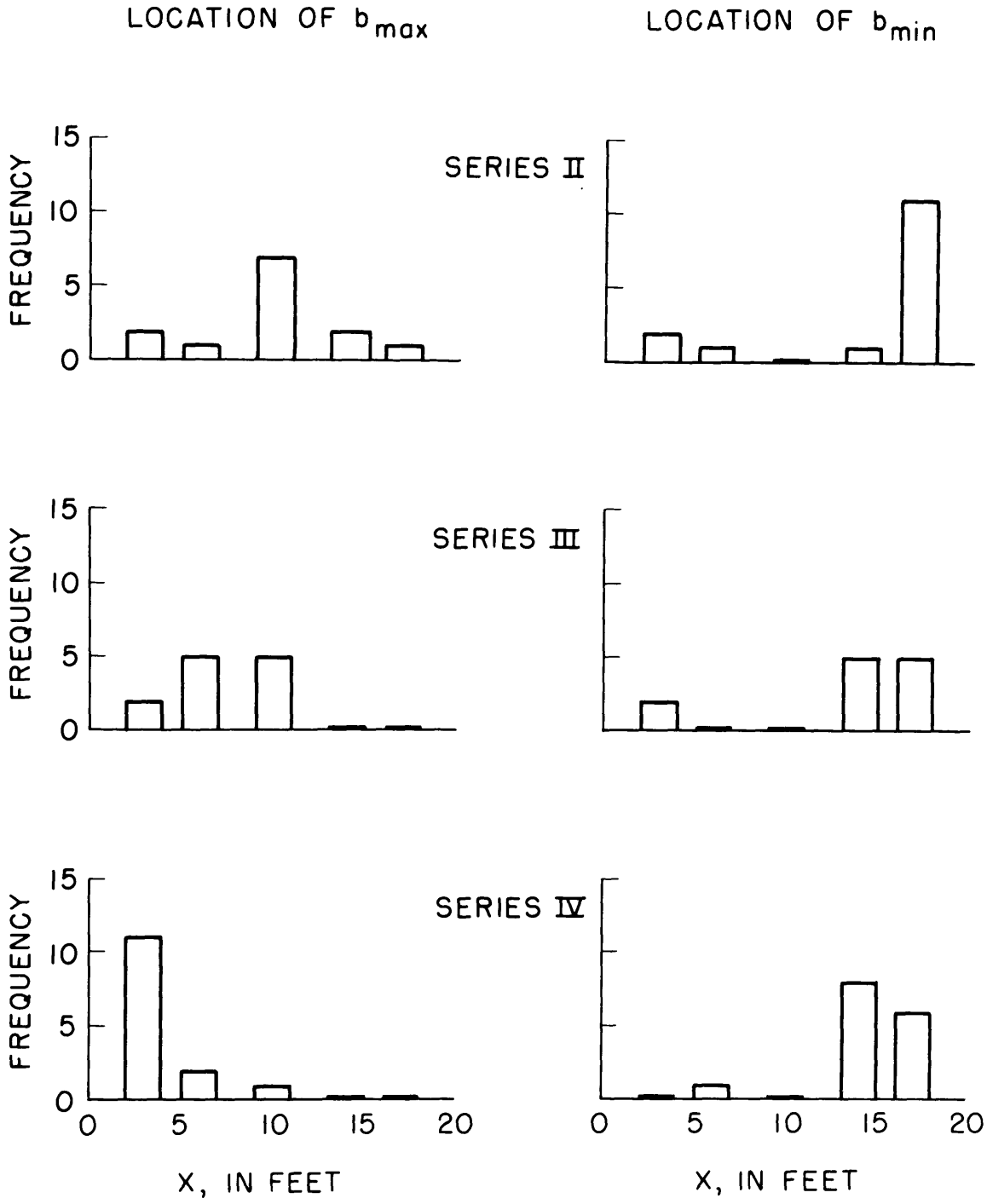

Figure 28. Location of Maximum and Minimum Breaker Distance along Test Beach

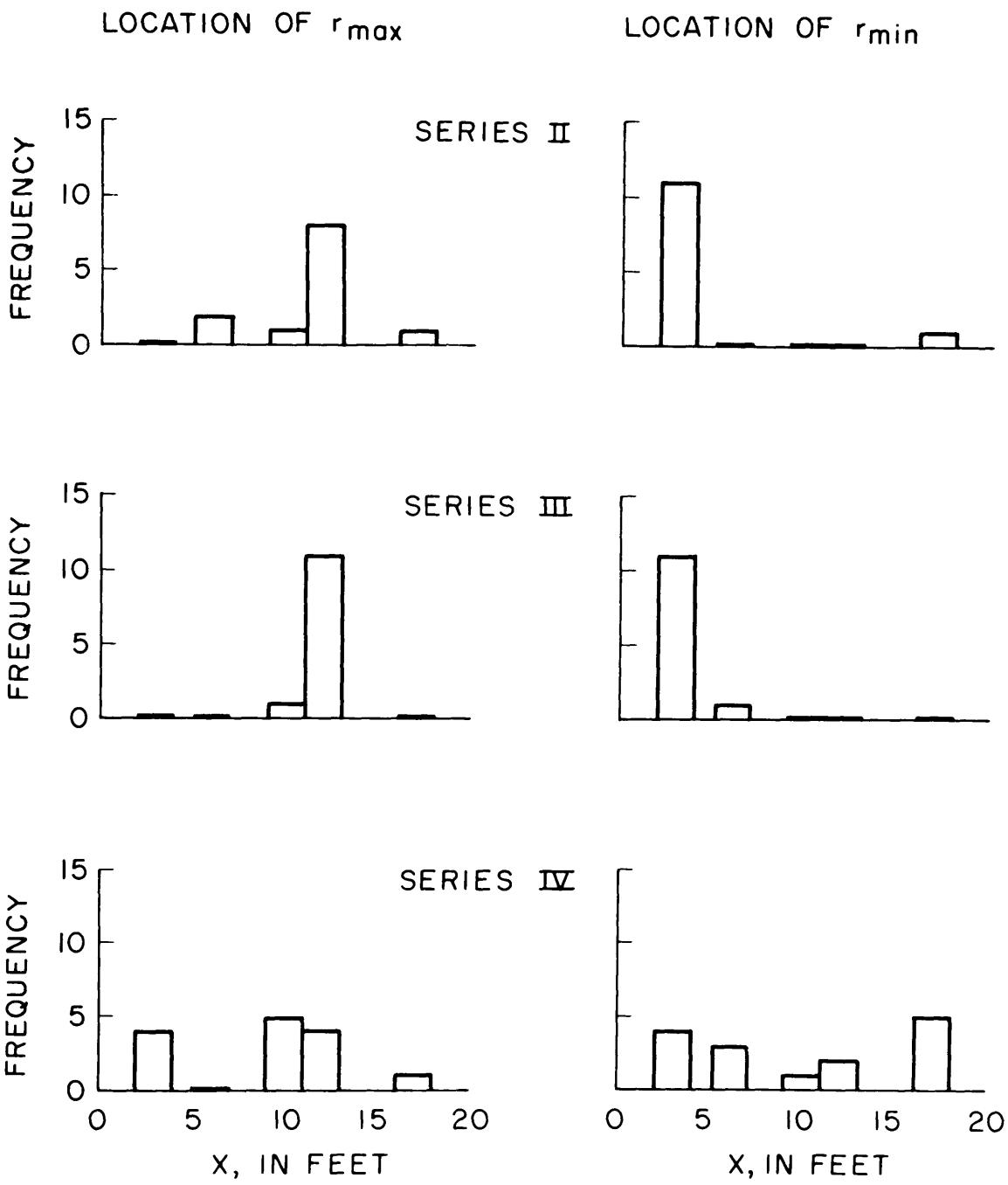

Figure 29. Location of Maximum and Minimum Runup Distance along Test Beach

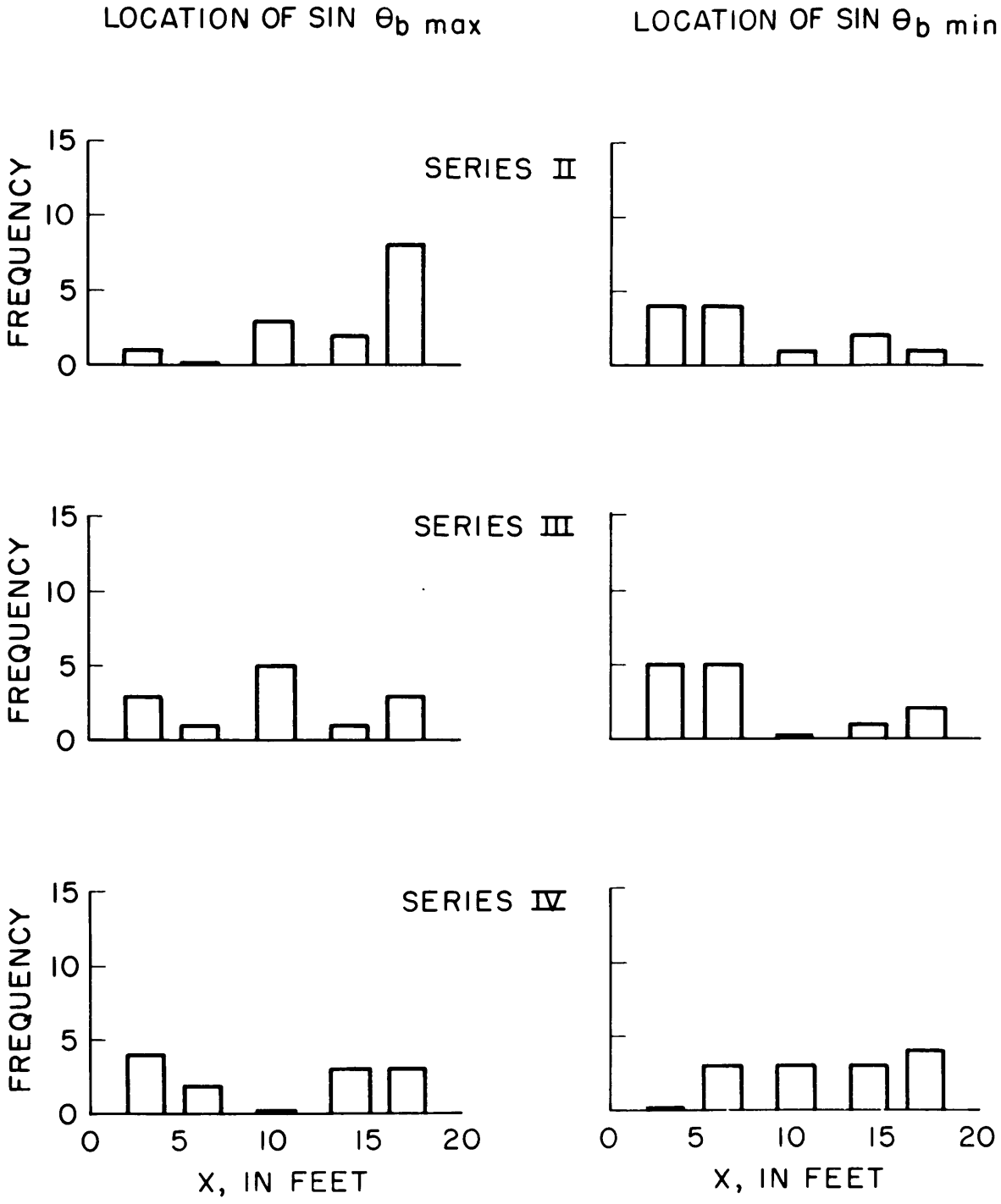

Figure 30. Location of Maximum and Minimum Breaker Angle along Test Beach

Figures 28 and 29 show an inverse correlation between b and r. In general, b is a minimum and r a maximum at the downstream end of the test beach, and the reverse holds at the upstream end.

It appears from these 4 figures that longshore currents carry more fluid with a higher velocity on the downstream end of the beach, and that because water level is raised downstream, the breaker point moves closer to shore and the runup limit moves higher up the beach. If water level is raised at the downstream end of the beach, there should be a local decrease in Θ_b because the waves have a slightly greater distance to refract before breaking. The histograms of Figure 30 present no clear evidence of this. Perhaps diffraction of waves around the end of the downstream training wall diminish this effect, or perhaps the effect is too small to measure.

5.8 Surf Characteristics for Tests II 4, III 4, IV 4

Samples of the data contained in the appendix are plotted in Figure 31 to show the relation of the measured variables in the longshore direction. The three tests are identical except for the plunger angle Θ_d.

The curves illustrate for specific cases the dependence of V and dV/dx on Θ_b, the interrelation between H_b and b (thus d_b) and between b and r, and the increase in e with x.

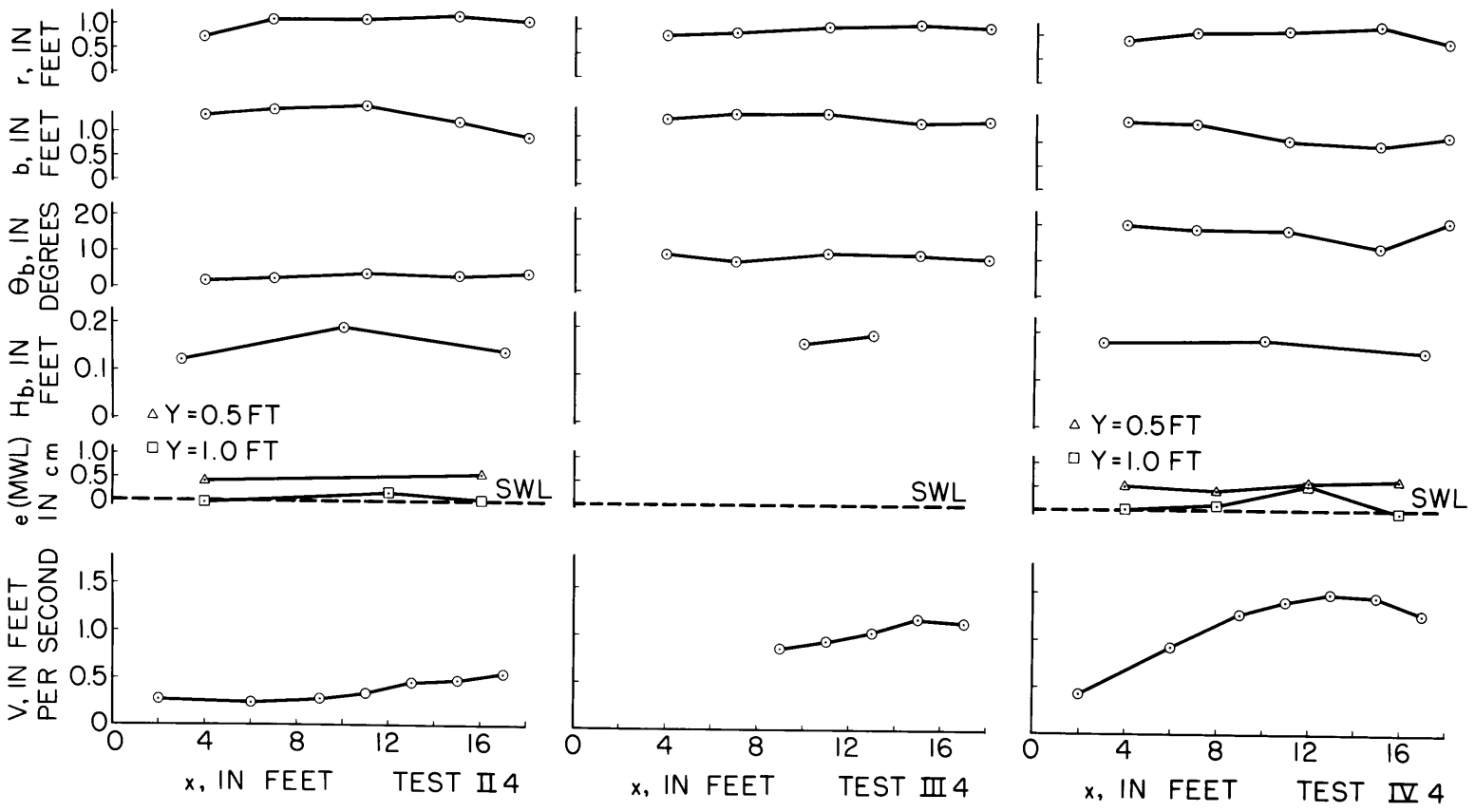

Figure 31. Variation with x for Conditions of Test 4

The variation of V with x and θ_b is typically illustrated in the lower set of curves. V versus x was typically convex upward in Series II, straight in Series III and convex downward in Series IV. V increases markedly with θ_b. The typical increase of e along the beach amounts to a few mm. in 20 feet. As usual, breaker height in the center of the beach is higher than at either end, and the increased height at x = 10 feet is reflected in increased b in Series II and III, but not IV. If there is a constant β, then b should increase if H_b does. The typically minimum values of r at the upstream end of the beach and maximum values at the downstream end are demonstrated in all three tests. The increase effect on b is also present but less clear, perhaps due to the variation in H_b.

5.9 Summary of Experimental Results

Measurements were made of wave height, shape, and speed; breaker and runup distances and breaker angle; change in MWL; longshore current velocity.

Principal experimental results include:

(1) wave speed is approximately described by solitary wave theory; $C_b = [g H_b (1 - \sigma + \beta)]^{1/2}$. (7a)

(2) MWL lies about 3/10 H_b above trough elevation for waves near breaking; $\sigma = 0.3$.

(3) MWL and SWL approximately coincide at the breaker position; $d_b = m\,b$.

(4) For these experiments $\beta = \frac{d_b}{H_b} = 0.85$.

(5) Measured breaker angle θ_b agrees with that predicted by small amplitude theory.

(6) Longshore current velocity increases significantly downstream, MWL increases slightly downstream; locations of maximum and minimum r are consistent with this change in MWL.

The experiments appear to justify most of the techniques used, particularly the measurement of MWL with damped piezometer, and visual measurement of breaker position and angle. The measurement of C_b needs to be refined.

6. QUALITATIVE ANALYSIS OF LONGSHORE CURRENTS

Longshore currents exist primarily amid the complex fluid motion which results when a wave moves onto a beach. In the shoaling zone offshore of the breaker point, wave motion approximates that predicted by the linear theory of small amplitude waves, and in the surf zone onshore of the breaker point, wave motion is of the kind approximated by the nonlinear theory of shallow water waves. Between these two regions is the controlling phenomenon of the breaking wave, for which there is, as yet, no adequate analytical description. To establish what is important in determining the motion of longshore currents, this section will summarize observations, experiments, and theory of waves on plane beaches as they relate to the formation of longshore currents.

6.1 Shoaling Zone

Waves moving onto a beach undergo transformations in height, speed, and direction. It has been shown experimentally (Eagleson, 1956; Wiegel, 1950) that the transformations in wave height and speed are adequately described by small amplitude theory up to a point close to where the wave breaks, and engineering experience (Dunham, 1951) indicates that the transformation in direction is also given to a good approximation by this theory. Throughout this motion, wave period remains constant.

As a consequence of the depth dependence of wave motion, waves moving onto a plane beach tend, by refraction, toward a propagation

direction normal to the shoreline of the beach. According to small amplitude theory, the amount of refraction is determined by wave direction in deep water, wave period, and beach slope. The total refraction, however derived, together with the wave height, determines the breaker angle θ_b. This angle, the direction of wave propagation at breaking, is critical in fixing the magnitude of the momentum flux available to drive the longshore current.

In addition to influencing wave direction, shoaling depths influence the wave form in three important aspects: (1) the wave length, or equivalently, the wave speed, is shortened, (2) wave height at first decreases slightly and then increases to the point of breaking, and (3) wave shape becomes doubly asymmetrical. The change in wave length and height is predicted by small amplitude theory and the predictions, which neglect reflection and dissipation, are approximately verified by experiment, even where finite amplitude invalidates the theory (Eagleson, 1956). There are two asymmetries in shape: one about the mean water level due to high peaked crests and shallow long troughs, and a second about a vertical axis due to steepening of the wave front and flattening of the wave back.

The change in wave form reflects the change in water particle motion within the wave. The particle paths, originally circular in deep water, become elliptical as the depth decreases, the minor axis of the ellipse gradually shrinking until in truly shallow water conditions the ellipse approximates a straight line. These simple paths, predicted by

small amplitude theory, have superimposed on them a net particle motion toward the shoreline due to the finite amplitude of the waves, so that the observed particle paths do not close on themselves after one orbit but are displaced toward the shoreline. With decreasing depths, the net particle velocities increase due to increasing wave asymmetry. This mass transported shoreward must be balanced by a return flow, or by flow along the beach in the longshore direction.

In summary, shoaling transforms a symmetrical deep water wave moving in one direction into a steeper, slower, asymmetrical wave usually moving in a somewhat different direction. The particle paths are deformed from nearly closed circles, in which vertical and horizontal displacements are approximately equal, to open ellipses in which vertical motion is negligible over all but a small part of the wave cycle.

6.2 Breaking Zone

As a wave on a beach moves into water whose mean depth roughly equals the wave height, the wave form, which has progressively deformed as the depth shoaled, becomes unstable and the discontinuity known as breaking occurs. The continuous spectrum of breaking wave forms are classified into surging, plunging, or spilling breakers (Ippen and Kulin, 1955). Only plunging breakers are treated here.

As the wave approaches the breaker point, water particle velocity at the crest increases relative to that lower in the wave. The crest

thus overtakes the lower part of the wave front resulting in an asymmetrical, steep-faced wave which, in the experiments described above, resembles a triangle more than any other simple shape (see Figure 32).

For waves which break by plunging, a point is reached where the crest of the wave stretches out beyond the retarded base of the wave forming a down-curved fluid sheet that strikes with a splash the water receding from the previous wave. Reaction to this incoming jet produces a second sheet of water which rises from the line along which the crest entered the water, splits into drops and individual jets, and falls again to the water surface. The plunge and splash-up is indicated on wave height envelopes through the breaker zone (see Figure 18). Accompanying these jets are the irregular turbulent motion in the main mass of water following the plunging crest, and the creation of air bubbles, splashed droplets, and noise - all of which indicate energy dissipation.

The details of this phenomenon have been observed on a laboratory beach and in part on photographs of plunging ocean waves. The exact ratio of mean depth to height at breaking, as discussed in Section 5.6, appears to depend on slope, wave period, the definition of the breaker point, and the observer.

6.3 Surf Zone

In addition to the splashup, the plunging crest and the main mass of the wave impulsively generate a distinct, steep-faced bore

Figure 32. Shape of Shoaling Wave near Breaking

(see Figure 7) which surges with diminishing height and speed across the surf zone to the limit of the runup region. As discussed in Section 5.2, the speed and height of the bore in the runup zone is lower and changes more rapidly than the speed and height of the wave before breaking (see Figure 20). The mean water level on which this bore travels rises from its intersection with the still water level, typically just shoreward of the breaker point in these experiments, to the runup limit where it intersects the beach surface (see Figures 22 and 33).

After a wave reaches the runup limit, the water drains back to meet the next bore advancing through the runup region. On the laboratory beach, this runback may form a reflected wave visible in low angle lighting which travels across the breaker point and into the offshore zone of the beach.

At present, a theory for bores on a beach based on shallow water wave equations is evolving (Ho and Meyer, 1962; Keller, Levine, and Whitham, 1960), but is apparently not yet entirely applicable to this problem, although one result is utilized in the order of magnitude analysis of the next section.

6.4 Longshore Currents

In many cases, the wave which moves across the surf zone is superimposed on a longshore current which moves parallel to the shoreline. The channel in which this current flows is bounded on the shoreward side by

the runup limit, on the bottom by the beach, and on the offshore side approximately by the breaker line.

The mean horizontal velocity distribution, as measuredin the laboratory, varied across the channel section in the y direction. On natural beaches, non-uniformity has been observed by some (Shepard, 1950), but not by others (Putnam, et al., 1949). The vertical variation on the laboratory beach was difficult to measure due to the shallow depths, but was found to be uniform to a good approximation on natural beaches (Inman and Quinn, 1951). The mean vertical velocity distribution in the current is necessarily limited by the geometry which fixes the depth on the order of a twentieth of the width.

The mean horizontal velocity near the bottom of the channel has an offshore (y) component of motion as shown by dye tests in the laboratory and measurement of neutrally buoyant floats in the field (Inman and Quinn, 1951). Such motion near the bottom is to be expected because there the pressure gradient of the setup has a more marked effect on the fluid whose kinetic energy is lowered by bottom shear. A compensating shoreward flow higher in the vertical section was observed using floats in the field (Inman and Quinn, 1951) and using dye in the runup region of the surf zone on the laboratory beach. This implies a circulation in the runup region: shoreward motion at the surface, seaward at the bottom, and probably rising motion at the breaker.

The important fact about the mean y velocity is that it is small. This smallness is also suggested by the fact that floats used to measure longshore current velocity stay in the longshore current.

The longshore current velocity, that is, the mean horizontal velocity in the x direction as measured along the 20 foot laboratory beach, usually increases with x (see Figure 31, and Table A 7 in Appendix) and at a given x, usually attains a maximum just offshore of the SWLine and decreases from there towards the breaker point (see Figure 24). Offshore of the breaker point, the x velocity drops rapidly, even becoming negative in some dye tests (see Section 5.5) and field observations (Shepard, 1950).

The trajectories, and thus the instantaneous velocity, of water particles in the longshore current have marked periodic fluctuation. In the vertical direction, a surface water particle in the longshore current rises abruptly as the runup wave passes, and then falls slowly to its original position. Particle trajectories have large y displacements at the shoreward edge of the longshore current channel, due to excursions and withdrawals of the runup. Minimum, but still substantial, periodic y displacements occur in the center of the channel, midway between the breaker point and runup limit. Particles on the outer edge of the channel participate in breaking and have an inpulsive-type motion in the y direction, moving suddenly shoreward at breaking, and ebbing slowly seaward once the shortlived breaking phenomena is over.

The path of the particles in the x direction is relatively smooth, although in many of these tests there was a tendency for the water particles, both on the surface and at depth, to leak seaward through the breaker line at the downstream (large x) section of the test beach. In no case was the water particle motion in the x-direction ever observed to reverse sign over any part of the wave cycle.

6.5 Qualitative Analysis

From this description of the longshore current, and from the experimental results of the preceding chapter, there emerges a qualitative understanding of the energy budget of longshore currents on a particular beach, and by extension, to other beaches as well.

The breaker, formed largely of fluid withdrawn from the surf zone, contributes mass, momentum, and energy to the surf zone. The mass contribution is a temporary one, being largely withdrawn to form the succeeding breaker. The energy contribution is partly spent in immediate dissipation, but a significant amount remains to form the bore which moves up the beach dissipating some of its kinetic energy by turbulence and bottom friction, and converting most of the remainder into potential energy at the runup limit. This potential energy is entirely dissipated in the runback when the withdrawing fluid meets the next bore. The longshore current is a side effect of this process. Energy not dissipated in the breaker and runup is available to maintain the longshore current.

The shoaling wave at breaking contains fluid particles drawn from the longshore current and moving in the longshore direction. Also, the wave form itself has a longshore component of motion. The mass of the breaking wave has a definite longshore component of motion. Thus, in breaking, the wave incidently adds mass moving with a longshore component, or equivalently, supplies momentum to the longshore current to keep it moving. The resulting current moves fast enough so that shear along the bottom balances the net rate at which momentum is added.

To make this analysis quantitative it is necessary to know how much energy is brought to the breaker zone and how this energy is divided among the various dissipative mechanisms. The next section contains an order of magnitude analysis of the energy budget in the breaker and surf zones for given laboratory conditions. A more detailed explanation should account for the gradual addition of mass and energy to the current which was observed experimentally on this relatively short test beach.

Unless some significant factor has been overlooked in this analysis, longshore currents generated by plunging breakers on other laboratory beaches and on natural beaches should behave in the same general way.

7. ENERGY BUDGET OF TEST III 2

This section attempts an order of magnitude analysis of the energy budget for test III 2 on the laboratory beach. The conditions of this test are outlined in the Appendix and repeated here for reference:

$\theta_d = 27^\circ$ $\quad V_{f_{10}} = 1.57$ ft./sec. $\quad r_{av} = 0.95$ ft.

$H_d = 0.19$ ft. $\quad V_{f_{16}} = 1.76$ ft./sec. $\quad b_{av} = 1.52$ ft.

$T = 1.00$ sec. $\quad m = 0.109$

$d_d = 1.15$ ft.

According to small amplitude theory, the power supplied (P) per unit width of wave crest of height 2a is

$$P = \frac{\gamma a^2}{2} \frac{C}{2} \left(1 + \frac{2Kd}{\sinh 2Kd}\right) \qquad (8)$$

For the conditions of test III 2, waves transmit shoreward 0.85 $\frac{\text{ft.lbs.}}{\text{sec.}}$ per foot of plunger, and this power is delivered to a beach segment that is longer than the plunger by the ratio $1/\cos\theta_d$. Conserving energy, this means that 0.77 $\frac{\text{ft.lbs.}}{\text{sec.}}$ is the power supplied per foot of shoreline. This is the power input from waves (E_w) per foot of beach.

According to the analysis of the preceding section, this incoming power dissipates by the following mechanisms:

1. Breaker dissipation.
2. Runup dissipation.
3. Longshore current bottom friction.
4. Kinetic energy flux off the test beach and offshore of the breaker in the return flow.
5. Reflection and eventual dissipation offshore.

7.1 Breaker Dissipation

Energy lost at breaking is unknown. A crude estimate of its magnitude may be obtained by comparing the wave at breaking with the bore which forms after breaking. From examination of wave envelopes in the surf zone for this test, it appears that bore height is on the order of one half the breaker height. Taking, as a crude approximation, energy proportional to the amplitude squared, this indicates a dissipation right in the breaker region of about 75 per cent.

7.2 Runup Dissipation

Energy dissipated in the runup is also difficult to evaluate. In the steady state it may be assumed that whatever energy enters the runup region in the bore dissipates there within one wave period. Shen and Meyer (1962) showed that the runup limit attained by a simple bore in ideal fluid on a beach represents the conversion to potential energy of the kinetic energy originally in the forward particle motion of the bore when it began to climb the beach. This result suggests a way of calculating runup dissipation. MWL is significantly raised above SWL in the

runup region (see Section 5.4) which means that energy is expended to maintain the mass of water above SWL. The mean position of this mass is the one for which the average rates of frictional and turbulent dissipation in the bore just balance the average rate that energy is supplied through the breaker.

The rate that energy is supplied varies over period T. The average rate of energy dissipation for the maintenance of the runup volume above SWL is

$$E_{pe} = (\text{mean elevation of volume})(\text{volume})(\frac{\text{density}}{\text{period}}) \qquad (9)$$

Limits can be put on E_{pe}. The maximum value is computed from the area under the curve in Figure 33 (based on the average e values measured along the beach) and the assumption that the mean elevation is 1/2 mr.

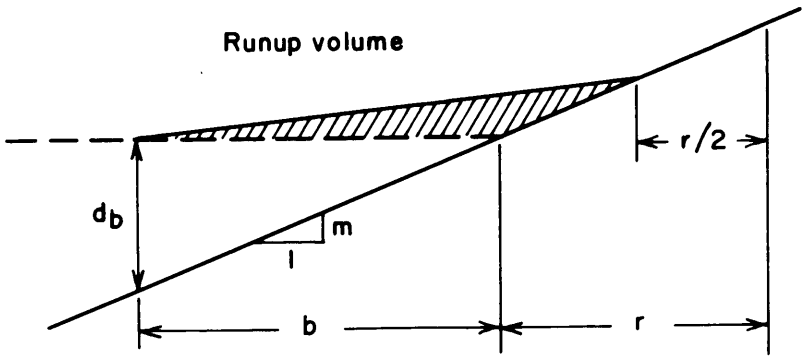

Figure 34. Definition of Runup Volume

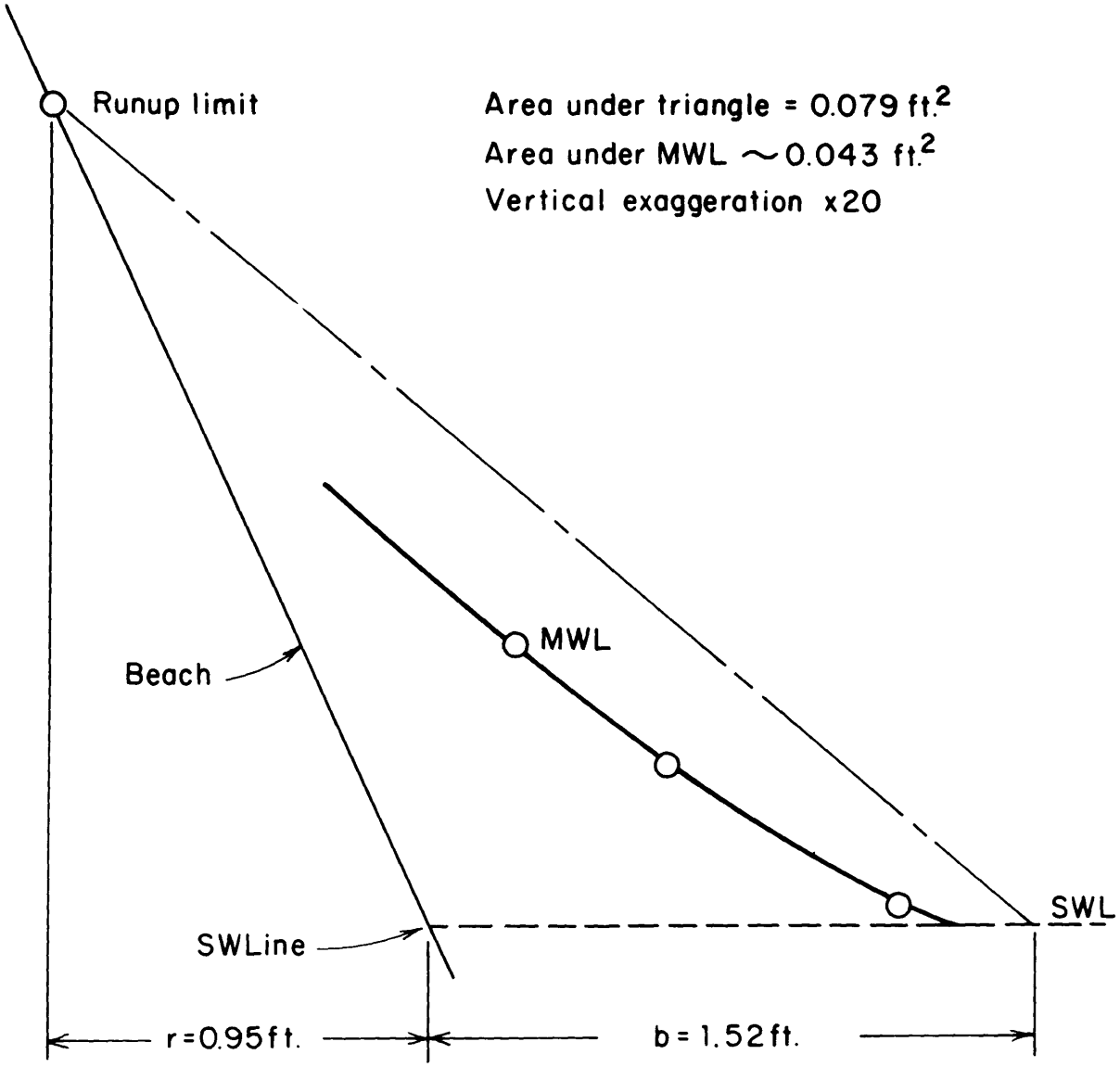

Figure 33. Mean Water Level in Surf Zone for Test III 2

The minimum value is probably the case for the volume in Figure 34 with a mean elevation 1/4 mr.

$$E_{pe} = 0.14 \frac{\text{ft.lb.}}{\text{sec.ft.}} \text{ (maximum)} \qquad (10a)$$

$$= 0.06 \qquad \text{(minimum)} \qquad (10b)$$

7.3 Longshore Current Bottom Friction

In test III 2, $\frac{4R}{k} \sim 330$, $\mathbb{R} = 4 \frac{VR}{\nu} \sim 5 \times 10^4$, giving from the conventional Moody diagram a Darcy-Weisbach friction factor $f \sim 0.026$. ($R = \frac{d_b}{2}$ and a k of 10^{-3} feet for smooth concrete was chosen). Per foot of beach and per pound of fluid flowing, the energy loss due to bottom friction of the longshore current is thus

$$h_f = f \frac{1}{4R} \frac{V^2}{2g} = 0.003 \text{ ft.lbs/lb/ft. of beach} \qquad (11)$$

For the total longshore current this is a rate of dissipation

$$E_f = h_f Q \gamma = 0.05 \text{ ft.lbs/sec/ft. of beach.} \qquad (12)$$

7.4 Kinetic Energy Flux

The kinetic energy flux leaving the test section of the beach is

$$E_{ke} = \frac{\rho}{2} V^3 A \text{ ft.lbs/sec for total beach} \qquad (13a)$$

$$= 0.88 \text{ ft.lbs/sec.} \qquad (13b)$$

Per foot of beach this averages out to 0.04 ft.lbs/sec., but most of the flux was attained in the first few feet of the beach. Energy flux out across the breaker into the shoaling zone is difficult to compute, but probably small (see Section 5.5).

7.5 Reflection

The reflection coefficient (reflected wave height divided by incident wave height) for a 1 on 10 beach is less than 0.1 (Herbich, 1956, p. 43) and was measured once for this beach to be 0.05. Since energy is proportional to the square of the reflection coefficient, energy lost by reflection is less than 0.01 ft.lb/sec per foot of beach.

7.6 Summary of Energy Budget

The following table shows that dissipation in the breaker region is the major, and most uncertain, energy consumer, and that energy

TABLE 11

SUMMARY OF ENERGY BUDGET

	rate of supply $\frac{\text{ft.lbs}}{\text{sec.}}$/ft. of beach	rates of loss $\frac{\text{ft.lbs}}{\text{sec.}}$/ft. of beach
Wave energy	0.77	
Breaker		$\sim$0.58
Runup		0.06 to 0.14
L.S.C. friction		0.05
L.S.C. flux		< 0.04
Reflection		< 0.01
	0.77	$\sim$ 0.74 to 0.82

consumed by flow in the longshore current is a relatively small fraction of the total energy. Comparison of rates of supply and loss also indicates that the analysis is not excessively in error.

7.7 Energy Loss in External Circuit

The test area of the basin is bounded by the plunger, the training walls, and the beach (see Figure 2). The external area of the basin is that part of the basin which is not the test area. The external circuit is the path followed by the fluid in flowing from the test beach to the plunger and back to the test beach through the external area.

Energy is supplied to the test area only by the motion of the 20 foot plunger at a rate of 17.0 ft.lbs/sec. (Section 7.1). Slightly more than 5 per cent of this energy leaves the test beach as the kinetic energy of the longshore current (Section 7.4). This is the energy supplied to the external circuit, and it is augmented by the energy in waves which diffract around the downstream training wall and the potential energy carried out by the longshore current in the runup region. Most of the diffracted energy is dissipated on the beach, and probably most of the potential energy in the runup is lost in immediate dissipation, as it is on the test section of the beach. As a first approximation assume that the kinetic energy flux in the longshore current is the total energy supplied to the external circuit.

The conditions in the test area may be affected by the necessity to supply energy to overcome losses in the external circuit, but the fact that the energy is needed at a rate which is only 5 per cent of the rate at which it is produced suggests that the effect is quite small. To demonstrate that this 5 per cent is sufficient to return the fluid through the external circuit to the plunger, an analysis of possible energy dissipation in the external circuit was made for the conditions of Test III 2.

The current which leaves the test beach continues to flow along the 8 foot stretch of beach downstream of the training wall, spreading out as it flows and diminishing in velocity. At the end of the beach it meets the basin wall, makes a right angle turn, and flows off the beach with a still lower velocity through a larger area. The fluid then moves slowly over a relatively unobstructed path to the plunger and passes under the plunger.

There appear to be four possible mechanisms of energy dissipation: Frictional dissipation in the continuation of the longshore current, head loss due to the right angle turn at the basin wall, frictional loss through the remainder of the external circuit, and head loss at the plunger.

For the given conditions (Section 7.1) the mass flux off the beach is $Q = 0.30$ cubic feet per second, and the velocity head at

x = 10 feet is 0.04 feet. The kinetic energy flux in the longshore current is 0.88 ft.lbs/sec.

Longshore current loss. Frictional dissipation per foot of beach due to the flow of the longshore current on the test beach is 0.05 ft.lbs/sec. It is a conservative assumption that energy is lost at the same rate over the 8 foot section of beach in the external circuit. This means a loss of 0.40 ft.lbs/sec.

Loss due to turn. For right angle turns in smooth pipes, head loss is about 0.2 or 0.3 times velocity head. Assume that the head loss in this case is 1/2 a velocity head and that the velocity head in question is that of x = 10 on the test beach.

$$E_{turn} = h_f Q \gamma \tag{14a}$$

$$= 0.37 \text{ ft.lbs/sec.} \tag{14b}$$

Friction loss after turn. Assume the fluid is concentrated in a channel which is 1 foot deep, 5 feet wide, and 40 feet long in returning to plunger. An appropriate Reynolds number from the given Q, area, and depth is 6×10^3, and assuming smooth flow, f is about 0.036.

$$h_f = f \frac{L}{4R} \frac{V^2}{2g} \tag{15a}$$

$$= 2 \times 10^{-5} \text{ ft.} \tag{15b}$$

$$E_f = h_f Q \gamma \tag{16a}$$

$$= 4 \times 10^{-4} \text{ ft.lbs/sec.} \tag{16b}$$

Flow under plunger. The mean elevation of the base of the 20 foot plunger is 0.40 feet. A head loss of several velocity heads through this varying orifice will result in energy loss less than 10^{-2} ft.lbs/sec.

Summary. This analysis, while uncertain in particulars, demonstrates that the kinetic energy supplied to the external circuit is of the order needed to overcome the losses there. According to the calculations outlined above, energy is supplied at a rate of 0.88 ft.lbs/sec., and dissipated at about that rate, chiefly on the continuation of the beach.

The head loss due to bottom friction over a 40 foot return path is less than 10^{-4} ft.lbs/lb whereas the precision of the piezometers used to measure water level is 3×10^{-3} feet.

It is concluded that external circuit losses must produce an energy gradient on the test beach which is a function of the particular laboratory apparatus used; however, the magnitude of this gradient in the present case is so small as to be negligible. There remains the possibility that the transition between test area and the external area at the downstream training wall may affect conditions on the downstream end of the test beach.

8. EQUATIONS OF MOTION OF LONGSHORE CURRENTS

8.1 Momentum Analysis of Putnam, Munk, and Traylor

Putnam, Munk, and Traylor (1949) published an analysis of the equations of motion for longshore currents based on the following assumptions:

1. A steady uniform state exists for which average longshore current velocity and mass flux and energy flux do not change along the beach.

2. The wave near breaking approximates a solitary wave.

3. At breaking a mass of water enters the surf zone with the propagation velocity of the equivalent solitary wave, and the volume of this mass is that contained above SWL in the crest of the equivalent solitary wave.

Under the first assumption, longshore currents must obey the following rules. The mass thrown into the surf zone by a breaking wave must be withdrawn before the next wave breaks (conservation of mass). The energy not otherwise used up in dissipation, or reflected or carried offshore, is dissipated in the uniform flow of the longshore current (conservation of energy). The flux of momentum into the longshore current in the longshore direction is balanced by the frictional force at the beach and the outward flux of momentum through the breaker line (conservation

of momentum). All of these conclusions follow from the assumption of steady state and a descriptive knowledge of the phenomena.

There are two parts to the analysis. The first is the energy approach which equates the fraction of energy (s) available to longshore currents to the energy consumed by frictional dissipation at the boundaries. Using solitary wave equations, the following relations were derived (in the notation of this report).

$$V = K \left[\frac{m H_b^2}{T} \sin 2\theta_b\right]^{1/3} \tag{17}$$

$$K^3 = 0.87\, g \left(\frac{8s}{f}\right) \tag{18}$$

where s is the ratio (rate of energy dissipation in the longshore current) /(rate of energy supplied at breaking).

The second part of the analysis is the momentum approach. The mass of the breaker added to the longshore current represents a flux of momentum into the current. The longshore component of this flux $(\frac{\text{Mass}}{T} C_b \sin\theta_b)$ is balanced by the frictional force at the solid boundary, and by a flux of momentum carried offshore in the return flow before the arrival of the next wave. This return flow is assumed to have a longshore component of velocity equal to the longshore current velocity V.

By balancing the net flux of momentum against the friction force, the analysis of Putnam, Munk, and Traylor results in

$$V^2 = a\,(C_b \sin \theta_b - V) \tag{19}$$

where

$$a = 2.61\,\frac{\delta_m}{fT}\,H_b \cos \theta_b \tag{20}$$

for solitary wave conditions. This equation can be solved either for friction factor, f, or for velocity, V. It was first solved for f using the measured velocities to obtain an average f for each test beach, and then the average f's were used to predict the velocities, which they did reasonably well.

8.2 Discussion of Momentum Analysis

In this section, the following aspects of the analysis of Putnam, Munk, and Traylor are discussed: the computed values of the friction factor, the computed percentage of the breaker energy dissipated by the longshore currents, the selection of the depth of breaking, and the proper formulation of the momentum approach.

Friction factor. Putnam et al. (p. 344) suggest the possibility that their friction coefficient, k, might be correlated with measured beach and wave characteristics in a manner similar to what has been done for pipe flow. Since the Moody pipe friction diagram is applicable as a first approximation to flow in open channels, and since the analysis treats longshore currents as a uniform open channel flow, existing

diagrams ought to provide an order of magnitude check on the friction factor computed from the analysis. The conventional Moody diagram has Reynolds number and friction factor, f, as coordinates with relative roughness as a parameter. The Darcy-Weisbach f is equivalent to 8k of Putnam, et al. The appropriate length is hydraulic radius which, for these triangular channels, is $1/2\ d_b$.

TABLE 12

FRICTION FACTOR, REYNOLDS NUMBER, AND RELATIVE ROUGHNESS FOR DATA FROM PUTNAM, ET AL. (1949)

Beach	f = 8k	IR	Relative Roughness	Moody f
Field	0.06	$>10^6$	>4000	0.014
Lab smooth concrete	0.06	10^5	1000 - 5000	0.02
Lab smooth concrete	0.32	10^5	500	0.025
Lab 1/4-inch gravel on concrete	3.08	10^5	25	0.07

Table 12 shows the friction factor for the different beaches of Putnam, et al. and order of magnitude values for Reynolds number and relative roughness. The Reynolds number and relative roughness along with the Moody diagram indicate that the values of Putnam, et al. are too high.

Energy distribution. These high values of computed f are probably induced by the analysis which allocates relatively large percentage of

the energy to the longshore current. The predicted energy dissipation by the longshore currents ranges from 0.15 to 0.33 of the total energy supplied by the waves for 3 of the beaches. Ordinarily, for the laboratory beach of this investigation (see Section 7.3), less than 10 per cent of the energy supplied is used by the longshore current.

Depth at breaker. From equation 3 of Putnam, et al., it appears that h is identical with d_b of this report. Therefore, its use as the trough elevation in the solitary wave equations (equations 5 through 8 of Putnam, et al.) is justified only if trough elevation approximates MWL.

For typical conditions of waves on natural beaches, an equation developed by Munk (1949, p. 386)

$$\bar{h} = h \left[1 + \frac{1}{T} \left(\frac{16H}{3g(1+\frac{H}{h})}\right)^{1/2}\right]$$

predicts a difference between trough elevation (h) and MWL ($\bar{h}$) of 5 to 10 per cent. However, some observations on natural beaches imply a greater difference; for example, to obtain wave heights, Inman and Quinn (1951) multiply the height of the wave crest above MWL by 4/3, implying that the difference between h and $\bar{h}$ approaches 25 rather than 5 per cent. In any case, as was shown in Section 5.2, this difference ($\bar{h} - h = a_t$ of this report, see Figure 19) is significant for the laboratory data of this report. For the conditions of these experiments, the elevation of the breaking wave crest above the beach is approximately $H_b (1 - \sigma + \beta)$ instead of $H_b (1 + \beta)$.

Momentum approach. In the derivation of the equations for conservation of momentum, it was assumed that the x-component of momentum flux into the surf zone has a mass moving with velocity $C_b \sin \Theta_b$ (equation 11 of Putnam, et al.) and this velocity is supposed to be larger than V. The mass flux out of the surf zone is assumed to move with an x-component of velocity V (equation 12 of Putnam, et al.). But since each breaking wave is made up primarily of fluid taken from the surf zone, it appears necessary to assume that the water particle in the breaking wave has an x-component of velocity which is better approximated by $V + C_b \sin \Theta_b$. In this case $C_b \sin \Theta_b$ is not necessarily larger than V.

In the analysis of Putnam, et al., the breaking wave will slow the longshore current velocities if $C_b \sin \Theta_b < V$, whereas the above considerations allow $C_b \sin \Theta_b$ to vary irrespective of V. All but one of 34 tests in Series II, III, and IV for which data are available show that $C_b \sin \Theta_b < V$ (see Table 13). For almost all tests, $C_b \sin \Theta_b < \frac{1}{2} V$ and in some cases $< \frac{1}{5} V$. C_b was computed from $(g H_b (1 - \sigma + \beta))^{1/2}$.

However, in this regard, there appears to be a basic difference between this set of data and those of Putnam, et al., for their data show that $C_b \sin \Theta_b$ can be greater than V. This difference might arise from methods of measurement, or in peculiarities of the experimental program. The laboratory data of Putnam, et al. (see Appendix) are characterized by uniformly high values of Θ_b - all greater than 10 degrees and 3 greater than 50 degrees - which makes $\sin \Theta_b$ high. Also, the depths h are greater

TABLE 13

COMPARISON OF $C_b \sin \theta_b$ WITH V

Series	II		III		IV	
Test	$C_b \sin \theta_b$* ft/sec	V** ft/sec	$C_b \sin \theta_b$ ft/sec	V ft/sec	$C_b \sin \theta_b$ ft/sec	V ft/sec
2	0.20	0.83	0.76	1.76	1.40	2.15
3	0.22	0.82	0.65	1.60	1.01	1.89
4	0.15	0.68	0.53	1.61	0.89	1.91
5	0.18	0.53	0.42	1.42	0.79	1.81
6	0.14	0.52	0.30	1.23	0.36	0.91
7	0.07	0.34	0.22	0.56	0.48	0.65
8	0.06	0.50	0.27	0.96	0.58	1.20
9	0.14	0.67	0.40	1.23	0.93	1.57
10	0.14	0.71	0.49	1.49	0.96	1.88
11	0.22	0.84	0.60	1.77	1.10	1.96
12	0.04	0.21	0.14	-	0.20	0.18
13	0.06	0.45	0.41	-	0.82	1.46

*C_b computed from $[g H_b (1 - \sigma + \beta)]^{1/2}$

$\sigma = 0.3$, $\beta = 0.85$, $H_b = \frac{mb}{\beta}$

**V is float velocity at x = 16 feet.

than the depths d_b obtained under comparable conditions in this investigation (compare Putnam, et al., test 15 for which $\beta = 1.33$ to test IV 2 for which $\beta = 0.83$ under similar conditions). With d_b and Θ_b both considerably higher in Putnam, et al. data, it becomes possible to have $C_b \sin \Theta_b > V$.

8.3 Revised Momentum Analysis

In this section a revised momentum equation for the non-uniform flow of longshore currents is presented. The control volume is the same as that used by Putnam, Munk, and Traylor (see Figure 35), but longshore current velocity is assumed to average V over the surf zone and to be V_b at the breaker line. Shear is assumed to be negligible at the fluid interface along the breaker line.

In the non-uniform case, there are 3 momentum fluxes in the x-direction to be balanced by shear on the control surfaces. They are the x-component of momentum flux of the fluid entering the control volume in the breaking wave, the x-component of momentum flux of the fluid leaving across the breaker line, and the net momentum flux of the fluid in the longshore current. The mass flux out across the breaker line is different from the mass flux in across the breaker line by the amount that the mass flux in the longshore current changes in the x-direction. The x-component of the fluid velocity in the breaking wave is $p C_b \sin \Theta_b + V_b$ where p is a constant <1 defined as the average shoreward particle velocity in the breaker divided by C_b. A_w is a cross

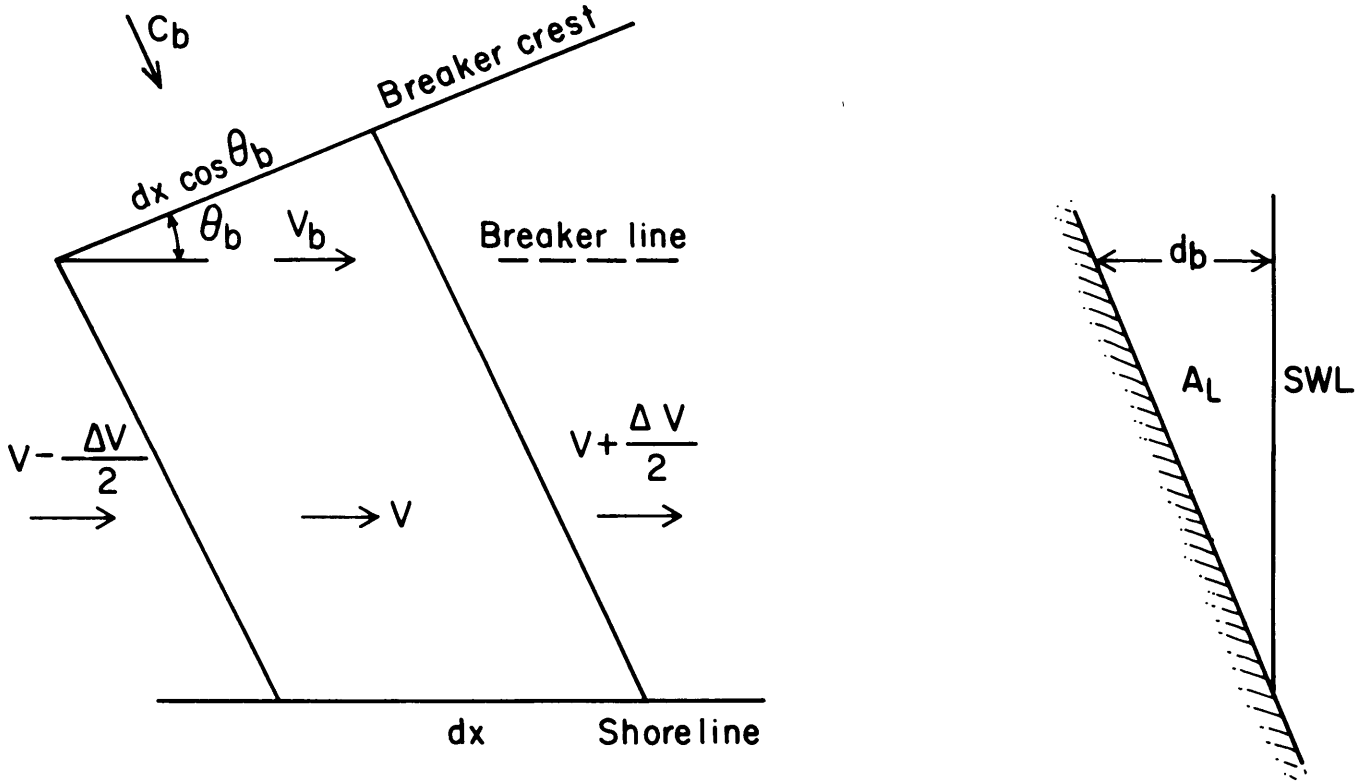

Figure 35. Control Volume for Momentum Equation

sectional area of the fluid in the breaking wave which enters the surf zone.

$$\text{Momentum flux in across breaker line} = \frac{A_w \rho}{T} (V_b + pC_b \sin\theta_b) \cos\theta_b \, dx \qquad (22a)$$

$$\text{Momentum flux out across breaker line} = (\frac{A_w \rho}{T} \cos\theta_b \, dx - A_L \rho dV) V_b \qquad (22b)$$

$$\text{Net Momentum flux of longshore current} = A_L \rho V \, dV \qquad (22c)$$

$$\text{Shear on bottom} = \frac{f}{8} \rho V^2 (b+r) \, dx \qquad (22d)$$

$$\text{Surface forces associated with wave breaking} = S \qquad (22e)$$

By equating the momentum fluxes to the forces, a momentum equation is obtained for the non-uniform flow of longshore currents

$$p C_b \sin 2\theta_b = \frac{f}{4} \frac{b+r}{A_w} T V^2 + \frac{2ST}{A_w \rho \, dx} + 2 \frac{A_L}{A_w} T V (1 - V') \frac{dV}{dx} \qquad (22)$$

in which V' equals V_b/V, and is assumed to be less than or equal to 1. The left hand side of Equation 22 is the wave term, the first term on the right hand side is the friction term, the second term on the right hand side is the breaking term, and the third term on the right hand side is a convective

acceleration term. S, in the breaking term, includes unknown forces associated with the breaking, impact, and splash of the wave, and it cannot now be expressed analytically. For lack of a better solution, it will be assumed proportional to the momentum flux in the entering wave and will be absorbed in the quantity p. Assumed negligible are the shear force on the fluid interface along the breaker line, and possible pressure forces due to a gradient of MWL in the x-direction. The shortened equation is thus

$$p C_b \sin 2\theta_b = \frac{f}{4} \frac{b+r}{A_w} T V^2 + 2 \frac{A_L}{A_w} T V (1 - V') \frac{dV}{dx} \qquad (23)$$

8.4 Velocity as a Function of x

The variation of velocity in the x-direction is a characteristic feature of the longshore currents observed in this investigation. For given test conditions, equation (6) becomes an equation in three variables V, V_b, and f. In particular, the left hand side is a constant which the right hand side must equal. It is desired to obtain the general form of the function V(x).

Differentiating with respect to x and solving for d^2V/dx^2, equation 23 becomes

$$D_2 (V - V_b) \frac{d^2V}{dx^2} = [D_2 (\frac{dV_b}{dx} - \frac{dV}{dx}) - D_1' f 2V] \frac{dV}{dx} - D_1' \frac{df}{dx} V^2 \qquad (24)$$

where

$$D_1' = \frac{T}{4} \frac{b+r}{A_w} \qquad (25)$$

$$D_2 = 2 \frac{A_L}{A_w} T \qquad (26)$$

f is small and varies little with x. Suppose, for example, longshore current velocity is negligible. The water in the surf zone still has an

average particle velocity due to the bore. The particle velocity at the head of the bore is given, (Keller, Levine, and Whitham, 1960) in notation of this report, by

$$u = \frac{1}{1-\sigma+\beta} C \tag{27a}$$

$$\sim \frac{2}{3} C \tag{27b}$$

where C is the local celerity of the bore in the runup region, and for measurements of these tests, has an average value $> \frac{1}{2} C_b$ (see Figure 20). Since u must go to zero once each half period, an average u is

$$u_{av} = \frac{1}{3} C \sim \frac{1}{6} C_b \tag{28}$$

In these tests u_{av} has a range from about 0.3 to 0.6 feet per second (see Figure 21) and V up to 2 feet per second. Therefore, the possible change in R along the beach will be less than an order of magnitude, and for the given relative roughnesses, f is a small quantity which should not vary by more than 20 per cent along the 20 foot test beach. For these reasons, the variation of f with x will be neglected and equation 24 rewritten as

$$D_2 (V - V_b) \frac{d^2V}{dx^2} = [D_2 (\frac{dV_b}{dx} - \frac{dV}{dx}) - D_1 2V] \frac{dV}{dx} \tag{29}$$

where

$$D_1 = \frac{f}{4} \frac{b+r}{A_w} T \tag{30}$$

The initial conditions for this equation are (Figure 40)

$$V(0) = p C_b \sin \theta_b \tag{31}$$

$$V_b(0) = 0 \tag{32}$$

Because V_b is defined as the average x-component of the velocity at the breaker with which the return flow escapes offshore, at the upstream training wall ($x = 0$), $V_b = 0$. But since the breaking wave enters the surf zone with a longshore component of motion proportional to the longshore component of the breaker velocity, $V = p C_b \sin \theta_b$ at the upstream training wall.

The shape of $V(x)$ will be convex upwards as long as the right hand side of (29) is positive. $2 D_1 V/D_2$ is on the order of $(f/d_b)\, p C_b \sin \theta_b$ near the upstream training wall, which can become a very small number for tests in Series II having small θ_b. Thus, for the case of small θ_b, the sign of d^2V/dx^2 will depend mainly on the relation between dV_b/dx and dV/dx. Because V goes from $p C_b \sin \theta_b$ to V_{max} along the beach, and V_b goes from 0 to near V_{max}, it is possible that dV_b/dx is larger than dV/dx over the upstream end of the beach and thus d^2V/dx^2 may be initially positive.

Figure 36 shows the ratio of the velocity at the breaker position indicated by the probe (V_{bp}) to the local mean velocity in the surf zone indicated by the probe (V), all for a given x. V_{bp} is the sum of the

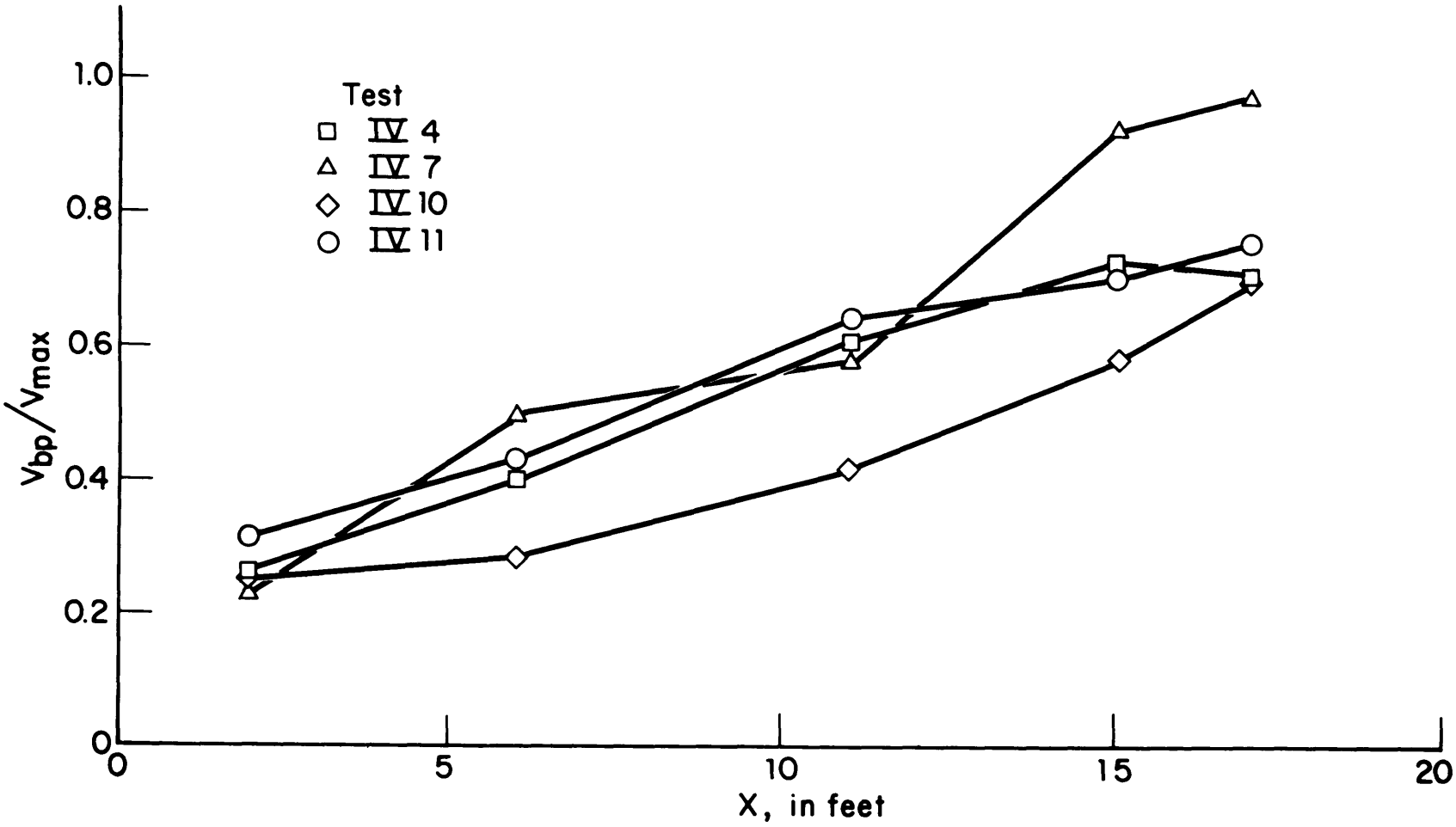

Figure 36. Ratio of Velocity Measured at Breaker to Mean Velocity as a Function of Distance along Beach

constant $p C_b \sin \theta_b$ and the variable velocity V_b, and incorporates possible error due to the probe responding differently at the outer edge of the surf zone from the calibrated response in the middle of the surf zone.

Because $p C_b \sin \theta_b$ and the possible error is probably constant along the beach, the variation shown on Figure 36 can be attributed to variation in V_b. This variation indicates that V_b increases more swiftly than V in the x-direction, but does not indicate whether the rate of increase is large enough to make d^2V/dx^2 positive.

Neglecting the variation in f, the friction term of equation 23 grows as the square of the velocity, but since the right hand side of (23) equals a constant, the velocity must approach an upper limit. Therefore, d^2V/dx^2 will always become negative if the beach is long enough, and V will tend toward a maximum.

Equation 23 predicts that V(x) may be concave upward initially, and must approach being horizontal eventually. Figures 37, 38, and 39 show typical velocity variation with x for 2 tests of each series. Series II tests show indications of being concave upward, which as pointed out above, is to be expected for the small θ_b of this series. The other two series demonstrate curves which reach a maximum.

V_{bp}/V, and thus V_b/V, was not observed to be greater than 1 in these tests which, according to equation 23, should be the case for curves

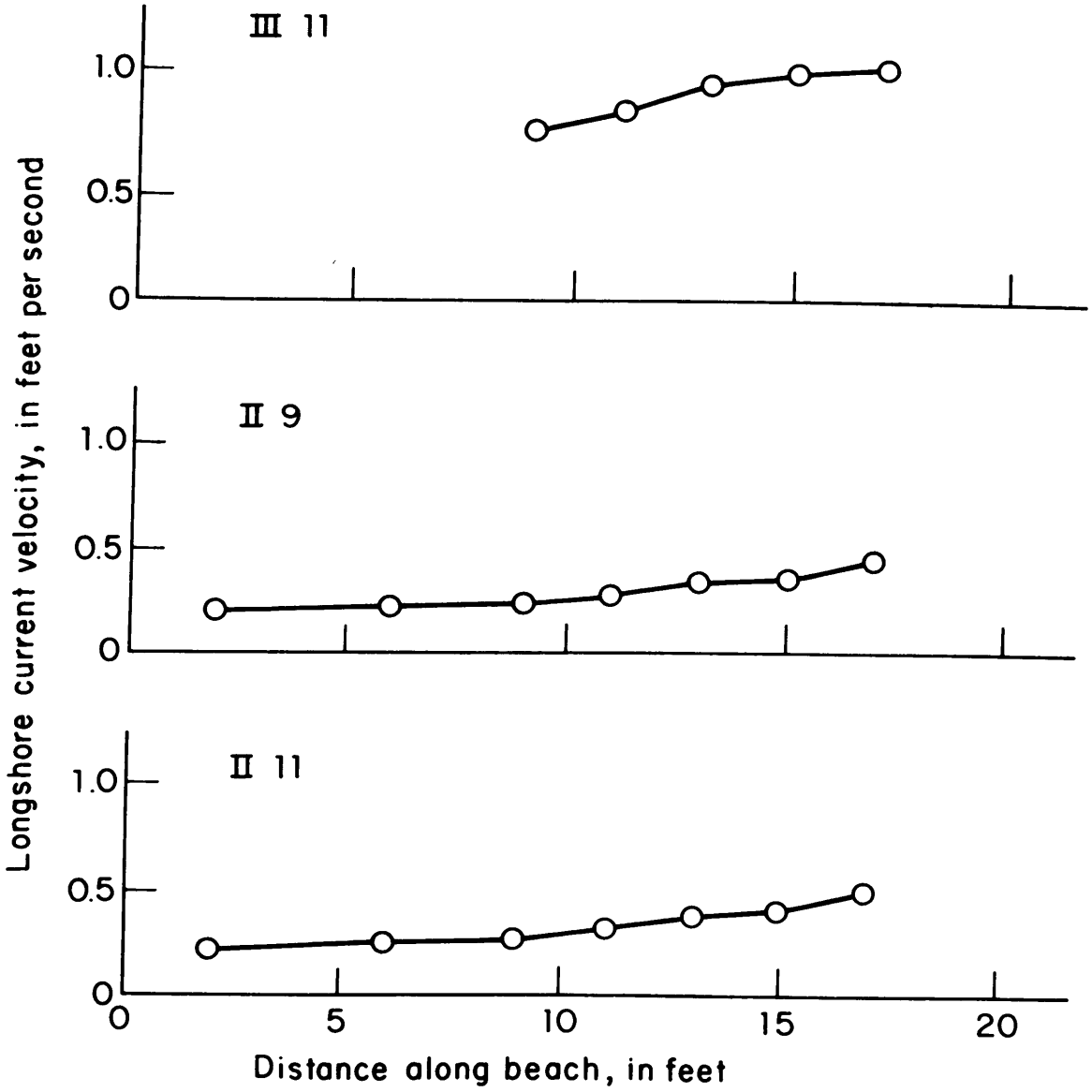

Figure 37. Variation of Mean Longshore Current Velocity with Distance along Beach

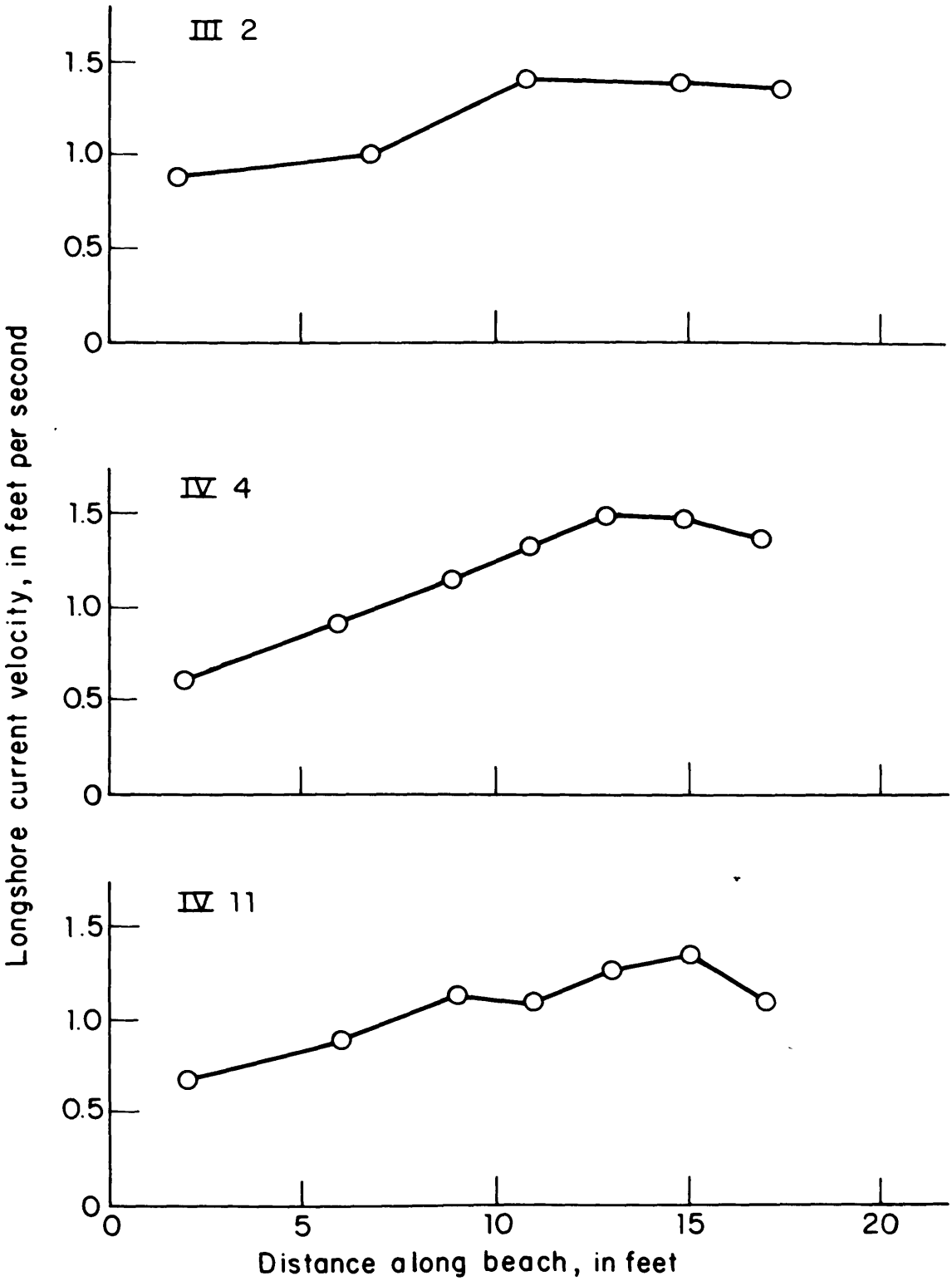

Figures 38, 39. Variation of Mean Longshore Current Velocity with Distance along Beach

which pass through a maximum. Pronounced offshore flow was frequently observed at the downstream end of the beach however.

Figure 40 demonstrates an idealized velocity distribution of longshore currents on the laboratory beach. The curves represent a composite of typical conditions from the plots of velocity distribution for 30 tests, but no single test demonstrated all the features displayed on the figure.

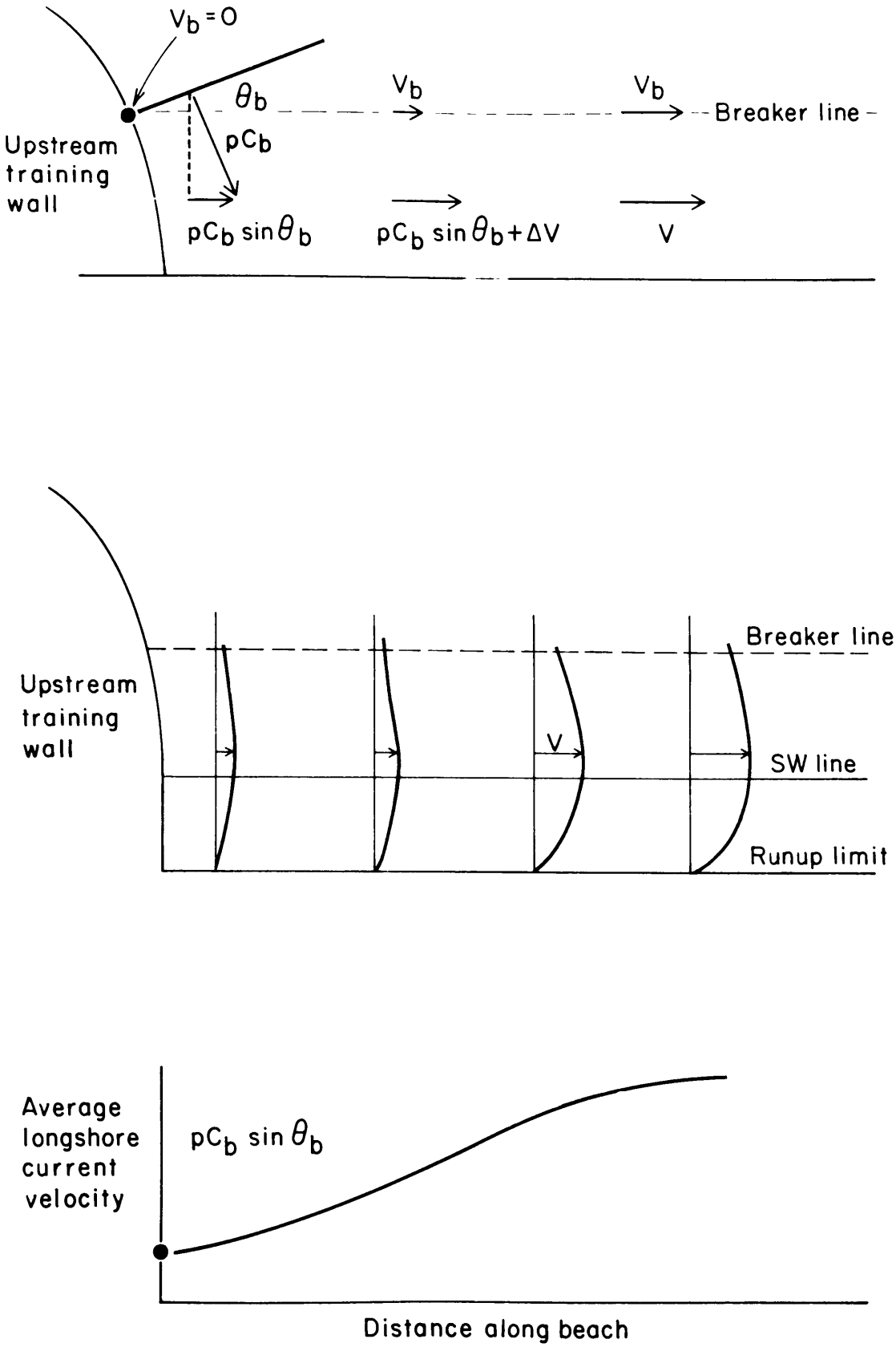

Figure 40. Idealized Velocity Distribution along a Laboratory Beach

8.5 Type of Solution Expected

It is not irrelevant to ask what type of solution can be expected from a given study. Whether useful equations of motion for longshore current motion can be expected from present knowledge of fluid mechanics is a legitimate question, especially since longshore current motion is compounded of two as yet incompletely described types of flow, open channel flow and wave movement in the surf zone.

Open channel flow in its simplest form - steady, uniform flow over a plane, immovable boundary - is still empirical, and the mechanics of waves in the surf zone are yet to be understood. Ultimately, all open channel flow predictions involve the use of empirically derived roughness or resistance coefficients, and even for the simplest cases, these coefficients are known with an accuracy suitable only for engineering computations. For waves at breaking, tests of existing theory "exhibit such a large degree of scatter that it is not possible to speak of confirmation in the sense in which physical laws can be checked in the laboratory", (Munk, 1949, p. 395).

As an open channel flow, longshore currents on a laboratory beach are flows in a triangular channel bounded by a plane surface on one side, water on a second side, and a very irregular and unsteady free surface above. This flow is driven by wave motion; it is not a gravity-driven system in the sense that typical open channel flows are. Energy is obtained from the periodic impact of the breaking wave and the motion of

the resulting bore in the surf zone. This periodic disturbance imparts to the water particle in the surf zone a transverse, reversing velocity which attains or exceeds the magnitude of the longshore current velocity. The Reynolds numbers (using longshore current velocity at $x = 10$ feet) and relative roughness (using a roughness $k = 10^{-3}$ feet for smooth concrete) can yield friction factors almost in the transition zone of the Moody diagram. For low longshore current velocities, it is a doubtfully valid assumption that longshore current velocities can be separated from the total velocity vector of the fluid in computing energy losses. Since there is no lower limit to possible longshore current velocities, there can always exist a velocity such that dissipation indicated by the Reynolds number of the longshore current is in the laminar range. Laminar flow is not expected in the surf zone. However, for large longshore current velocities, friction factor is determined largely or solely by relative roughness, and this separation of energy becomes a better, but not completely accurate, assumption.

Even supposing that friction loss can be computed, the energy dissipated by the friction is only a small fraction of the total energy dissipated (see Section 7.6), and the friction force is a small part of the total force. Equations of motion based on the conservation of energy or the x-component of momentum flux must therefore rely on the small differences of large quantities to predict longshore current velocity, and the quantities which describe the principal dissipation phenomena in the surf zone are very uncertain.

It is concluded that a relation to predict longshore current velocity is expected to be empirical, and that the wave-driven character of the flow will add to the number of variables needed to define the coefficients.

9. CONTINUITY CORRELATION

9.1 The Correlation

An empirical correlation is possible between two groups of measured variables for some of the available field and laboratory data. In one form, this correlation is between the mass flux in the longshore current, Q_L, and a hypothetical mass flux, identified as Q_W, equal to the product of a velocity $C_b \sin \theta_b$ and an area of height H_b and length $1/2\ L_b \cos \theta_b$.

$$Q_L = A_L V = \frac{1}{2} m b^2 V \tag{33}$$

$$Q_W = A_W C_b \sin \theta_b = (\frac{1}{2} H_b L_b \cos \theta_b)(C_b \sin \theta_b) \tag{34}$$

$$Q_R = Q_L / Q_W \tag{35}$$

Using equations 6 and 7 in (33) and using the equation for solitary wave speed and a trigonometric identity in (34), Q_L and Q_W are rewritten

$$Q_L = \frac{1}{2} \beta^2 \frac{H_b^2}{m} V \tag{36}$$

$$Q_W = \frac{1}{4} g T H_b^2 (1 - \sigma + \beta) \sin 2 \theta_b \tag{37}$$

Data from Putnam et al. (1949), and Inman and Quinn (1951) together with data from this investigation are plotted as Q_L and Q_W on Figure 41. Some selection of the data has been made. Only those points

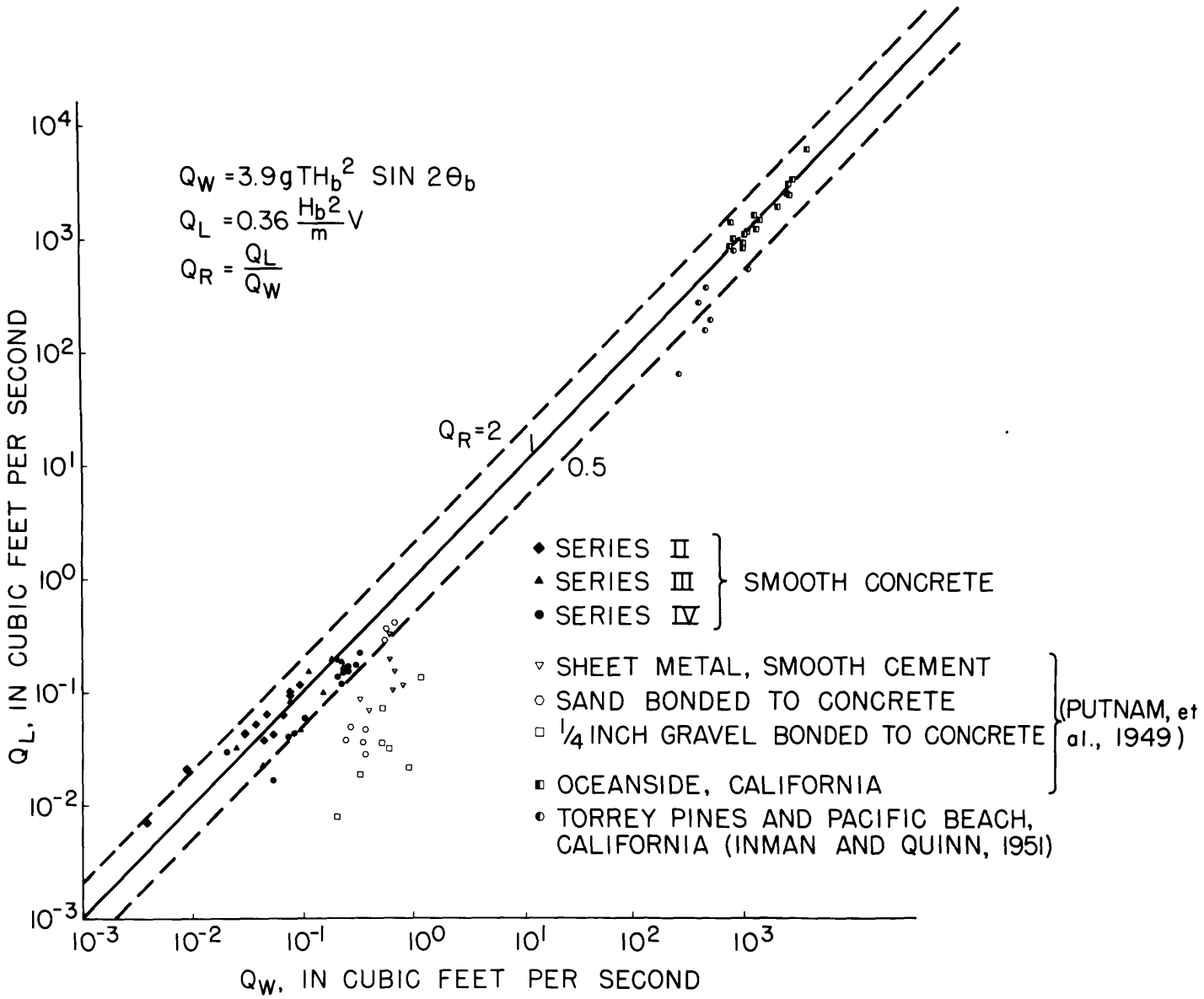

Figure 41. Continuity Correlation

have been taken from Inman and Quinn for which the mean velocity exceeds the standard deviation of the velocity, thus eliminating the tests for which an upstream longshore current was most significant. It is possible that part of the reason why the data of Inman and Quinn fall below the line $Q_R = 1$ is that even in the selected tests, the velocities listed by Inman and Quinn are the average over 15 stations, some of which are directed upstream.

Tests 13 and 17 of the Putnam, et al. field data were eliminated because of high following winds. Only those laboratory data of Putnam, et al. are plotted which have $d_b/L_o < 0.04$ (see Figure 25) are used. This is the range within which the tests of this investigation and the field data fall. The omitted laboratory points would plot generally in the same position as the plotted points, but it is apparent from Figure 25, that either experimental conditions or the definition of breaker position in the laboratory experiments of Putnam, et al. differed considerably from those of this investigation. No information on the definition of breaker position, or the measurement of wave height and depth of breaking is included in the original report (Putnam, Munk, and Traylor, 1949, p. 340). All available data from Series II, III, and IV are used.

For all data, the values $\sigma = 0.3$, $\beta = 0.85$ were used, and in evaluating data in Series II, III, and IV, equation 33 was used instead of (37), in order to eliminate scatter introduced by erratic values of H_b.

Using (36) and (37) to evaluate (35), Q_R becomes

$$Q_R = \frac{2\beta^2}{1-\sigma+\beta} \frac{V}{g\,m\,T \sin 2\theta_b} \tag{38}$$

This permits a relation of the following form

$$V = K_1\, g\, m\, T \sin 2\theta_b \tag{39}$$

From the plot of the data on Figure 41, Q_R, for some series of tests, can be approximated by a constant on the order of 1, and from the values of β and σ found in this investigation, $\frac{1-\sigma+\beta}{2\beta^2}$ is also a constant on the order of 1, so that K_1 has a value near 1.

The average K_1 for the 16 usable field tests of Putnam, et al. is 1.02. Individual K's are within 25 per cent of the average K in 13 of the 16 tests, and the use of K_{av} tends to be conservative at higher velocities, that is, predicted velocities are higher than measured velocities.

If this correlation holds and K can be evaluated for representative natural beaches, the velocity of longshore currents can be predicted from a simple relation involving the product of 3 independent variables. For engineering purpose, slope might be measured in the field or estimated from hydrographic charts. Wave period might be estimated from meteorologic data (Bretschneider, 1958), and breaker angle estimated from refraction diagrams. This correlation may make available an estimate of the velocity

of longshore currents for engineers contemplating building structures on a coastline, or for geomorphologists trying to interpret the history of coastal land forms. Work must yet be done to relate the velocity to sediment transporting capacity of the longshore current.

9.2 Possible Explanation of Correlation

Empirical correlations, such as the continuity correlation, must reflect some cause. The cause may be a trivial one, such as the chance grouping of limited sets of data representing conditions under which some important variables cancel or do not vary. Since correlation in Figure 41 exists only for the data of this investigation and for the field data of Putnam, et al., this is a possibility. There is a need to test the correlation on laboratory beaches with lower slopes or on natural beaches for small waves.

Another cause may be that a basic physical law has accidently been formulated. The flow of longshore currents may then represent conditions for which this physical law has the simple form of equation 39. Because it appears that longshore currents contribute only in minor way to the complicated balancing of forces or dissipation of energy in the surf zone, it would appear that the simple form of the correlation could hardly be an expression of the conservation of momentum or energy.

There remains, however, another basic law of physics, even more elementary than the conservation of momentum or energy, and just as rigid

in its demands - the conservation of mass, or the so-called continuity equation. For the conservation of mass in the surf zone, the flow of the longshore current is the dominating phenomenon, not a side effect as it is in the conservation of momentum and energy.

The manner in which the correlation is first formulated (equations 33, 34, and 35) suggests that continuity may be involved. But the application of the continuity equation is not straight forward because, for steady uniform flows, the breaking wave does not permanently contribute any mass to the longshore current. However, for the increment Δx of beach length bordered on one side by the upstream training wall and on the other by section b (Figure 42), the breaker must contribute to the longshore current.

Because the longshore current velocity is the mean velocity in the x-direction of water in the surf zone, the fact that the wave in breaking moves with a longshore component of motion creates a longshore velocity.

So the flux of mass into the surf zone across Δx is balanced by the flux out across Δx and the flux downstream across b. If it can be assumed that the wave at breaking is moving in pure translation with speed C_b, then the flux out across b will be related to the product of the x-component of the wave velocity at breaking ($C_b \sin \Theta_b$) and the cross sectional area of the breaking wave projected against the normal section b (A_W). A_W has been assumed to be the area $1/2\ H_b L_b \cos \Theta_b$ which can be

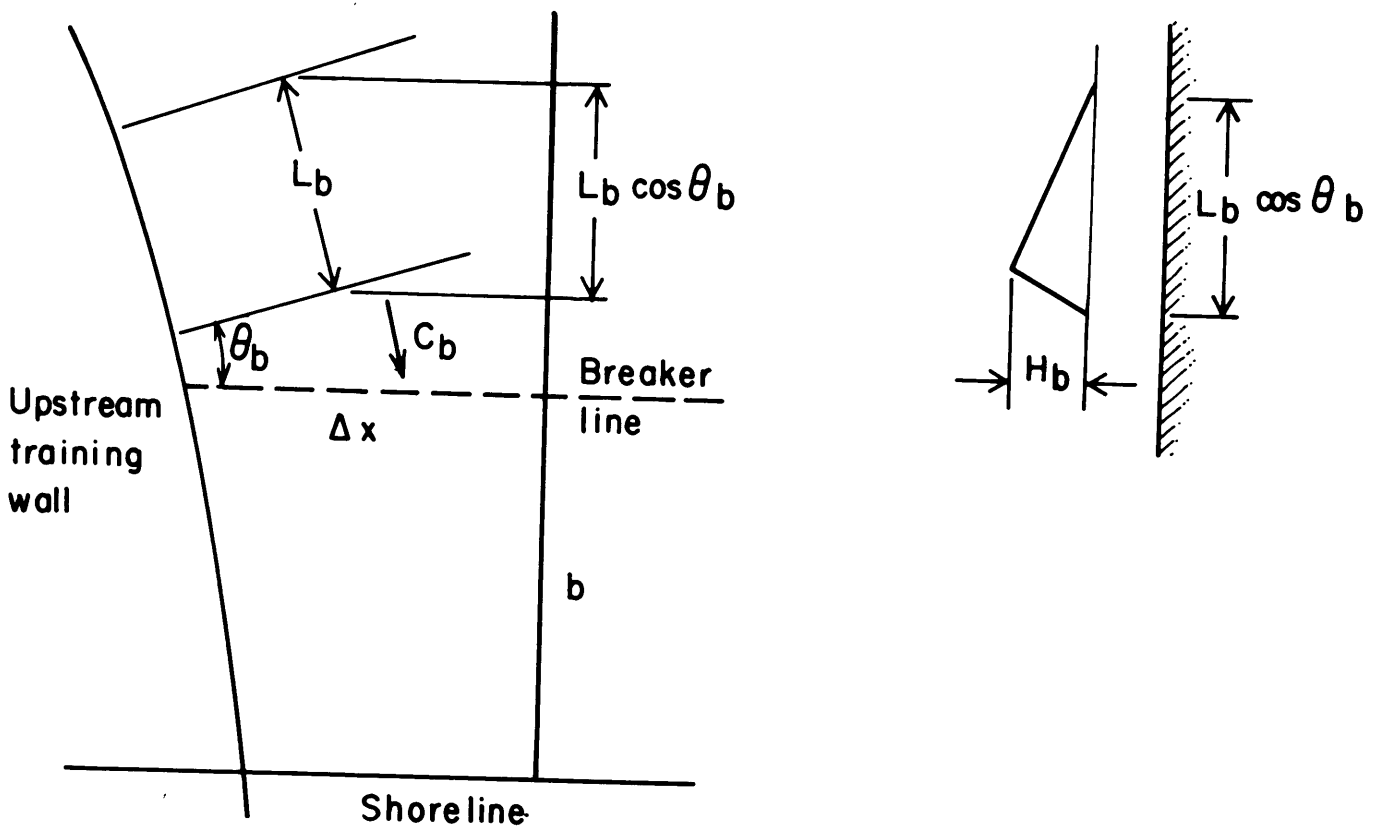

Figure 42. Continuity Control Volume

interpreted either as the projected triangular wave, $L_b \cos \theta_b$ long and H_b high, or approximately half the projected area in the wave averaging H_b deep and $1/2\ L_b \cos \theta_b$ long.

Interpreted this way, it is seen that a continuity equation is involved, that is, Q_W is in some way proportional to Q_L. Why the proportionality constant should approach so nearly to 1 is not apparent, for it is clear that waves at breaking are not in pure translation (see Figure 15, Iverson, 1952; Figure 9, Ippen and Kulin, 1955), but only approach C_b at the crest. It is interesting that the geometrical constraint, β = constant, proportions the size of the wave to the size of the longshore current channel, and thus eliminates wave height from equation 39.

10. SUMMARY

10.1 Approach

The purpose of this investigation has been to describe, by experiment, the characteristics of longshore currents, and to develop an analytical technique for predicting longshore current velocity. The two objectives are prompted by the need to understand the mechanics of sediment transport by longshore currents on natural beaches.

The results of this investigation, both experimental and analytical, are based on experiments made on the 20 foot test section of a plane, smooth concrete beach with a 1 on 10 slope. The experiments performed on the beach provided data concerning breaking waves and longshore currents, and these observations led to an analysis of energy dissipation in the surf zone, an analytical description of the non-uniform flow of longshore currents, and an empirical correlation between the velocity of longshore currents, and the wave conditions and beach geometry.

10.2 Experimental Results

Description of the breaker. The mean water level at the breaker point on the laboratory beach was found to be at, or slightly lower than, the still water level. It was found that waves broke when the ratio, β, of mean water depth to wave height was approximately 0.85. The value of β appeared to be relatively independent of wave height, position along

the beach, or breaker angle. It was found to be considerably lower than reported by other investigators, and it came closest to agreeing with previous results for oscillatory waves on a similar beach slope, and for the breaking of solitary waves. The level of the trough at breaking was found to about 0.3 H_b below mean water level.

Wave speed at breaking is given approximately by the solitary wave equation, $C_b = [g H_b (1 - \sigma + \beta)]^{1/2}$. Wave height at breaking varied with position along the beach, perhaps due to the geometry of the basin. At the upstream and downstream ends of the beach, the height at breaking was lower than that predicted by small amplitude theory, and in the middle of the test beach, height at breaking was higher than that predicted by small amplitude theory.

The breaker angle, given as the average of measurements by two observers, agreed well with the angle predicted by small amplitude theory.

Description of the runup region. The mean water level was found to rise smoothly in the onshore direction towards an intersection with the beach at or below the runup limit. For the conditions of these experiments the still water line was located slightly inshore of the middle of the surf zone. The shape of the bore in the surf zone is more symmetric about a horizontal axis than the shape of the wave at breaking; trough elevation occurred at an elevation about 0.4 H below mean water level. As far as could be measured, bore speed in the runup region diminishes uniformly toward the shore, but at a point close to the runup limit, the

bore still moves with a speed which is 1/4 to 1/2 the speed of the wave at breaking.

Velocity distribution in longshore current. At a given position on the beach, the maximum measured longshore current velocity occurred just offshore of the still water line. Shoreward from this point, the velocity remained high, as far as it could be measured. Seaward from the maximum, the velocity gradually decreased to some value V_b at the breaker point.

The mean longshore current velocity, V, increased with distance from the upstream training wall. It was reasoned that very close to the training wall, V was proportional to the longshore component of the breaking wave velocity, and that V_b was 0. Measurements indicate that V_b increases faster than V in the downstream direction. The rate at which V increases varies along the beach and with the given test conditions. For tests with small breaker angles, the velocity gradient in the x-direction increased downstream, but for most tests the velocity gradient was constant over the upstream half of the beach and decreased over the downstream half of the test beach.

Within the surf zone there is a circulation imposed on the water which drifts the surface fluid shoreward and drives the bottom fluid toward the breaker line. However, flow out of the surf zone across the breaker line was rarely observed except at the downstream end of the beach.

Variation in the x-direction. In addition to velocity, the measured mean water level, breaker position, and runup limit varied in the x-direction. Mean water level usually increased and the breaker position and runup limit usually moved shoreward at the downstream end of the beach, observations which are consistent with each other.

10.3 Experimental Apparatus and Procedure

The breaker position was defined in such a way that it could be measured visually with a simply designed breaker locator. Tests showed that the method is reliable, and that agreement between different operators making the same measurement is good. Measurement of breaker angle with the locator showed consistent differences of 2 or 3 degrees between two operators, but the average of the two observations agreed well with the angle predicted by small amplitude refraction theory.

Wave speed, wave shape, wave height, and wave height envelopes in the surf zone were measured with platinum wire resistance gages modified for use in the surf zone. For the conditions used, the gages gave linear calibrations, which did not drift with time and were relatively insensitive to variation in spacing and nearness to conducting boundaries. The measurement of wave speed from the recorded phase lag of two simultaneous wave traces is subject to error because the gages interfere with one another electronically, and because it is difficult to identify on the two traces the same point and the same wave.

Measurement of mean water level with damped piezometers in the surf zone agrees with the mean water level obtained from the graphical integration of the wave form. From this experimental check and from theoretical considerations, the piezometers appear to measure the mean hydrostatic head.

Longshore current velocity was measured with miniature current meters (velocity probe) calibrated against the velocity of surface floats. The relation between float and probe velocities is linear for given ranges of breaker angle. Onshore of the still water line, the measured velocity is probably too low because the probe is exposed over part of the wave cycle, and at and offshore of the breaker position, the measured velocity may be too high due to the more pronounced oscillatory motion of the waves.

10.4 Analytical Results

Energy dissipation in the surf zone. Most of the energy brought to the beach by shoaling waves is immediately dissipated there in the breaking process. Perhaps less than 25 per cent of the energy then remains to be dissipated by motion of the bore through the runup region and by bottom friction due to the flow of longshore currents, or to be convected downstream as increased kinetic energy of the longshore current, or to be reflected from the beach.

Of these secondary mechanisms, energy dissipated by the bore in the runup region is probably the most important. This dissipation

can be computed from the potential energy stored in the runup region, which is related to the rise in mean water level in the runup region measured by the piezometers. This potential energy must be obtained by conversion from kinetic energy in the bore. Energy equal to the mean potential energy of the runup region must be supplied, and thus dissipated, each period.

Frictional dissipation of the longshore current is relatively unimportant. In only 7 of 30 tests was it computed to be more than 10 per cent, and for 11 of the 30 tests it was less than 1 per cent of the incoming wave energy given by small amplitude theory. This percentage depends strongly on breaker angle. Computations of frictional dissipation are uncertain because fluid in the surf zone has a longshore and a periodic onshore-offshore motion which complicates the choice of proper friction factor.

The rate at which the kinetic energy of the longshore current increases downstream may be the same order of magnitude as the frictional dissipation of the current. Reflection and eventual dissipation of energy offshore of the breaker appears to be negligible.

The effect of the external area on the test area of the basin also appears to be small. Dissipation in the external circuit by the fluid returning to the test area of the beach can be accounted for by the flux of kinetic energy off the test beach. It is unlikely to have a measurable effect on the slope of the water surface anywhere in the basin.

Momentum equation. The momentum approach of Putnam, Munk, and Traylor (1949) was reformulated for the non-uniform flow of longshore currents. Momentum flux in the x-direction into and out of the control volume was balanced against the frictional force of the longshore current, and pressure forces due to a possible gradient in mean water level and frictional forces on the fluid interface at the breaker line were neglected. The important step in formulating the equation was the assumption that fluid flows out across the breaker line with a longshore component of velocity, V_b, which is lower than the average longshore current, V, and that this velocity V_b is still present when the fluid is lifted up to form the next breaker.

The resulting differential equation has two initial conditions which result from supposing the current to start from a wall: $V_b(0) = 0$, and $V(0)$ = a velocity proportional to the longshore component of the velocity of the breaking wave. The second derivative of the solution $V(x)$ must eventually be negative but may be initially positive, if the first derivative of $V_b(x)$ is large enough. In all cases, the first derivative of V must be positive. The equation predicts that a negative second derivative is most likely for small breaker angle.

The measured variation of the longshore current in the longshore direction agrees qualitatively with the equation. At some low breaker angles, the curve of $V(x)$ versus x is concave upward, while in others the curve is initially straight and eventually concave downward.

Continuity correlation. Velocity of the longshore current is found to be proportional to the product of beach slope, wave period, breaker angle, and g. The proportionality constant has a value near 1. This empirical correlation holds for the field data of Putnam, Munk, and Traylor (1949) and, with some dependence on breaker angle, for the measurements of this investigation. If it can be verified elsewhere, the correlation will provide engineers and geologists with an easy method for predicting longshore current velocities on plane beaches.

11. CONCLUSIONS

11.1 Results

The results of this investigation which appear most applicable to the flow of longshore currents on natural beaches are these:

1. Relative importance of dissipative mechanisms in the surf zone. Immediate dissipation in the breaking process accounts for most of the energy dissipated on a beach. Of secondary dissipative mechanisms, the bore passing through the runup region is quantitatively the most important. Energy dissipation by the longshore current is small and may be less than 1 per cent of the energy brought to the beach by shoaling waves.

2. Longshore current velocity. Longshore current velocity depends on beach slope, wave period, and breaker angle, as well as distance from a barrier (groin, jetty, cape, upstream training wall). For a given wave on a given natural beach, current may erode the shoreline to a shape such that the breaker angle and the distance from the barrier combine to give an equilibrium rate of sediment transport along the beach.

The local longshore current velocity at the breaker point, V_b, initially increases faster in the downstream direction than does the average longshore current V. This is a result of the lateral spreading of the longshore current in the downstream direction and may contribute

to sediment deposition offshore of the breaker.

3. Gradient of mean water level. Mean water level rises toward the shore from the breaker region and possibly rises in the downstream direction. The resulting pressure gradient may cause the observed offshore spread of the longshore current, and possibly cause rips.

4. Analytical techniques. (a) The mean potential energy of the mass stored in the runup region must be supplied, and dissipated, once each period. This permits calculation of energy dissipation by the bore in the runup region, provided the mean water level is known. The way in which energy is dissipated in the runup region probably determines the local slope of the beach.

(b) A momentum analysis of the non-uniform flow of the longshore current may give qualitative prediction of the growth of longshore current velocity. According to the analysis, longshore current velocity may initially increase fast enough that d^2V/dx^2 is positive, but eventually d^2V/dx^2 must be negative. The initial positive second derivative is possible if dV_b/dx is sufficiently larger than dV/dx. The rate of growth of V will affect the shape of the shoreline downstream from a barrier.

5. Empirical prediction of velocity. The average velocity of longshore currents is approximately equal to $g\,m\,T \sin 2\theta_b$ for tests on one laboratory and one natural beach. Predictions for other plane beaches

may be possible with this formula. It is interesting that this relation is independent of wave height.

11.2 Suggestions for Future Work

Probably, best progress will be made toward understanding fluid motion in the surf zone if future work concentrates on solving one basic problem at a time. The principal problem is where and why a wave breaks, and in breaking, how is the energy dissipated. Until this is understood, the prediction of sediment motion in the surf zone must remain uncertain.

The bore which forms after the breaking of the wave is an interesting problem in shallow water wave theory, and a phenomenon of importance second only to that of the breaker in the surf zone. In its simplest form, the motion of a bore into quiet water could easily be investigated experimentally, and the results checked with theoretical solutions based on ideal fluid motion in order to gain insight into energy dissipation by this mechanism. The major experimental problem would be the generation of the bore, which might perhaps be done by pulling a gate between a channel and a large body of water. The resistance wave gages could be used to measure bore speed if they were only slightly submerged and if the junction between bore and still water is sharp enough.

The possible connection between the variation of velocity and mean water level in the longshore direction and the generation of rip currents should be investigated. The transverse pressure gradient due to a rise in

mean water level in the downstream direction may become large enough to deflect the longshore currents offshore as a rip.

The continuity correlation should be tested on laboratory beaches with lower slopes and with facilities for larger variation in wave conditions.

APPENDIX

TABLE A 1

DEFINITION OF TEST NUMBERS

Test Number	Period (T) (seconds)	Waveheight at Plunger (H_d) (feet)
1	0.90	0.211
2	1.00	0.191
3	1.125	0.167
4	1.25	0.143
5	1.375	0.121
6	1.50	0.105
7	1.25	0.050
8	1.25	0.098
9	1.25	0.124
10	1.25	0.130
11	1.25	0.156
12	1.50	0.062
13	1.0	0.110
14	1.0	0.073
15	1.0	0.146
16	1.0	0.213

Series	θ_d
I	0°
II	10°
III	27°
IV	51°

TABLE A 2

DATA AVAILABLE

Test No.	Series	I				II				III				IV			
	Data Type	A	B	C	D	A	B	C	D	A	B	C	D	A	B	C	D
1				x													
2				x			x	x	x	H_b	x	x	x	x	x	x	x
3						C_b	x	x	x	H_b	x		x	x	x		x
4				x		x	x	x	x	H_b	x		x	x	x	x	x
5						x	x	x	x	x	x		x	x	x		x
6				x		C_b	x	x	x	x	x	x	x	x	x	x	x
7						C_b	x	x	x	x	x			x	x	x	x
8						x	x	x	x	H_b	x		x	x	x		x
9						C_b	x	x	x	x	x		x	x	x	x	x
10						x	x		x	x	x			x	x		x
11						x	x		x	x	x		x	x	x		x
12						x	x		V_f	x	x				x		V_p
13						C_b	x		V_f	x	x				x		V_p
14				x											x		
15				x													
16				x													

x indicates data complete

TABLE A 3

AVERAGE BREAKER AND RUNUP DATA,

AND FLOAT VELOCITIES

Series	Test	b_{av}	$d_{b_{av}}$	r_{av}	$\theta_{b_{av}}$	$V_{f_{10}}$	$V_{f_{16}}$
		ft	ft	ft	degrees	ft/sec	ft/sec
II	2	1.62	0.177	1.01	5.7	0.73	0.83
	3	1.53	0.167	1.06+	6.3	0.65	0.82
	4	1.33	0.145	1.07+	4.1	0.42	0.68
	5	1.24	0.135	1.15+	3.6	0.60	0.53
	6	1.17	0.128	1.04	4.4	0.45	0.52
	7	0.62	0.068	0.62	3.2	0.25	0.34
	8	0.87	0.095	0.77	4.8	0.27	0.50
	9	1.21	0.132	1.03	4.7	0.35	0.67
	10	1.07	0.117	1.03	4.6	0.40	0.71
	11	1.44	0.157	1.08+	4.7	0.38	0.84
	12	0.76	0.083	0.78	1.1	0.21	0.21
	13	0.98	0.107	0.75	5.9	0.52	0.45
III	1	-	-	-	-	1.41	1.81
	2	1.52	0.166	0.95	14.5	1.57	1.76
	3	1.51	0.165	1.05	12.1	1.43	1.60
	4	1.44	0.157	1.05	10.9	1.29	1.61
	5	1.13	0.123	1.05	9.3	1.32	1.42
	6	1.04	0.113	1.06	8.1	1.06	1.23
	7	0.68	0.074	0.61	7.1	0.60	0.56
	8	0.85	0.093	0.75	7.0	0.86	0.96
	9	1.11	0.121	0.89	10.5	1.16	1.23
	10	1.33	0.145	1.01	11.1	1.27	1.49
	11	1.55	0.169	1.10	12.7	1.35	1.77
	12	0.77	0.084	0.76	5.0	-	-
	13	0.94	0.102	0.67	10.3	-	-

TABLE A 3 (cont'd)

AVERAGE BREAKER AND RUNUP DATA,

AND FLOAT VELOCITIES

Series	Test	b_{av}	$d_{b_{av}}$	r_{av}	$\theta_{b_{av}}$	$V_{f_{10}}$	$V_{f_{16}}$
		ft	ft	ft	degrees	ft/sec	ft/sec
IV	2	1.40	0.153	0.84	30.7	1.83	2.15
	3	1.15	0.125	0.88	22.1	1.77	1.89
	4	1.22	0.133	1.02	19.3	1.72	1.91
	5	1.32	0.144	1.17	16.0	1.71	1.81
	6	0.91	0.099	0.90	7.3	1.04	0.91
	7	0.69	0.075	0.59	13.4	0.87	0.65
	8	0.83	0.090	0.79	16.8	1.20	1.20
	9	1.19	0.130	0.86	20.4	1.44	1.57
	10	1.27	0.138	0.97	22.2	1.73	1.88
	11	1.29	0.141	1.12	25.0	1.93	1.96
	12	0.57	0.062	0.54	8.8	0.40	0.18
	13	0.88	0.096	0.72	22.5	1.31	1.46
	15	1.11	0.121	0.79	19.0	-	-

TABLE A 4

WAVE HEIGHT AND CELERITY AT BREAKING

Test	x ft	Series II H_b ft	Series II C_b ft/sec	Series III H_b ft	Series III C_b ft/sec	Series IV H_b ft	Series IV C_b ft/sec
3	3	0.192	-	-	-	-	-
4		0.130	3.94	-	-	0.179	2.60
5		0.192	-	-	-	-	-
6		-	-	-	-	-	2.50
7		0.023	-	-	-	0.162	2.30
8		0.075	-	-	-	-	-
9		0.141	-	-	-	0.155	3.20
10		0.154	-	-	-	-	-
11		0.171	-	-	-	-	-
2	10	-	-	-	-	0.176	3.55
3		0.230	2.91	-	-	0.204	3.22
4		0.170	3.28	-	-	0.185	2.66
5		0.218	3.12	0.192	2.21	0.167	3.16
6		-	2.88	0.157	1.78	0.101	2.22
7		0.045	1.88	0.091	1.15	0.166	2.90
8		0.157	2.70	0.126	-	0.125	2.74
9		0.211	3.26	0.149	2.01	0.152	2.89
10		0.198	2.79	0.170	2.37	0.167	3.08
11		0.224	2.60	0.167	2.39	0.237	3.38
12		0.065	2.76	0.109	1.58	-	-
13		0.088	2.79	0.107	2.24	-	-

TABLE A 4 (cont'd)

WAVE HEIGHT AND CELERITY AT BREAKING

Test	x	Series II		Series III		Series IV	
		H_b	C_b	H_b	C_b	H_b	C_b
	ft	ft	ft/sec	ft	ft/sec	ft	ft/sec
1	13	-	-	0.177	-	-	-
2		-	-	0.168	-	-	-
3		-	-	0.186	-	-	-
4		-	-	0.187	-	-	-
5		-	-	-	2.50	-	-
3	17	0.198	-	-	-	-	-
2		-	-	-	-	-	3.92
4		0.130	3.64	-	-	0.160	2.86
5		0.154	-	-	-	-	-
7		0.032	-	-	-	0.147	1.40
8		0.102	-	-	-	-	-
9		0.186	-	-	-	0.130	3.25
10		0.177	-	-	-	-	-
11		0.177	-	-	-	-	-

TABLE A 5

LOCAL BREAKER POINT, BREAKER ANGLE AND RUNUP LIMIT

x	b ft	r ft	θ_b degrees	b ft	r ft	θ_b degrees	b ft	r ft	θ_b degrees
	(II 2)			(II 3)			(II 4)		
4	1.38	0.88	2.5	1.46	1.01	2	1.37	0.75	3.5
7	1.67	1.08	6	1.58	1.06	7.5	1.49	1.13	3
11	1.82	1.05	5	1.68	1.09+	6	1.59	1.12+	5
15	1.94	1.02	7	1.70	1.11	7.5	1.25	1.22+	4.5
18	1.28	1.04	8	1.21	1.03	8.5	0.96	1.13	4.5
	(II 5)			(II 6)			(II 7)		
4	1.41	1.22	-1.5	1.22	0.87	5	0.57	0.47	3.5
7	1.38	1.28+	2	1.11	0.96	2	0.66	0.56	1.5
11	1.35	1.09+	6.5	1.22	1.09+	5.5	0.77	0.75	3.5
15	1.16	1.19	3	1.16	1.19+	3.5	0.58	0.76	3
18	0.92	0.96	8	1.13	1.09	6	0.53	0.55	4.5
	(II 8)			(II 9)			(II 10)		
4	0.82	0.59	3.5	1.19	0.74	4	1.29	0.73	3
7	0.91	0.70	3	1.35	0.99	3	1.39	1.02	3.5
11	0.96	0.91	5.5	1.44	1.12	5	1.51	1.09	6
15	0.85	0.91	4.5	1.07	1.21	4.5	1.12	1.21	3.5
18	0.82	0.75	7.5	1.01	1.07	7	1.05	1.11	7
	(II 11)			(II 12)*			(II 13)		
4	1.45	0.80	2	0.80	0.60	4	1.00	0.64	2
7	1.62	1.12	3	0.67	0.72	2	1.06	0.82	3.5
11	1.78	1.12+	6	0.79	0.83	0.5	0.96	0.69	5.5
15	1.32	1.22+	4	0.73	0.80	0	1.04	0.83	6
18	1.03	1.14+	8.5	0.81	0.97	-1	0.83	0.77	6.5

*θ_b by CJG. All other θ_b by RLB

TABLE A 5 (cont'd)

LOCAL BREAKER POINT, BREAKER ANGLE

AND RUNUP LIMIT

x	b ft	r ft	θ_b degrees	b ft	r ft	θ_b degrees	b ft	r ft	θ_b degrees
	(III 2)			(III 3)*			(III 4)		
4	1.58	0.81	9.5	1.58	0.86	11	1.38	0.90	12
7	1.68	0.83	13.5	1.69	1.01	16	1.51	0.97	9.5
11	1.62	1.00	16.5	1.68	1.11+	15	1.54	1.10	11.5
15	1.40	1.07	16	1.37	1.19	9	1.35	1.16	12
18	1.31	1.05	17	1.23	1.07	9.5	1.40	1.12	9.5
	(III 5)			(III 6)			(III 7)		
4	0.95	0.94	5	1.10	0.96	9	0.73	0.44	10.5
7	1.27	1.03	11	0.98	0.85	7	0.67	0.63	4.5
11	1.26	1.11+	12.5	1.23	1.12+	11.5	0.74	0.66	7
15	1.05	1.19	10	0.98	1.22+	7.5	0.65	0.76	7
18	1.12	1.00	8	0.93	1.13	5.5	0.62	0.58	6.5
	(III 8)			(III 9)			(III 10)		
4	0.93	0.62	9	1.21	0.64	11.5	1.35	0.80	11
7	0.85	0.72	4.5	1.14	0.89	8	1.43	0.99	9
11	0.89	0.75	7	1.16	0.96	10	1.39	0.99	12
15	0.75	0.95	6	0.98	1.05	11	1.17	1.18	11.5
18	0.85	0.73	8.5	1.05	0.90	12	1.29	1.09	12
	(III 11)			(III 12)			(III 13)		
4	1.54	0.96	12.5	0.83	0.47	9	0.89	0.46	9.5
7	1.54	1.06	10	0.64	0.61	8	1.07	0.73	10
11	1.75	1.09	14	0.90	0.96	2	0.95	0.70	11
15	1.41	1.22+	14.5	0.73	0.92	3	0.97	0.75	11
18	1.52	1.14+	12.5	0.76	0.82	3	0.82	0.71	10

*θ_b by CJG. All other θ_b by RLB.

TABLE A 5 (cont'd)

LOCAL BREAKER POINT, BREAKER ANGLE

AND RUNUP LIMIT

x	b ft	r ft	θ_b degrees	b ft	r ft	θ_b degrees	b ft	r ft	θ_b degrees
	(IV 2b)			(IV 3)*			(IV 4)*		
4	1.56	0.71	26	1.56	1.03	24.5	1.45	0.90	21
7	1.49	0.91	30.5	1.02	0.74	21.5	1.42	1.09	20
11	1.60	1.12+	31	1.08	1.12+	15	1.08	1.12+	20.5
15	1.39	0.92	33.5	1.00	0.76	23	0.98	1.21	14
18	1.16	0.96	32.5	1.11	0.97	26.5	1.16	0.87	21
	(IV 5)*			(IV 6)*			(IV 7)		
4	1.67	1.11	21	1.16	1.00	11	0.88	0.58	14.5
7	1.41	1.29	19	0.84	0.91	3.5	0.86	0.56	16
11	1.31	1.12+	16	1.00	0.89	6.5	0.72	0.56	14
15	0.96	1.14	18	0.82	0.94	8.5	0.49	0.64	15.5
18	1.25	1.14+	6	0.74	0.81	7	0.51	0.58	7
	(IV 8)			(IV 9)			(IV 10)		
4	1.02	0.84	19	1.44	0.81	23	1.52	0.84	24
7	1.05	0.79	17	1.39	0.91	23	1.53	1.08	21
11	0.89	0.81	15.5	1.06	1.12+	21	1.18	1.12+	25
15	0.59	0.71	19	1.08	1.00	17	1.06	1.13	19
18	0.62	0.82	13.5	1.00	0.71	18	1.08	0.82	22
	(IV 11)			(IV 12)*			(IV 13)		
4	1.63	1.01	24.5	0.69	0.60	10	1.10	0.68	22
7	1.62	1.20	23.5	0.57	0.52	15	0.79	0.69	22.5
11	1.08	1.12+	26	0.65	0.58	5	0.82	0.80	19.5
15	1.06	1.22+	26	0.40	0.51	15 to 9	0.82	0.69	25.5
18	1.06	1.05	25	0.54	0.52	4 to -1	0.86	0.82	23

*θ_b by CJG. All other θ_b by RLB.

TABLE A 5 (cont'd)

LOCAL BREAKER POINT, BREAKER ANGLE

AND RUNUP LIMIT

x	b ft	r ft	θ_b degrees
(IV 15)*			
	1.29	0.74	18.5
	1.07	0.85	23
	1.09	1.12	14
	1.18	0.84	20.5
	0.94	0.73	19

*θ_b by CJG. All other θ_b by RLB.

TABLE A 6.1

CHANGE IN MEAN SEA LEVEL ON BEACH (SERIES I)

Tap No.	x = 0 ft y ft	e cm	12 ft y ft	e cm	0 ft y ft	e cm	12 ft y ft	e cm
	(I 1)				(I 4)			
1	0.22	1.13	0.44	1.08	0.27	1.03	0.49	0.85
2	0.72	0.87	0.94	0.83	0.77	0.42	0.99	0.74
3	1.22	0.37	1.44	0.08	1.27	-0.27	1.49	0.62
4	2.72	-0.10	2.94	-0.22	2.77	-0.06	2.99	-0.12
	(I 6)				(I 14)			
1	0.25	0.45	0.47	0.39	0.28	0.60	0.50	0.10
2	0.75	-0.05	0.97	0.02	0.78	-0.40	1.00	0
3	1.25	-0.15	1.47	-0.10	1.28	-0.40	1.50	-0.40
4	1.75	-0.04	2.97	-0.08	2.78	-0.10	3.00	-0.10
	(I 15)				(I 16)			
1	0.28	0.63	0.50	0.50	0.35	1.15	0.57	1.30
2	0.78	0.16	1.00	-0.02	0.85	0.64	1.07	0.90
3	1.28	-0.10	1.50	-0.14	1.35	0.25	1.57	-0.33
4	2.78	-0.05	3.00	-0.05	2.85	0.09	3.07	-0.24

	x = 0 ft		4 ft		8 ft		12 ft		16 ft	
	(I 2)									
1	0.27	1.04	0.27	1.00	0.35	0.98	0.49	0.92	0.37	0.72
2	0.77	0.52	0.77	0.52	-	-	0.99	0.73	-	-
3	1.27	0.08	1.27	-0.18	1.35	-0.20	1.49	0.70	1.37	-0.15
4	2.77	-0.08	2.77	-0.22	2.85	-0.12	2.99	-0.12	2.87	-0.08

TABLE A 6.2

CHANGE IN MEAN SEA LEVEL ON BEACH (SERIES II AND IV)

On all piezometer channels, piezometer taps have the following spacing:

tap number	1	2	3	4	5	6
distance from tap no. 1, in feet	0	0.5	1.0	2.5	5.0	8.0

For series II and IV, the y coordinate of tap no. 1 at various x values is:

x of piezometer channel, in feet:	4	8	12	16	20	24	28
y of tap no. 1, in feet:	0.11	0.18	0.30	0.25	0.27	0.30	0.71

e cm

Test	tap no.	x = 4 ft	8 ft	12 ft	16 ft	20 ft	24 ft	28 ft
II 2	1	-	-	0.58	1.06	-	-0.30	0.22
	2	0.47	-	-	-	0.17	-0.34	-
	3	-0.32	-0.10	0.02	-0.04	-0.30	-0.11	-
	4	-0.14	-0.13	-0.16	-0.15	-0.12	-0.05	-
	5	-	-0.04	-0.09	-0.06	-0.07	-	-
	6	-0.04	-0.12	-0.01	-0.03	-0.03	-	-0.05
II 3	1	1.12	-	-	0.73	-	-0.10	0.10
	2	0.46	-	0.46	-	0.10	-0.30	-
	3	-0.23	-0.10	-0.08	-0.22	-0.32	-0.14	-
	4	-0.14	-0.15	-0.14	-0.12	-0.09	-	-
	5	-	-0.04	-0.05	-0.09	-0.05	-	-
	6	-0.05	-0.04	-0.02	-0.04	-0.02	-	-0.03
II 4	1	0.40	-	-	0.82	-	0.76	0.01
	2	0.30	-	0.41	-	-0.16	-0.08	-
	3	-0.14	0	-0.20	-0.25	-0.25	-0.04	-
	4	-0.08	0	-0.13	-0.08	-0.08	0.01	-
	5	-	0.10	-0.08	-0.04	-0.03	-	-
	6	0	-0.20	-0	-0.01	0.03	-	0

TABLE A 6.2 (cont'd)

CHANGE IN MEAN SEA LEVEL ON BEACH (SERIES II AND IV)

e cm

Test	tap no.	x = 4 ft	8 ft	12 ft	16 ft	20 ft	24 ft	28 ft
II 5	1	1.18	-	-	0.72	-	0.05	0.02
	2	0.40	-	-0.01	-	-0.14	-0.22	-
	3	-0.25	-0.24	-0.16	-0.19	-0.12	-0.03	-
	4	-0.16	-0.12	-0.05	-0.07	-0.09	0.01	-
	5	-	-0.02	-0.01	-0.03	-0.05	-	-
	6	-0.06	-0.15	0	-0.01	-0.02	-	0.04
II 6	1	0.02	-	-	0.62	-	1.19	-0.06
	2	0	-	-0.10	-	-0.43	-0.20	-
	3	-0.28	-0.17	-0.20	-0.17	-0.15	-0.13	-
	4	-0.19	-0.08	-0.09	-0.10	-0.09	-0.08	-
	5	-	-0.03	-0.05	-0.04	-0.05	-	-
	6	-0.14	-0.20	-0.04	0.03	0.10	-	-0.03
II 7	1	-	-	-	0.04	-	-0.08	0.04
	2	-0.09	-	-0.13	-	-0.03	0.02	-
	3	-0.04	-0.05	-0.03	-0.04	-0.01	0.03	-
	4	0.01	0	0.00	0	0.02	0.02	-
	5	-	0.03	0.01	0	0	-	-
	6	0.03	0.04	0.01	0.04	0.02	-	0.05
II 8	1	0.06	-	-	0.48	-	-0.10	-0.01
	2	-0.10	-	-0.18	-	-0.24	-0.05	-
	3	-0.07	-0.14	-0.12	-0.10	-0.12	-0.04	-
	4	-0.05	-0.06	-0.04	-0.04	-0.05	-0.02	-
	5	-	-0.03	-0.03	-0.03	-0.04	-	-
	6	-0.04	-0.05	-0.12	0.04	0.03	-	-0.03

TABLE A 6.2 (cont'd)

CHANGE IN MEAN SEA LEVEL ON BEACH (SERIES II AND IV)

Test	tap no.	x = 4 ft	8 ft	12 ft	e cm 16 ft	20 ft	24 ft	28 ft
II 9	1	0.78	-	-	0.70	-	0.01	0.01
	2	0.22	-	0.37	-	-0.12	-0.01	-
	3	-0.05	-0.20	-0.20	-0.20	-0.19	-0.03	-
	4	-0.09	-0.10	-0.10	-0.08	-0.08	-0.02	-
	5	-	-0.04	-0.05	-0.03	-0.03	-	-
	6	-0.05	-0.05	-0.03	-0.02	0	-	-0.01
IV 2	1	1.14	0.63	1.07	0.86	0.30	-	0.74
	2	0.32	-	0.27	-	0.30	0.06	0.54
	3	-0.04	0.18	-0.13	-0.07	-0.10	-0.14	0.20
	4	-0.14	0.10	-0.11	-0.09	-0.10	-0.03	-0.05
	5	-0.08	0.05	-0.07	-0.05	-0.07	-0.04	-0.05
	6	-	0.04	-0.04	-0.00	-0.03	0	-0.05
IV 4	1	1.02	0.62	0.87	0.73	-	0.56	0.20
	2	0.31	-	-	-	-0.04	-0.50	0.18
	3	-0.09	0	-	-	-0.19	-	0.06
	4	-0.14	0	-0.15	-0.14	-0.12	-0.07	0.04
	5	-	0	-	-0.09	-0.09	-	-0.05
	6	-0.08	-0.09	-	-0.05	-0.03	0.08	-0.04
IV 6	1	0.62	0.14	0.30	0.35	-	-0.12	0.02
	2	-0.02	-	-	-	-	-0.14	-
	3	-0.04	-0.17	-0.07	-0.10	-0.05	-0.05	-
	4	-0.08	-0.15	-	-0.05	0	-0.02	-
	5	-	-	-	-0.02	-	-	-
	6	-0.02	-	-	-0.03	-	-	0

TABLE A 6.2 (cont'd)

CHANGE IN MEAN SEA LEVEL ON BEACH (SERIES II AND IV)

Test	tap no.	x = 4 ft	8 ft	12 ft	e cm 16 ft	20 ft	24 ft	28 ft
IV 7	1	0.46	0.35	0.12	0.18	-	-0.05	0.03
	2	-0.10	-	-	-	-	-0.05	-
	3	-0.05	-0.12	0.03	-0.04	-0.04	-0.05	-
	4	-0.04	-0.10	-	-0.03	-0.01	-0.02	-
	5	-	-	-	-0.02	-	-	-
	6	-0.01	-	-	0	-	-	0.05
IV 9	1	0.78	0.51	0.65	0.60	-	0.12	0.17
	2	0.18	-	-	-	-	-0.22	-
	3	-0.10	-0.13	-0.09	-0.07	-0.04	-0.07	-
	4	-0.07	-0.07	-	-0.04	-0.02	-0.02	-
	5	-	-	-	-0.02	-	-	-
	6	-0.01	-	-	-0.01	-	-	-0.05

TABLE A 6.3

CHANGE IN MEAN SEA LEVEL ON BEACH (SERIES III)*

Test	tap no.	x = 0 ft		4 ft		8 ft		12 ft		16 ft		20 ft		24 ft		28 ft	
		y ft	e cm	y ft	e cm	y ft	e cm	y ft	e cm	y ft	e cm	y ft	e cm	y ft	e cm	y ft	e cm
III 2a		d_d = 0.99 ft															
	3	-0.24	2.00	-0.24	1.81	-0.16	1.75	0	1.62	0.01	1.39	0.10	1.46	0.10	0.82	0.37	0.28
	4	1.26	0.43	1.26	0.32	1.34	-0.23	1.5	-0.17	1.51	-0.13	1.60	-0.15	1.60	-0.08	1.87	0.14
	5	3.76	-0.05	-	-	-	-	4.0	0.43	4.01	-0.05	4.10	-0.04	4.10	-0.02	4.37	-0.01
	6	6.76	-0.05	-	-	6.84	-0.02	-	-	-	-	7.00	-0.02	7.00	-0.02	7.37	-0.01
III 2b		d_d = 1.14 ft															
	1	0.11	0.42	0.12	1.12	0.19	1.05	0.31	1.10	0.26	0.96	-	-	0.31	0.10	0.72	0.42
	2	0.61	0.79	0.62	0.42	-	-	-	-	-	-	-	-	0.81	-0.56	1.22	0.42
	3	1.11	0.30	1.12	0.08	1.19	-0.12	1.31	-0.27	1.26	-0.37	-	-	1.31	-0.49	1.72	-0.27
	4	2.61	-0.13	2.62	-0.17	2.69	-0.20	2.81	-0.19	2.76	-0.17	-	-	2.81	-0.08	3.22	-0.05
	5	5.11	-0.13	-	-	-	-	5.31	-0.12	-	-	-	-	5.31	-0.09	5.72	-0.05
	6	-	-	-	-	-	-	-	-	-	-	-	-	-	-	8.72	-0.08
III 2c		d_d = 1.18 ft															
	1	0.22	0.78	0.23	0.85	0.30	0.45	0.42	0.65	0.37	0.75	-	-	0.42	-0.06	0.83	0.45
	2	0.72	0.30	0.73	0.30	0.80	-	0.92	0	-	-	0.92	-0.30	0.92	-0.27	1.33	0.37
	3	1.22	-0.15	1.23	-0.15	1.30	-0.15	1.42	-0.10	1.37	-0.20	1.42	-0.20	1.42	-0.12	1.83	0.78
	4	2.72	-0.07	2.73	-0.12	2.80	-0.10	2.92	-0.10	2.87	-0.10	2.92	-0.10	2.92	-0.05	3.33	0.17

*Series III data for e are 3 runs of test III 2, at different still water levels. y coordinates good to only ± 0.04 feet.

TABLE A 7

TWO-DIMENSIONAL VELOCITY DISTRIBUTION

Series	Test	y ft	x = 2 ft	6 ft	9 ft	11 ft	13 ft	15 ft	17 ft
II	2	-0.17	0.36	0.25	0.54	0.50	0.37	0.34	0.57
		0.33	0.43	0.33	0.60	0.47	0.49	0.52	0.68
		0.83	0.44	0.35	0.58	0.42	0.47	0.49	0.77
		1.33	0.17	0.25	0.25	0.35	0.42	0.45	0.53
		1.83	0.19	0.24	0.16	0.24	0.23	0.35	0.28
	3	-0.17	0.17	0.21	0.46	0.51	0.38	0.38	0.50
		0.33	0.32	0.32	0.53	0.59	0.57	0.64	0.71
		0.83	0.31	0.34	0.49	0.49	0.51	0.60	0.68
		1.33	0.19	0.24	0.28	0.38	0.43	0.51	0.52
		1.83	0.15	0.18	0.16	0.19	0.29	0.29	0.29
	4	-0.17	0.18	0.24	0.32	0.31	0.37	0.42	0.54
		0.33	0.32	0.27	0.32	0.37	0.48	0.53	0.67
		0.83	0.31	0.27	0.30	0.40	0.51	0.50	0.45
		1.33	0.19	0.19	0.18	0.24	0.28	0.31	0.34
		1.83	0.15	0.18	0.18	0.17	0.16	0.16	0.17
	5	-0.17	0.27	0.21	0.51	0.47	0.41	0.34	0.37
		0.33	0.30	0.24	0.52	0.50	0.62	0.50	0.64
		0.83	0.28	0.26	0.31	0.43	0.49	0.45	0.34
		1.33	0.21	0.18	0.16	0.28	0.27	0.33	0.32
		1.83	0.17	0.15	0.19	0.16	0.17	0.15	0.19
	6	-0.17	0.24	0.15	0.24	0.27	0.19	0.27	0.37
		0.33	0.45	0.44	0.41	0.40	0.42	0.38	0.50
		0.83	0.27	0.47	0.37	0.38	0.41	0.41	0.35
		1.33	0.16	0.26	0.27	0.27	0.28	0.28	0.25

TABLE A 7 (cont'd)

TWO-DIMENSIONAL VELOCITY DISTRIBUTION

Series	Test	y	x = 2	6	9	11	13	15	17
		ft	ft	ft	ft	ft	ft	ft	ft
II	7	-0.17	0.0	0.0	0.13	0.13	0.12	0.16	0.10
		0.33	0.19	0.20	0.24	0.23	0.23	0.23	0.21
		0.83	0.14	0.14	0.13	0.16	0.17	0.16	0.15
		1.33	0.14	0.13	0.13	0.14	0.13	0.12	0.14
	8	-0.17	0.0	0.0	0.13	0.13	0.14	0.15	0.14
		0.33	0.23	0.25	0.25	0.28	0.37	0.29	0.32
		0.83	0.14	0.16	0.20	0.21	0.23	0.28	0.21
		1.33	0.15	0.15	0.13	0.17	0.14	0.13	0.16
		1.83	0.15	0.15	0.15	0.15	0.15	0.14	0.15
	9	-0.17	0.12	0.16	0.25	0.31	0.30	0.28	0.42
		0.33	0.31	0.26	0.30	0.36	0.41	0.43	0.60
		0.83	0.27	0.29	0.31	0.35	0.39	0.49	0.42
		1.33	0.17	0.19	0.15	0.17	0.25	0.26	0.27
		1.83	0.17	0.16	0.16	0.17	0.14	0.14	0.15
	10	-0.17	0.13	0.19	0.17	0.34	0.34	0.30	0.45
		0.33	0.32	0.30	0.28	0.38	0.46	0.51	0.62
		0.83	0.27	0.27	0.31	0.40	0.43	0.50	0.40
		1.33	0.18	0.22	0.16	0.20	0.26	0.27	0.27
		1.83	0.17	0.16	0.17	0.17	0.14	0.14	0.14
	11	-0.17	0.15	0.14	0.27	0.30	0.35	0.49	0.51
		0.33	0.25	0.27	0.31	0.39	0.54	0.63	0.72
		0.83	0.29	0.28	0.28	0.29	0.57	0.58	0.57
		1.33	0.27	0.23	0.27	0.30	0.39	0.41	0.45
		1.83	0.19	0.17	0.17	0.17	0.20	0.20	0.19

TABLE A 7 (cont'd)

TWO-DIMENSIONAL VELOCITY DISTRIBUTION

Series	Test	y ft	x = 2 ft	7 ft	9 ft	11 ft	13 ft	15 ft	17 ft
III	2	0.30	1.10	1.23	-	1.68	-	1.68	1.49
		0.53	1.08	1.20	-	1.62	-	1.76	1.55
		0.80	0.77	1.20	-	1.49	-	1.64	1.67
		1.06	-	1.22	-	-	-	1.57	1.50
		1.47	-	0.98	-	-	-	1.15	1.20
		1.76	-	0.63	-	-	-	0.93	0.92
		1.97	-	0.35	-	-	-	-	-
	3	-0.06	-	-	1.20	1.32	1.17	1.10	1.03
		0.24	-	-	1.30	1.51	1.65	1.57	1.57
		0.54	-	-	1.23	1.40	1.69	1.61	1.69
		0.84	-	-	1.24	1.42	1.57	1.56	1.59
		1.24	-	-	0.98	1.10	1.30	1.23	1.32
		1.64	-	-	0.55	0.59	0.79	0.85	0.93
	4	0.26	-	-	1.15	1.32	1.53	1.71	1.45
		0.46	-	-	1.25	1.33	1.49	1.75	1.70
		0.76	-	-	1.27	1.38	1.45	1.61	1.63
		1.06	-	-	1.04	1.07	1.11	1.32	1.40
		1.46	-	-	0.62	0.64	0.81	0.87	0.98
		1.73	-	-	-	0.35	0.43	0.52	-
	5	-0.06	-	-	0.82	1.20	0.63	0.83	0.76
		0.24	-	-	1.00	1.41	1.51	1.38	1.33
		0.54	-	-	0.97	1.35	1.66	1.53	1.38
		0.84	-	-	1.06	1.16	1.36	1.33	1.30
		1.24	-	-	0.67	0.69	0.31	0.88	0.96
		1.64	-	-	0.32	0.27	0.34	0.39	0.45

TABLE A 7 (cont'd)

TWO-DIMENSIONAL VELOCITY DISTRIBUTION

Series	Test	y ft	x = 2 ft	7 ft	9 ft	11 ft	13 ft	15 ft	17 ft
III	6	-0.06	-	-	0.74	0.99	0.97	0.78	0.82
		0.24	-	-	1.07	1.30	1.22	1.21	1.07
		0.54	-	-	1.12	1.29	1.27	1.27	1.15
		0.84	-	-	0.97	1.02	1.13	1.19	1.05
		1.14	-	-	0.60	0.59	0.70	0.77	0.75
		1.54	-	-	0.32	0.32	0.36	0.43	0.45
	8	-0.06	-	-	0.57	0.64	0.36	0.44	0.46
		0.24	-	-	0.96	0.95	0.73	1.03	0.90
		0.54	-	-	0.88	0.85	0.90	0.95	0.88
		0.84	-	-	0.59	0.66	0.85	0.70	0.70
		1.14	-	-	0.23	0.27	0.44	0.46	0.49
		1.53	-	-	0.15	0.20	0.15	0.17	0.15
	9	-0.07	-	-	0.95	1.00	0.80	0.74	0.57
		0.22	-	-	-	1.13	1.25	1.30	1.23
		0.54	-	-	1.12	1.17	1.30	1.42	1.35
		0.84	-	-	0.95	1.02	1.04	1.10	1.19
		1.24	-	-	0.51	0.56	0.75	0.72	0.80
		1.64	-	-	0.23	0.25	0.27	0.30	0.36
	11	-0.06	-	-	1.07	1.21	1.27	1.30	0.98
		0.24	-	-	1.25	1.34	1.58	1.75	1.58
		0.54	-	-	1.27	1.38	1.53	1.75	1.72
		0.84	-	-	1.28	1.44	1.44	1.63	1.74
		1.24	-	-	1.06	1.15	1.15	1.23	1.36
		1.64	-	-	0.59	0.67	0.84	0.92	0.90

TABLE A 7 (cont'd)

TWO-DIMENSIONAL VELOCITY DISTRIBUTION

Series	Test	y	x = 2	6	9	11	13	15	17
		ft	ft	ft	ft	ft	ft	ft	ft
IV	2	0.28	1.23	1.49	1.74	1.75	2.07	2.18	2.17
		0.78	0.92	1.49	1.75	1.53	1.85	2.04	2.05
		1.28	0.56	1.26	1.18	1.19	1.41	1.46	1.42
		1.78	0.55	0.53	0.57	0.58	0.70	0.80	0.80
	3	0.28	1.07	1.67	1.73	1.74	1.73	1.88	2.00
		0.78	0.89	1.66	1.63	1.51	1.71	1.61	1.75
		1.28	0.59	1.09	0.81	0.78	1.07	1.00	0.99
		1.78	0.51	0.53	0.48	0.50	0.56	0.65	0.69
	4	0.31	1.23	1.51	1.63	1.91	2.04	1.96	1.73
		0.81	0.95	1.39	1.73	1.53	1.79	1.80	1.62
		1.31	0.50	0.97	0.95	0.81	0.98	1.08	1.03
		1.81	0.50	0.48	0.48	0.51	0.53	0.60	0.64
	5	0.31	1.10	1.42	1.62	1.93	1.82	1.74	1.57
		0.81	0.82	1.33	1.56	1.45	1.74	1.56	1.49
		1.31	0.50	0.90	0.82	0.78	0.99	1.05	1.03
		1.81	0.52	0.48	0.50	0.55	0.51	0.60	0.57
	6	0.31	0.97	1.05	0.97	0.98	1.02	0.82	0.86
		0.81	0.54	0.92	0.77	0.77	0.85	0.78	0.77
		1.31	0.47	0.43	0.48	0.42	0.46	0.57	0.52
		1.81	0.50	0.43	0.44	0.40	0.41	0.44	0.42
	7	0.31	1.00	0.92	0.94	0.93	0.84	0.78	0.71
		0.81	0.42	0.63	0.50	0.52	0.61	0.68	0.61
		1.31	0.44	0.44	0.42	0.40	0.41	0.47	0.47

TABLE A 7 (cont'd)

TWO-DIMENSIONAL VELOCITY DISTRIBUTION

Series	Test	y	x = 2	6	9	11	13	15	17
		ft	ft	ft	ft	ft	ft	ft	ft
IV	8	0.28	1.12	1.07	1.19	1.27	1.24	1.11	1.12
		0.78	0.48	0.94	0.78	0.81	0.97	0.97	0.92
		1.28	0.46	0.43	0.43	0.42	0.43	0.51	0.48
		1.78	0.46	0.44	0.42	0.40	0.40	0.41	0.39
	9	0.31	1.15	1.25	1.48	1.57	1.60	1.49	1.44
		0.81	0.77	1.27	1.14	1.08	1.33	1.24	1.24
		1.31	0.36	0.54	0.55	0.55	0.64	0.70	0.72
		1.81	0.49	0.49	0.48	0.46	0.47	0.49	0.47
	10	0.31	1.26	1.44	1.59	1.85	1.90	1.87	1.71
		0.81	0.94	1.32	1.49	1.12	1.59	1.59	1.50
		1.31	0.48	0.81	0.78	0.72	0.86	0.92	0.93
		1.81	0.51	0.49	0.48	0.49	0.48	0.51	0.56
	11	0.31	1.22	1.53	1.77	1.92	2.16	2.08	1.80
		0.81	1.00	1.40	1.66	1.56	1.74	1.92	1.59
		1.31	0.56	1.05	1.12	1.00	1.11	1.25	1.19
		1.81	0.51	0.51	0.52	0.57	0.59	0.61	0.65
	12	0.31	0.67	0.63	0.53	0.53	0.47	0.46	0.50
		0.81	0.43	0.53	0.51	0.51	0.50	0.47	0.44
		1.31	0.43	0.40	0.42	0.40	0.49	0.48	0.41
	13	0.31	1.09	1.09	1.31	1.46	1.50	1.57	1.51
		0.81	0.73	1.15	0.88	0.97	0.99	1.09	1.11
		1.31	0.46	0.50	0.46	0.55	0.53	0.57	0.58
		1.81	0.44	0.44	0.42	0.46	0.43	0.42	0.46

TABLE A 8

LONGSHORE CURRENT DATA

PMT refers to Putnam, Munk, and Traylor (1949)

IQ refers to Inman and Quinn (1951)

PMT F SERIES

C	T	M	B	D	H	SINF	V	CODF
10.00	0.016	0.00	0.00	5.00	0.258	2.50	2001.
9.00	0.020	0.00	0.00	5.50	0.208	2.20	2002.
9.00	0.023	0.00	0.00	7.00	0.258	3.00	2003.
7.00	0.017	0.00	0.00	6.00	0.131	1.80	2004.
10.00	0.031	0.00	0.00	5.00	0.174	3.60	2005.
10.00	0.022	0.00	0.00	8.00	0.174	2.80	2006.
10.00	0.023	0.00	0.00	8.00	0.174	2.30	2007.
12.00	0.020	0.00	0.00	6.50	0.174	2.40	2008.
12.00	0.020	0.00	0.00	4.50	0.174	2.40	2009.
12.00	0.019	0.00	0.00	4.50	0.174	2.70	2010.
12.00	0.019	0.00	0.00	4.50	0.174	2.10	2011.
15.00	0.016	0.00	0.00	6.50	0.087	1.70	2012.
7.00	0.022	0.00	0.00	8.00	0.301	5.20	2013.
8.00	0.030	0.00	0.00	5.00	0.174	3.30	2014.
8.00	0.020	0.00	0.00	8.50	0.208	2.50	2015.
15.00	0.026	0.00	0.00	5.00	0.087	2.40	2016.
8.00	0.019	0.00	0.00	9.00	0.258	5.50	2017.
8.00	0.019	0.00	0.00	9.00	0.258	3.90	2018.

PMT SERIES

C T	M	B	D	H	SINE	V	CODE
1.00	0.066	0.00	0.75	0.47	0.314	0.78	1001.
1.06	0.066	0.00	0.44	0.32	0.238	0.64	1002.
1.14	0.066	0.00	0.56	0.40	0.252	0.82	1003.
1.15	0.066	0.00	0.41	0.31	0.218	0.68	1004.
1.25	0.066	0.00	0.39	0.30	0.203	0.76	1005.
1.32	0.066	0.00	0.40	0.32	0.203	0.75	1006.
1.40	0.066	0.00	0.37	0.29	0.189	0.64	1007.
1.90	0.144	0.00	0.24	0.16	0.302	0.75	1008.
2.13	0.144	0.00	0.23	0.15	0.296	0.66	1009.
2.22	0.144	0.00	0.24	0.15	0.297	0.50	1010.
0.72	0.241	0.00	0.48	0.28	0.312	1.33	1011.
0.92	0.241	0.00	0.52	0.35	0.284	1.27	1012.
1.14	0.241	0.00	0.28	0.22	0.180	0.53	1013.
1.22	0.241	0.00	0.27	0.22	0.184	0.69	1014.
0.99	0.100	0.00	0.32	0.24	0.470	1.68	1015.
1.32	0.100	0.00	0.27	0.22	0.388	1.45	1016.
1.63	0.100	0.00	0.23	0.16	0.322	0.96	1017.
1.98	0.100	0.00	0.22	0.16	0.316	0.76	1018.
0.83	0.139	0.00	0.43	0.28	0.835	2.46	1019.
0.91	0.139	0.00	0.33	0.23	0.711	2.31	1020.
1.00	0.139	0.00	0.29	0.22	0.627	2.22	1021.
1.12	0.139	0.00	0.24	0.20	0.548	1.93	1022.
1.35	0.139	0.00	0.25	0.20	0.516	1.52	1023.
0.80	0.260	0.00	0.62	0.34	0.843	3.78	1024.
0.90	0.260	0.00	0.43	0.29	0.793	3.34	1025.
0.98	0.260	0.00	0.41	0.28	0.734	3.00	1026.
1.23	0.260	0.00	0.26	0.20	0.537	1.91	1027.
1.27	0.260	0.00	0.23	0.22	0.528	1.76	1028.
0.95	0.098	0.00	0.36	0.26	0.502	1.03	1029.
1.33	0.098	0.00	0.27	0.21	0.365	0.46	1030.
1.67	0.098	0.00	0.20	0.16	0.309	0.20	1031.
1.99	0.098	0.00	0.19	0.12	0.282	0.15	1032.
1.08	0.143	0.00	0.47	0.33	0.506	1.32	1033.
1.36	0.143	0.00	0.38	0.29	0.416	0.63	1034.
1.58	0.143	0.00	0.27	0.20	0.330	0.36	1035.
1.91	0.143	0.00	0.26	0.20	0.316	0.32	1036.
2.32	0.143	0.00	0.30	0.22	0.327	0.18	1037.

IO SERIES

C T	M	B	D	H	SINE	V	CODE
15.00	0.027	0.00	0.00	2.80	0.113	0.38	3001.
8.50	0.027	0.00	0.00	3.10	0.026	0.04	3002.
8.00	0.027	0.00	0.00	3.70	0.070	0.22	3003.
14.00	0.027	0.00	0.00	3.60	0.000	0.04	3004.
8.00	0.027	0.00	0.00	4.90	0.087	0.84	3005.
7.00	0.027	0.00	0.00	3.80	0.087	0.21	3006.
12.50	0.027	0.00	0.00	3.40	0.000	0.55	3007.
8.00	0.035	0.00	0.00	2.60	0.000	0.04	3008.
9.50	0.035	0.00	0.00	3.00	0.156	0.01	3009.
10.00	0.035	0.00	0.00	2.70	0.000	0.15	3010.
13.50	0.035	0.00	0.00	3.50	0.000	0.09	3011.
13.00	0.035	0.00	0.00	4.90	0.000	0.21	3012.
10.00	0.035	0.00	0.00	2.90	0.000	0.50	3013.
12.00	0.035	0.00	0.00	4.60	0.000	0.80	3014.
8.00	0.028	0.00	0.00	3.70	0.000	0.20	3015.
12.00	0.027	0.00	0.00	5.10	0.150	0.29	3016.
14.00	0.027	0.00	0.00	4.70	0.122	0.53	3017.
15.00	0.027	0.00	0.00	4.50	0.070	0.70	3018.
12.00	0.027	0.00	0.00	4.80	0.070	1.19	3019.
12.00	0.027	0.00	0.00	4.20	0.078	0.40	3020.
12.00	0.027	0.00	0.00	2.00	0.078	0.36	3021.
8.00	0.027	0.00	0.00	1.70	0.122	0.23	3022.
15.00	0.027	0.00	0.00	2.90	0.087	0.56	3023.
6.00	0.027	0.00	0.00	1.60	0.087	0.11	3024.
14.00	0.014	0.00	0.00	6.20	0.087	0.54	3025.
16.00	0.014	0.00	0.00	3.10	0.122	0.62	3026.
12.00	0.014	0.00	0.00	4.50	0.052	0.49	3027.
14.00	0.014	0.00	0.00	3.50	0.070	0.17	3028.
16.00	0.014	0.00	0.00	2.70	0.061	0.13	3029.
13.00	0.014	0.00	0.00	4.70	0.122	1.37	3030.
11.50	0.014	0.00	0.00	2.60	0.035	0.04	3031.
14.50	0.014	0.00	0.00	2.00	0.070	0.11	3032.
12.00	0.014	0.00	0.00	1.80	0.044	0.06	3033.

II SERIES

C	T	M	B	D	H	SINE	V	CODE
1.00	0.109	1.62	0.18	0.00	0.087	0.83	4002.
1.12	0.109	1.53	0.17	0.21	0.072	0.82	4003.
1.25	0.109	1.33	0.15	0.14	0.052	0.68	4004.
1.37	0.109	1.24	0.14	0.19	0.064	0.53	4005.
1.50	0.109	1.17	0.13	0.00	0.052	0.52	4006.
1.25	0.109	0.62	0.07	0.03	0.035	0.34	4007.
1.25	0.109	0.87	0.10	0.12	0.023	0.50	4008.
1.25	0.109	1.21	0.13	0.17	0.051	0.67	4009.
1.25	0.109	1.07	0.12	0.17	0.051	0.71	4010.
1.25	0.109	1.44	0.16	0.19	0.072	0.84	4011.
1.50	0.109	0.76	0.08	0.07	0.019	0.21	4012.
1.00	0.109	0.98	0.11	0.09	0.024	0.45	4013.

III SERIES

C	T	M	B	D	H	SINE	V	CODE
0.90	0.109	0.00	0.00	0.18	0.000	1.81	6001.
1.00	0.109	1.52	0.00	0.17	0.243	1.76	6002.
1.12	0.109	1.51	0.00	0.19	0.209	1.60	6003.
1.25	0.109	1.44	0.00	0.19	0.175	1.61	6004.
1.37	0.109	1.13	0.00	0.19	0.159	1.42	6005.
1.50	0.109	1.04	0.00	0.16	0.119	1.23	6006.
1.25	0.109	0.68	0.00	0.09	0.106	0.56	6007.
1.25	0.109	0.85	0.00	0.13	0.115	0.96	6008.
1.25	0.109	1.11	0.00	0.15	0.151	1.23	6009.
1.25	0.109	1.33	0.00	0.17	0.170	1.49	6010.
1.25	0.109	1.55	0.00	0.17	0.192	1.77	6011.
1.50	0.109	0.77	0.00	0.11	0.064	0.00	6012.
1.00	0.109	0.94	0.00	0.11	0.168	0.00	6013.

IV SERIES

C	T	M	B	D	H	SINE	V	CODE
1.00	0.109	1.40	0.00	0.18	0.469	2.15	5002.
1.12	0.109	1.15	0.00	0.00	0.372	1.89	5003.
1.25	0.109	1.22	0.00	0.19	0.318	1.91	5004.
1.37	0.109	1.32	0.00	0.00	0.271	1.81	5005.
1.50	0.109	0.91	0.00	0.10	0.149	0.91	5006.
1.25	0.109	0.69	0.00	0.16	0.231	0.65	5007.
1.25	0.109	0.83	0.00	0.13	0.247	1.20	5008.
1.25	0.109	1.19	0.00	0.16	0.336	1.57	5009.
1.25	0.109	1.27	0.00	0.00	0.337	1.88	5010.
1.25	0.109	1.29	0.00	0.00	0.383	1.96	5011.
1.50	0.109	0.57	0.00	0.00	0.104	0.18	5012.
1.00	0.109	0.88	0.00	0.00	0.344	1.46	5013.
1.00	0.109	1.11	0.00	0.00	0.324	0.00	5015.

REFERENCES

Bass, N.W., and others, Origin and distribution of Bartlesville and Burbank shoestring sands in parts of Oklahoma and Kansas, Am. Assoc. Petroleum, Geol. Bull, 21, pp. 30-66, 1937.

Beach Erosion Board, Shore protection planning and design, Technical Report No. 4, Beach Erosion Board, 1961.

Brebner, A., and Kennedy, R.J., Littoral drift in Lake Ontario Harbors: Eng. Journ. Eng. Inst. of Canada, 42, No. 9.

Bretschneider, C.L., Revision in wave forecasting: deep and shallow water, in Proceedings of Sixth Conf. on Coastal Engineering, edited by J.W. Johnson, Council on Wave Research, Richmond, California, 1958.

Caldwell, J.M., Wave action and sand movement near Anaheim Bay, California, Beach Erosion Board Technical Memo. No. 68, 1956.

Dean, R.G., Interaction of a fixed, semi-immersed circular cylinder with a train of surface waves, doctoral theses, MIT, Dept. of Civ. Engineering, 1959.

Dunham, J.W., Refraction and diffraction diagrams, in Proceedings First Conf. on Coastal Engineering, edited by J.W. Johnson, pp. 33-49, Council on Wave Research, Richmond, Calif., 1950.

Eagleson, P.S., Properties of shoaling waves by theory and experiment, J. Geophys. Res., 37, 565-572, 1956.

Eaton, R.O., Littoral process on sandy coasts, in Proc. First Conf. on Coastal Eng., edited by J.W. Johnson, pp. 140-154, Council on Wave Research, Richmond, Calif, 1951.

Emery, K.O., The sea off Southern California, John Wiley and Sons, New York, 1960.

Friedman, G.M., Distinction between dune, beach, and river sands from their textural characteristics, J. Sed. Petrography, 31, pp. 514-529, 1961.

Handin, J.W., The source, transportation, and deposition of beach sediment in Southern California, Beach Erosion Board Tech. Memo, No. 22, 1950.

Herbich, J.B., Experimental studies of wave filters and absorbers, St. Anthony Falls Hydraulic Lab. Project Report No. 44, 1956.

Ho, D.V., and Meyer, R.E., Climb of a bore on a beach, J. Fluid Mechanics, 14, pp. 305-318, 1962.

REFERENCES (cont'd)

Inman, D.L., and Quinn, W.H., Currents in the surf zone, in Proceedings of Second Conf. on Coastal Engineering, edited by J.W. Johnson, pp. 24-36, Council on Wave Research, Richmond, Calif., 1951.

Iverson, H.W., Laboratory study of breakers, Gravity Waves, National Bureau of Standards Circular 521, pp. 9-35, 1952.

Ippen, A.T., and Kulin, G., Shoaling and breaking characteristics of the solitary wave, MIT Hydrodyn. Lab. TR No. 15, 1955.

Johnson, J.W., Dynamics of nearshore sediment movement, Am. Assoc. Petroleum Geol. Bull, 40, pp. 2211-2232, 1956.

Johnson, J.W., Sand transport by littoral currents, Proceedings, Fifth Hydraulic Conf., State Univ. of Iowa, Studies of Eng. Bull. 34, 1952.

Johnson, J.W., O'Brien, M.P., and Isaacs, J.D., Graphical construction of wave refraction diagrams, Hydrographic Office Pub. No. 605, 1948.

Johnson, D.W., Shore processes and shore line development, John Wiley and Sons, New York, 1919.

Keller, H.B., Levine, D.A., and Whitham, G.B., Motion of bore over a sloping beach, J. Fluid Mechanics, 7, pp. 302-316, 1960.

Kuenen, P.H., Marine geology, John Wiley and Sons, New York, 1950.

LeMehaute, B., Theoretical Study of a wave breaking at an angle with a shoreline, J. Geophys. Res., 66, pp. 495-500, 1961.

McCowan, J., On the highest wave of permanent type, Phil. Mag., 38, p. 351, 1894.

Miche, R., Movements ondulatoires de la mer, Ann. Ponts and Chausses, 114, pp. 25-78, 131-164, 270-292, 369-406, 1944.

Munk, W.H., The solitary wave theory and its application to surf problems, N.Y. Acad. Sci, 51, pp. 376-424, 1949.

Per Bruun, Longshore currents and longshore troughs, J. Geophys. Res., 68, pp. 1065-1078, 1963.

Putnam, J.A., Munk, W.H., and Traylor, M.A., The prediction of longshore currents, Trans. Am. Geophys. Union, 30, pp. 337-345, 1949.

REFERENCES (cont'd)

Savage, R.P., Laboratory determination of littoral-transport rates, J. Waterways and Harbors Div., Am. Soc. Civil Engineers, 88, pp. 69-92, 1962.

Shen, M.C., and Meyer, R.E., Wave run-up on beaches, Nonr 562-34 Tech. Rept. No. 3, Brown University, 1962.

Shepard, F. P., Longshore current observations in Southern California, Beach Erosion Board Tech Memo No. 13, 1950.

Shepard, F.P., and Inman, D.L., Nearshore water circulation related to bottom topography and wave refraction, Trans. Am. Geophys. Union, 31, pp. 196-212, 1950.

Svendson, S., Munch-Peterson's littoral drift formula, Bull. Beach Erosion Board, 4, pp. 1-31, 1950.

Topping, J., Errors of observation and their treatment, Reinhold Publ. Corp., New York, 1960.

Wiegel, R.L., Parallel wire resistance wave meter, in Coastal Engineering Instruments, edited by R.L. Wiegel, pp. 39-43, Council on Wave Research, Richmond, Calif., 1956.

Wiegel, R.L., Gravity Waves, tables of functions, Council on Wave Research, Richmond, Calif. 1954.

Wiegel, R.L., Experimental study of surface waves in shoaling water, Trans. Amer. Geophys. Union, 31, 377 - 385 pp., 1950.

BIOGRAPHICAL NOTE

The writer was born in 1935 in Jersey City, New Jersey, the first of the ten children of Cyril Jerome and Veronica Lawlor Galvin. He graduated from Saint Peter's Prep, Jersey City, in 1953, received a bachelor of science degree in geological engineering from Saint Louis University, Saint Louis, Missouri, in 1957, and a master of science degree in geology from Massachusetts Institute of Technology, Cambridge, Massachusetts, in 1959. His professional experience includes four years as a research assistant at the Hydrodynamics Laboratory and two years as a teaching assistant in the Department of Geology and Geophysics of the Massachusetts Institute of Technology. He worked two summers as a geologist with the Fuels Branch, United States Geological Survey, and one summer as assistant mining geologist, Fluorite Division, Minerva Oil Company, Elizabethtown, Illinois. He is a member of the Geological Society of America and the American Association for the Advancement of Science, and an associate member of the American Geophysical Union and the American Society of Civil Engineers.

Publications

Galvin, C. J., 1963, Age-frequency analysis of geologic maps (abstract): Geological Society of America, Special Paper No. 73, p. A57.

Galvin, C. J., 1963, Discussion of "Laboratory determination of littoral-transport rates" by R.P. Savage, J. of Waterways and Harbors Div., Am. Soc. Civil Engineers, v. 89, no. WW1, pp. 57-59.

Reed, B., Galvin, C. J., and Miller, J. P., 1962, Some aspects of drumlin geometry: Am. J. of Science, v. 260, pp. 200-210.

Harleman, D.R.F., McDougall, D. W., Galvin, C. J., and Hoopes, J. A., 1961, An analysis of one-dimensional convective diffusion phenomena in an idealized estuary: MIT Hydrodynamics Laboratory Technical Report No. 42, 32 pp.